EXHIBIT 4

Analyses of Groundwater Flow, Contaminant Fate and Transport, and Distribution of Drinking Water at Tarawa Terrace and Vicinity, U.S. Marine Corps Base Camp Lejeune, North Carolina: Historical Reconstruction and Present-Day Conditions

Chapter I: Parameter Sensitivity, Uncertainty, and Variability Associated with Model Simulations of Groundwater Flow, Contaminant Fate and Transport, and Distribution of Drinking Water

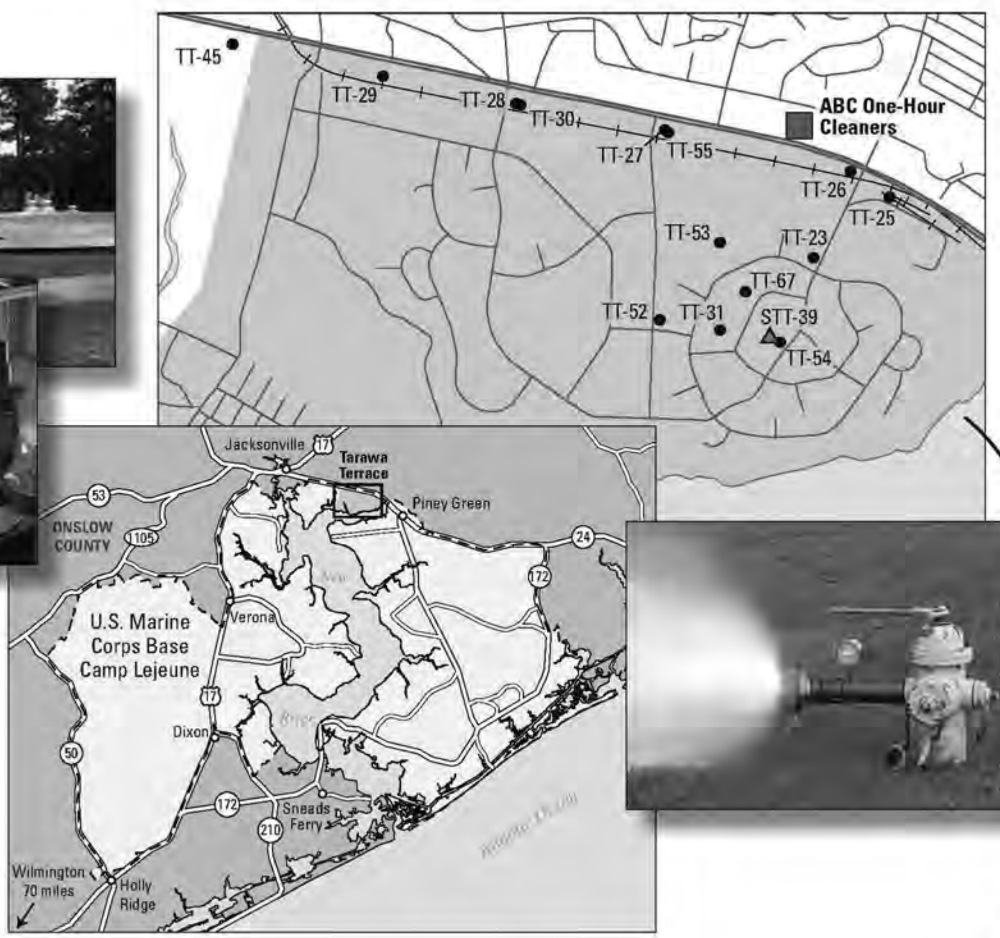

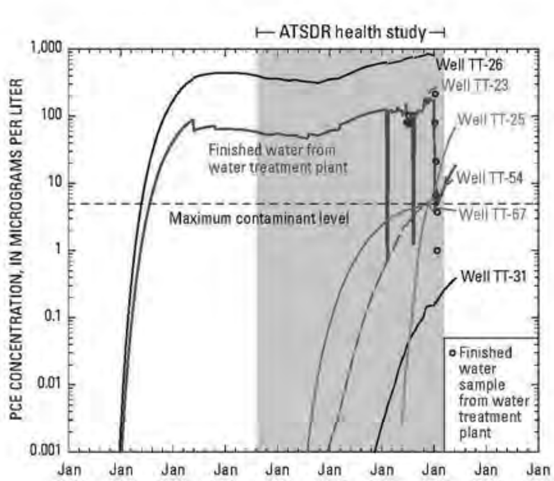

ATSDR
AGENCY FOR TOXIC SUBSTANCES AND DISEASE REGISTRY

DEPARTMENT OF HEALTH & HUMAN SERVICES · USA

Atlanta, Georgia–February 2009

Front cover: Historical reconstruction process using data, information sources, and water-modeling techniques to estimate historical exposures

Maps: U.S. Marine Corps Base Camp Lejeune, North Carolina; Tarawa Terrace area showing historical water-supply wells and site of ABC One-Hour Cleaners

Photographs on left: Ground storage tank STT-39 and four high-lift pumps used to deliver finished water from tank STT-39 to Tarawa Terrace water-distribution system

Photograph on right: Equipment used to measure flow and pressure at a hydrant during field test of the present-day (2004) water-distribution system

Graph: Reconstructed historical concentrations of tetrachloroethylene (PCE) at selected water-supply wells and in finished water at Tarawa Terrace water treatment plant

Analyses of Groundwater Flow, Contaminant Fate and Transport, and Distribution of Drinking Water at Tarawa Terrace and Vicinity, U.S. Marine Corps Base Camp Lejeune, North Carolina: Historical Reconstruction and Present-Day Conditions

Chapter I: Parameter Sensitivity, Uncertainty, and Variability Associated with Model Simulations of Groundwater Flow, Contaminant Fate and Transport, and Distribution of Drinking Water

By Morris L. Maslia, René J. Suárez-Soto, Jinjun Wang, Mustafa M. Aral, Robert E. Faye, Jason B. Sautner, Claudia Valenzuela, and Walter M. Grayman

Agency for Toxic Substances and Disease Registry
U.S. Department of Health and Human Services
Atlanta, Georgia

February 2009

Authors

Morris L. Maslia, MSCE, PE, D.WRE, DEE
Research Environmental Engineer and Project Officer
Exposure-Dose Reconstruction Project
Agency for Toxic Substances and Disease Registry
Atlanta, Georgia

René J. Suárez-Soto, MS EnvE, EIT
Environmental Health Scientist
Division of Health Assessment and Consultation
Agency for Toxic Substances and Disease Registry
Atlanta, Georgia

Jinjun Wang, MSCE
Ph.D. Candidate
Multimedia Environmental Simulations Laboratory
School of Civil and Environmental Engineering
Georgia Institute of Technology
Atlanta, Georgia

Mustafa M. Aral, PhD, PE
Director and Professor
Multimedia Environmental Simulations Laboratory
School of Civil and Environmental Engineering
Georgia Institute of Technology
Atlanta, Georgia

Robert E. Faye, MSCE, PE
Civil Engineer/Hydrologist
Robert E. Faye and Associates, Inc.
Consultant to Eastern Research Group, Inc.
Lexington, Massachusetts

Jason B. Sautner, MSCE, EIT
Environmental Health Scientist
Division of Health Assessment and Consultation
Agency for Toxic Substances and Disease Registry
Atlanta, Georgia

Claudia Valenzuela, MSCE
Post Graduate Research Fellow
Formerly, Oak Ridge Institute for Science and Education
Agency for Toxic Substances and Disease Registry
Atlanta, Georgia
Now, National Commission for the Environment
(CONAMA), Santiago, Chile

Walter M. Grayman, PhD, PE
Consulting Engineer
W.M. Grayman Consulting Engineer
Cincinnati, Ohio

For additional information write to:

Project Officer
Exposure-Dose Reconstruction Project
Division of Health Assessment and Consultation
Agency for Toxic Substances and Disease Registry
4770 Buford Highway, N.E., Mail Stop F-59
Atlanta, Georgia 30341

Suggested citation:
Maslia ML, Suárez-Soto RJ, Wang J, Aral MM, Faye RE, Sautner JB, Valenzuela C, and Grayman WM. Analyses of Groundwater Flow, Contaminant Fate and Transport, and Distribution of Drinking Water at Tarawa Terrace and Vicinity, U.S. Marine Corps Base Camp Lejeune, North Carolina: Historical Reconstruction and Present-Day Conditions—Chapter I: Parameter Sensitivity, Uncertainty, and Variability Associated with Model Simulations of Groundwater Flow, Contaminant Fate and Transport, and Distribution of Drinking Water. Atlanta, GA: Agency for Toxic Substances and Disease Registry; 2009.

Foreword

The Agency for Toxic Substances and Disease Registry (ATSDR), an agency of the U.S. Department of Health and Human Services, is conducting an epidemiological study to evaluate whether in utero and infant (up to 1 year of age) exposures to volatile organic compounds in contaminated drinking water at U.S. Marine Corps Base Camp Lejeune, North Carolina, were associated with specific birth defects and childhood cancers. The study includes births occurring during the period 1968–1985 to women who were pregnant while they resided in family housing at the base. During 2004, the study protocol received approval from the Centers for Disease Control and Prevention Institutional Review Board and the U.S. Office of Management and Budget.

Historical exposure data needed for the epidemiological case-control study are limited. To obtain estimates of historical exposure, ATSDR is using water-modeling techniques and the process of historical reconstruction. These methods are used to quantify concentrations of particular contaminants in finished water and to compute the level and duration of human exposure to contaminated drinking water.

Final interpretive results for Tarawa Terrace and vicinity—based on information gathering, data interpretations, and water-modeling analyses—are presented as a series of ATSDR reports. These reports provide comprehensive descriptions of information, data analyses and interpretations, and modeling results used to reconstruct historical contaminant levels in drinking water at Tarawa Terrace and vicinity. Each topical subject within the water-modeling analysis and historical reconstruction process is assigned a chapter letter. Specific topics for each chapter report are listed below:

- **Chapter A**: Summary of Findings
- **Chapter B**: Geohydrologic Framework of the Castle Hayne Aquifer System
- **Chapter C**: Simulation of Groundwater Flow
- **Chapter D**: Properties and Degradation Pathways of Common Organic Compounds in Groundwater
- **Chapter E**: Occurrence of Contaminants in Groundwater
- **Chapter F**: Simulation of the Fate and Transport of Tetrachloroethylene (PCE) in Groundwater
- **Chapter G**: Simulation of Three-Dimensional Multispecies, Multiphase Mass Transport of Tetrachloroethylene (PCE) and Associated Degradation By-Products
- **Chapter H**: Effect of Groundwater Pumping Schedule Variation on Arrival of Tetrachloroethylene (PCE) at Water-Supply Wells and the Water Treatment Plant
- **Chapter I**: Parameter Sensitivity, Uncertainty, and Variability Associated with Model Simulations of Groundwater Flow, Contaminant Fate and Transport, and Distribution of Drinking Water
- **Chapter J**: Field Tests, Data Analyses, and Simulation of the Distribution of Drinking Water
- **Chapter K**: Supplemental Information

An electronic version of this report, *Chapter I: Parameter Sensitivity, Uncertainty, and Variability Associated with Model Simulations of Groundwater Flow, Contaminant Fate and Transport, and Distribution of Drinking Water*, will be made available on the ATSDR Camp Lejeune Web site at *http://www.atsdr.cdc.gov/sites/lejeune/index.html*. Readers interested solely in a summary of this report or any of the other reports should refer to *Chapter A: Summary of Findings* that also is available at the ATSDR Web site.

Contents

Figures

Tables

Conversion Factors

Multiply	By	To obtain
	Length	
inch (in.)	2.54	centimeter (cm)
inch (in.)	25.4	millimeter (mm)
foot (ft)	0.3048	meter (m)
mile (mi)	1.609	kilometer (km)
mile, nautical (nmi)	1.852	kilometer (km)
yard (yd)	0.9144	meter (m)
	Area	
square foot (ft^2)	0.09290	square meter (m^2)
	Volume	
gallon (gal)	3.785	liter (L)
gallon (gal)	0.003785	cubic meter (m^3)
million gallons (MG)	3,785	cubic meter (m^3)
	Flow rate	
foot per day (ft/d)	0.3048	meter per day (m/d)
cubic foot per day (ft^3/d)	0.02832	cubic meter per day (m^3/d)
million gallons per day (MGD)	0.04381	cubic meter per second (m^3/s)
inch per year (in/yr)	25.4	millimeter per year (mm/yr)
	Density	
pound per cubic foot (lb/ft^3)	1.602×10^1	kilogram per cubic meter (kg/m^3)
	Hydraulic conductivity	
foot per day (ft/d)	0.3048	meter per day (m/d)

Concentration Conversion Factors

Unit	To convert to	Multiply by
microgram per liter (µg/L)	milligram per liter (mg/L)	0.001
microgram per liter (µg/L)	milligram per cubic meter (mg/m^3)	1
microgram per liter (µg/L)	microgram per cubic meter (µg/m^3)	1,000
parts per billion by volume (ppbv)	parts per million by volume (ppmv)	1,000

Vertical coordinate information is referenced to the National Geodetic Vertical Datum of 1929 (NGVD 29).

Horizontal coordinate information is referenced to the North American Datum of 1983 (NAD 1983).

Altitude, as used in this report refers to distance above the vertical datum.

Glossary and Abbreviations

Definitions of terms and abbreviations used throughout this report are listed below.

2-COMP	a two-compartment storage-tank mixing model	
ATSDR	Agency for Toxic Substances and Disease Registry	
CD–ROM	compact disc, read-only memory	
CI	cast iron	
CLW	Camp Lejeune water document	
CRWQME	continuous recording water-quality monitoring equipment	
CSTR	continuous stirred-tank reactor, also referred to as a complete mixing storage-tank model	
DCE	1,1-DCE	1,1-dichloroethylene or 1,1-dichloroethene
	1,2-DCE	1,2-dichloroethylene or 1,2-dichloroethene
	1,2-cDCE	*cis*-1,2- dichloroethylene or *cis*-1,2-dichloroethene
	1,2-tDCE	*trans*-1,2- dichloroethylene or *trans*-1,2-dichloroethene
DVD	digital video disc	
EPANET 2	a water-distribution system model developed by USEPA (Rossman 2000)	
EPS	extended period simulation; a simulation method used to analyze a water-distribution system	
FIFO	a first-in, first-out plug-flow storage-tank mixing model	
FORTRAN	formula translation, a computer coding language for scientific and engineering computations and analyses	
gal/min	gallons per minute	
kriging	geostatistical techniques used to interpolate the value of random parameters (for example, porosity) at an unobserved location from observations of its value at nearby locations	
LIFO	a last-in, first-out plug-flow storage-tank mixing model	
MCL	maximum contaminant level; a legal threshold limit set by the USEPA on the amount of a hazardous substance that is allowed in drinking water under the Safe Drinking Water Act; usually expressed as a concentration in milligrams or micrograms per liter. Effective dates for MCLs are as follows: trichloroethylene (TCE) and vinyl chloride (VC), January 9, 1989; tetrachloroethylene (PCE) and *trans*-1,2-dichloroethylene (1,2-tDCE), July 6, 1992 (40 CFR, Section 141.60, Effective Dates, July 1, 2002, ed.)	
MC simulation	Monte Carlo simulation, also referred to as Monte Carlo analysis; a computer-based method of analysis that uses statistical sampling techniques to obtain a probabilistic approximation to the solution of a mathematical equation or model (USEPA 1997)	
MESL	Multimedia Environmental Simulations Laboratory, School of Civil and Environmental Engineering, Georgia Institute of Technology, Atlanta, Georgia; an ATSDR cooperative agreement partner	
mL	milliliter; 1/1000th of a liter	
MODFLOW	a three-dimensional groundwater-flow model developed by the U.S. Geological Survey; versions of MODFLOW used for the Tarawa Terrace analyses are MODFLOW-96 (Harbaugh and McDonald 1996) and MODFLOW-2000 (Harbaugh et al. 2000)	
MT3DMS	a three-dimensional mass transport, multispecies model developed by C. Zheng and P. Wang on behalf of the U.S. Army Engineer Research and Development Center, Vicksburg, Mississippi	

NPL	National Priorities List
PCE	tetrachloroethene, tetrachloroethylene, 1,1,2,2-tetrachloroethylene, or perchloroethylene; also known as PERC® or PERK®
PDF	probability density function
PEST	a model-independent parameter estimation and uncertainty analysis tool developed by Watermark Numerical Computing (Doherty 2005)
PRNG	pseudo-random number generator; an algorithm for generating a sequence of numbers that approximates the properties of random numbers
probabilistic	an analysis in which frequency distributions are assigned to represent uncertainty analysis or variability in model parameters. The output of a probabilistic analysis is a distribution (Cullen and Frey 1999)
PVC	polyvinyl chloride
realization	a set of uncertain parameter values obtained by using a pseudo-random number generator; an MC simulation consists of multiple realizations
RMS	root-mean-square
SCADA	supervisory control and data acquisition
sensitivity analysis	an analysis method used to ascertain how a given model output (for example, concentration) depends upon the input parameters (for example, pumping rate, mass loading rate). Sensitivity analysis is an important method for checking the quality of a given model, as well as a powerful tool for checking the robustness and reliability of its analysis
SG simulation	sequential Gaussian simulation; a process in which a field of values (such as hydraulic conductivity) is obtained multiple times assuming the spatially interpolated values follow a Gaussian (normal) distribution
TCE	1,1,2-trichloroethene, 1,1,2-trichloroethylene, or trichloroethylene
uncertainty	the lack of knowledge about specific factors, parameters, or models (for example, one is uncertain about the mean value of the concentration of PCE at the source)
uncertainty analysis	determination of the uncertainty (e.g., standard deviation) of the output variables' expected value (e.g., mean) due to uncertainty in model parameters, inputs, or initial state by stochastic modeling techniques (Schnoor 1996)
USEPA	U.S. Environmental Protection Agency
USGS	U.S. Geological Survey
variability	observed differences attributable to heterogeneity or diversity in a model parameter, an exposure parameter, or a population
variogram	also known as semivariogram; a statistically-based (geostatistical), quantitative description of the spatial continuity or roughness of a dataset (Barnes 2003)
VC	vinyl chloride or chloroethene
VOC	volatile organic compound
WTP	water treatment plant

Use of trade names and commercial sources is for identification only and does not imply endorsement by the Agency for Toxic Substances and Disease Registry or the U.S. Department of Health and Human Services.

Analyses of Groundwater Flow, Contaminant Fate and Transport, and Distribution of Drinking Water at Tarawa Terrace and Vicinity, U.S. Marine Corps Base Camp Lejeune, North Carolina: Historical Reconstruction and Present-Day Conditions

Chapter I: Parameter Sensitivity, Uncertainty, and Variability Associated with Model Simulations of Groundwater Flow, Contaminant Fate and Transport, and Distribution of Drinking Water

By Morris L. Maslia,[1] René J. Suárez-Soto,[1] Jinjun Wang,[2] Mustafa M. Aral,[2] Robert E. Faye,[3] Jason B. Sautner,[1] Claudia Valenzuela,[4] and Walter M. Grayman[5]

Abstract

Two of three water-distribution systems that have historically supplied drinking water to family housing at U.S. Marine Corps Base Camp Lejeune, North Carolina, were contaminated with volatile organic compounds (VOCs). Tarawa Terrace was contaminated mostly with tetrachloroethylene concentrations up to 215 micrograms per liter (µg/L), and Hadnot Point was contaminated mostly with trichloroethylene concentrations up to 1,400 µg/L. Because scientific data relating to the harmful effects of VOCs on a child or fetus are limited, the Agency for Toxic Substances and Disease Registry (ATSDR), an agency of the U.S. Department of Health and Human Services, is conducting an epidemiological study to evaluate potential associations between in utero and infant (up to 1 year of age) exposures to VOCs in contaminated drinking water at Camp Lejeune and specific birth defects and childhood cancers. The study includes births occurring during the period 1968–1985 to women who were pregnant while they resided in family housing at Camp Lejeune. Because limited measurements of contaminant and exposure data are available to support the epidemiological study, ATSDR is using modeling techniques to reconstruct historical conditions of groundwater flow, contaminant fate and transport, and the distribution of drinking water contaminated with VOCs delivered to family housing areas. This report, Chapter I, provides detailed information and interpretations of parameter sensitivity, variability, and uncertainty associated with model simulations of groundwater flow, contaminant fate and transport, and distribution of drinking water at Tarawa Terrace and vicinity. It relies on information, data, and simulation results from calibrated models presented in previously published ATSDR reports on Tarawa Terrace—Chapters A, B, C, E, and F. Future analyses and reports will present information and data about contamination of the Hadnot Point water-distribution system.

[1] Agency for Toxic Substances and Disease Registry, Atlanta, Georgia.

[2] Multimedia Environmental Simulations Laboratory, School of Civil and Environmental Engineering, Georgia Institute of Technology, Atlanta, Georgia.

[3] Consultant to Eastern Research Group, Inc., Lexington, Massachusetts.

[4] Formerly, Oak Ridge Institute for Science and Education, Oak Ridge, Tennessee, now at National Commission for the Environment (CONAMA), Santiago, Chile.

[5] W.M. Grayman Consulting Engineer, Cincinnati, Ohio.

Background

The Agency for Toxic Substances and Disease Registry (ATSDR), an agency of the U.S. Department of Health and Human Services, is conducting an epidemiological study to evaluate whether in utero and infant (up to 1 year of age) exposures to drinking water contaminated with volatile organic compounds (VOCs) at U.S. Marine Corps Base Camp Lejeune, North Carolina, were associated with specific birth defects and childhood cancers. The study includes births occurring during the period 1968–1985 to pregnant women who resided in family housing at the base. Because limited measurements of contaminant and exposure data are available to support the epidemiological study, ATSDR is using water-modeling techniques to provide the epidemiological study with quantitative estimates of monthly contaminant levels in the drinking water. Results obtained by using water-modeling techniques, along with information from the mother on her water use, can be used by the epidemiological study to estimate the level and duration of exposures to the mother during her pregnancy and to the infant (up to 1 year of age). Using water-modeling techniques in such a process is referred to as historical reconstruction (Maslia et al. 2001). Calibrated models were developed for groundwater flow (Faye and Valenzuela 2007), contaminant fate and transport (Faye 2008), and the distribution of drinking water (Sautner et al. 2007, In press 2009) for Tarawa Terrace and vicinity (Figure I1). These models required data that are usually not readily

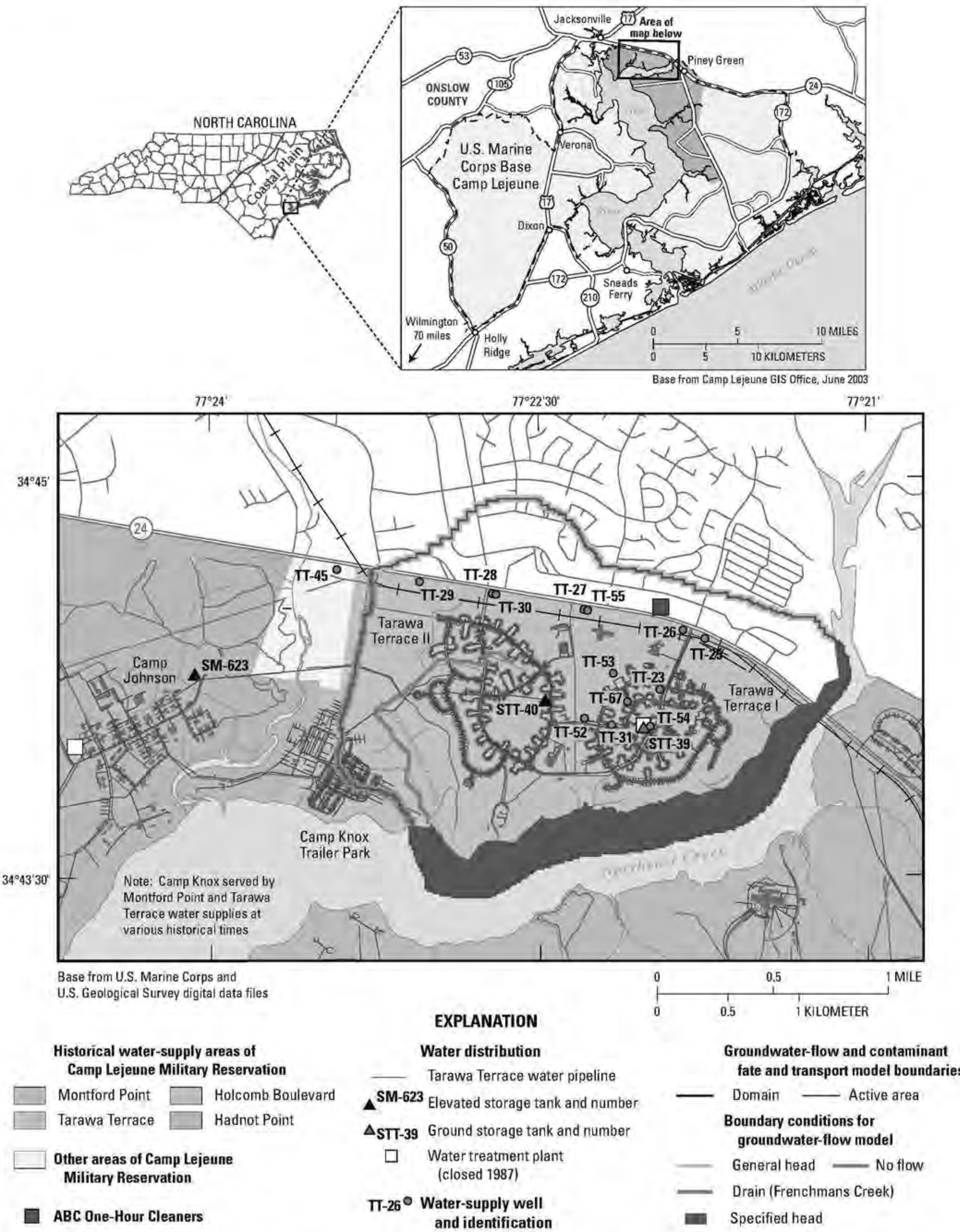

Figure I1. Location of groundwater-flow and contaminant fate and transport modeling domain and water-supply facilities used for historical reconstruction analyses, Tarawa Terrace and vicinity, U.S. Marine Corps Base Camp Lejeune, North Carolina.

available and inherently contain errors of approximation and interpretation. Moreover, all models and associated parameters contain uncertainties—both in the approximation of solutions to mathematical equations and in parameter values. Analyses subsequent to model calibration are required to describe, understand, and quantify sources of variability and uncertainty resulting from the application of models. Descriptions of the Tarawa Terrace models, calibration procedures, and simulation results are summarized in the Chapter A report (Maslia et al. 2007). Comprehensive details pertaining to the development, calibration, and simulation results of the Tarawa Terrace models are provided in Chapter C for groundwater flow (Faye and Valenzuela 2007), Chapter F for contaminant fate and transport (Faye 2008), and Chapter J for the distribution of drinking water (Sautner et al. In press 2009).

Purpose and Scope

The goal of the water-modeling analyses and the historical reconstruction process is to quantify the concentration of tetrachloroethylene (PCE) in groundwater, at Tarawa Terrace water-supply wells, and in finished drinking water[6] at the Tarawa Terrace water treatment plant (WTP) for the period 1951–1994. To achieve this goal, a number of models were used. Groundwater flow was simulated using the model code MODFLOW-96 (Harbaugh and McDonald 1996), contaminant fate and transport was simulated using the model code MT3DMS (Zheng and Wang 1999), the concentration of contaminants in finished water at the WTP was calculated using a flow-weighted materials mass balance model (Masters 1998, Maslia et al. 2007, Faye 2008), and the distribution of contaminated drinking water was simulated using the model code EPANET 2 (Rossman 2000). A discussion and description of all models used for the Tarawa Terrace analyses is presented in Chapter A of this report series (Maslia et al. 2007).

All models, including the aforementioned models, are subject to varying degrees of uncertainty which are associated with: (1) limited or lack of data, (2) erroneous data due to precision and accuracy limitations, and (3) simplifications of mathematical equations represented by the model. As defined by Schnoor (1996), an uncertainty analysis allows one to determine the uncertainty (standard deviation) of an output variable's expected value (mean) due to uncertainty in model parameters, inputs, or initial state by stochastic modeling techniques. Therefore, sensitivity and uncertainty analyses are a requisite of the model building and implementation process (Anderson and Woessner 1992). The purpose of this chapter report (Chapter I) is to characterize the uncertainty of model output (that is, simulated results) due to model input parameter uncertainty and variability. Several methods are frequently used to evaluate and quantify uncertainty. Two such methods are sensitivity and probabilistic analyses. Within the generalized classification of probabilistic analysis, Monte Carlo (MC) simulation is a particularly well-known numerical method. For this study, four types of sensitivity analyses and two sets of MC simulations were conducted using the calibrated Tarawa Terrace models (Faye and Valenzuela 2007, Faye 2008). The uncertainty methods discussed in this report are shown graphically in Figure I2 and are described below:

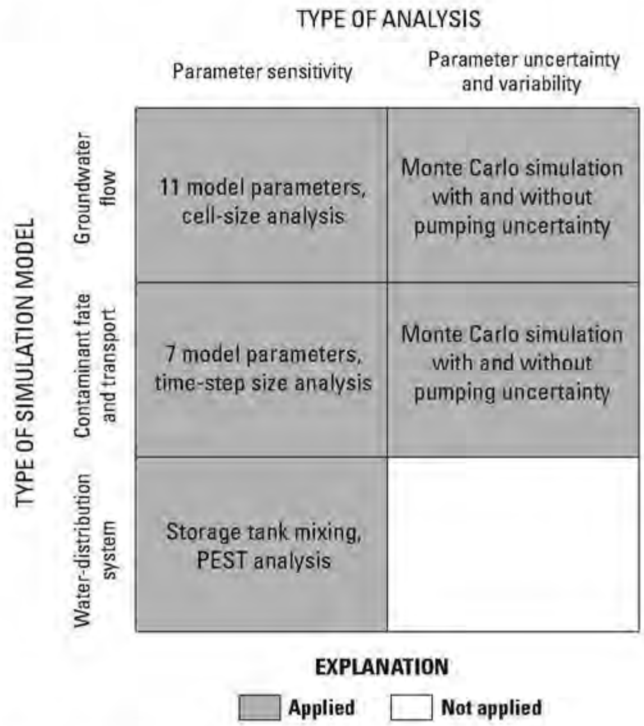

Figure I2. Types of uncertainty analyses applied to simulation models, Tarawa Terrace and vicinity, U.S. Marine Corps Base Camp Lejeune, North Carolina. [PEST, sensitivity analysis using PEST model code (Doherty 2005)]

1. a sensitivity analysis conducted using parameters of the groundwater-flow and contaminant fate and transport models. This sensitivity analysis included 11 parameters associated with the groundwater-flow model and 7 parameters associated with the contaminant fate and transport model;
2. a sensitivity analysis conducted to quantify the effect of the finite-difference grid cell size on groundwater-flow model output; [7]

[6] For the Tarawa Terrace study, finished drinking water is defined as groundwater that has undergone treatment at the WTP and delivered to a person's home. The concentration of contaminants in treated water at the WTP is considered the same as the concentration in the water delivered to a person's home. This assumption is tested and verified in the Chapter J report (Sautner et al. In press 2009). Hereafter, the term "finished water" will be used when referring to treated water.

[7] Refer to the Chapter C report (Faye and Valenzuela 2007) for details specific to the computational grid and model boundaries used to simulate groundwater flow.

3. a sensitivity analysis conducted to quantify the effect of time-step size on contaminant fate and transport model output; [8]

4. a sensitivity analysis conducted to quantify the relative importance of water-distribution system model parameters by conducting analyses of storage-tank mixing models and by utilizing the parameter estimation tool, PEST (Doherty 2005); [9]

5. a probabilistic analysis based on MC simulation using selected groundwater-flow model parameters with and without pumping uncertainty; and

6. a probabilistic analysis based on MC simulation using selected contaminant fate and transport model parameters, with and without pumping uncertainty.

The probabilistic analyses described in items 5 and 6 were conducted to determine the variability and uncertainty of model output caused by input parameter uncertainty. To quantify the variability and uncertainty of the model results, a series of MC simulations was conducted using the groundwater-flow and contaminant fate and transport models described in Faye and Valenzuela (2007) and Faye (2008), respectively. Two simulation scenarios were considered using MC simulations (Figure I2). Scenario 1 assumed no uncertainty associated with the allocation of groundwater pumping. Scenario 2 assumed uncertainty was associated with the allocation of groundwater pumping.[10]

Description of Calibrated Models

Given the paucity of measured historical contaminant-specific data and the lack of historical exposure data during most of the period relevant to the epidemiological study (January 1968–December 1985), ATSDR decided to apply the concepts of historical reconstruction to synthesize and estimate the spatial and temporal distributions of contaminant-specific concentrations in the drinking-water supply at Tarawa Terrace. Historical reconstruction typically includes the application of simulation tools, such as models, to recreate (or synthesize) past conditions. For this study, historical reconstruction included the linking of contaminant fate and transport models with materials mass balance (simple mixing) and water-distribution system models. In a simulation approach, a calibration process is used so that the combination of various model parameters—regardless of whether a model is simple or complex—appropriately reproduces the behavior of real-world systems (for example, migration of PCE) as closely as possible. A hierarchical approach for model calibration was used to estimate concentrations of PCE in finished water at the Tarawa Terrace WTP. A description of this approach is provided in the Chapter A report (Maslia et al. 2007). Specific details relative to models used to simulate groundwater flow, contaminant fate and transport, and the distribution of drinking water are provided in the Chapter C report (Faye and Valenzuela 2007), the Chapter F report, (Faye 2008), and the Chapter J report (Sautner et al. In press 2009), respectively. In the following sections of this report, summaries are provided that describe each of the aforementioned calibrated models.

Groundwater Flow

Steady-state and transient groundwater flow were simulated using the model code MODFLOW-96 (Harbaugh and McDonald 1996). The location of the model domain and active model area used for simulating groundwater flow are shown in Figure I1. The modeling grid consists of 7 layers, 200 rows, and 270 columns. Each cell represents an area of 250 square feet (ft^2)—50 feet (ft) per side—and every layer consists of 54,000 cells, of which 27,642 cells are within the active domain of the model. The following boundary conditions, described in Faye and Valenzuela (2007) are imposed on the modeled area.

1. A no-flow boundary is assigned to the eastern, western, and southern perimeters of the active model domain for all model layers.

2. A specified-head boundary with an assigned value of 0 ft, representing sea level, is assigned in layer 1 to Northeast Creek, extending east to the mid-channel line.

3. A general-head (head-dependent) boundary is used to represent the northern boundary for all layers and also generally conforms to a topographic divide. A general-head (head-dependent) boundary is assigned because of the proximity of water-supply wells to the boundary in the northwestern and north-central parts of the active model domain.

4. A drain is used to represent Frenchmans Creek in model layer 1 in the western part of the model domain.

Transient simulations were conducted using monthly stress periods of 28, 29, 30, or 31 days that corresponded to January 1951–December 1994 for a total of 528 stress periods. A listing of simulation stress periods and the corresponding month and year can be found in Appendix I1 of this report. The locations of water-supply wells used for the transient simulations are listed in Table I1. A complete listing of data pertaining to pumpage rates assigned to specific water-supply wells and the corresponding stress periods when the wells were operated in the model is provided in the Chapter C (Faye and Valenzuela 2007) and Chapter K (Maslia et al. In press 2009) reports. Calibrated groundwater-flow model parameter

[8] Refer to the Chapter F report (Faye 2008) for details specific to the computational time step used to simulate contaminant fate and transport analyses.

[9] Refer to the Chapter J report (Sautner et al. In press 2009) for details specific to the simulation of the distribution of water within the Tarawa Terrace water-distribution system.

[10] Refer to the Chapter H report (Wang and Aral 2008) for detailed analyses of the effect of groundwater pumping schedule variation on arrival of PCE at water-supply wells and at the Tarawa Terrace WTP.

Table I1. Locations of water-supply wells used for simulating groundwater flow and contaminant fate and transport, Tarawa Terrace and vicinity, U.S. Marine Corps Base Camp Lejeune, North Carolina.

[ft, feet]

Well[1]	Groundwater-flow model location[2]			Location coordinates[3]	
	Layer	Row	Column	Easting (ft)	Northing (ft)
TT-23	3	84	175	2491015	363195
TT-25	3	67	194	2491965	364045
TT-26	3	61	184	2491465	364345
TT-27	3	52	135	2489015	364795
TT-28	3	47	96	2487065	365045
TT-29	3	41	61	2485315	365345
TT-30	3	47	97	2487115	365045
TT-31	1 and 3	104	152	2489865	362195
TT-52	1 and 3	101	136	2489065	362345
TT-53	1	81	151	2489815	363345
TT-54	1 and 3	106	167	2490615	362095
TT-55	1	53	136	2489065	364745
TT-67	3	93	158	2490165	362745

[1]Water-supply wells #6, #7, and TT-45 are located external to the model domain and are not included in groundwater-flow and contaminant fate and transport model simulations. They are included in computations of water volume supplied to the Tarawa Terrace water treatment plant (Maslia et al. 2007, Faye 2008)

[2]Refer to Faye and Valenzuela (2007) for details describing groundwater-flow model grid

[3]Location coordinates are North Carolina State Plane coordinates, North American Datum of 1983

values, reported by Faye and Valenzuela (2007) are listed in Table I2. Calibration statistics are summarized in the Chapter A report (Maslia et al. 2007) and are discussed in detail in the Chapter C report (Faye and Valenzuela 2007).

Contaminant Fate and Transport

The contaminant fate and transport model uses simulated cell-by-cell specific discharge (Darcy velocities) derived from the calibrated groundwater-flow model to simulate the fate and transport of a contaminant in the subsurface. The same model domain, active area, cell sizes, and boundary conditions used for groundwater-flow simulation were used for contaminant fate and transport simulations. The model code MT3DMS (Zheng and Wang 1999) was applied to output from the Tarawa Terrace groundwater-flow model to simulate contaminant fate and transport. The following boundary conditions unique to simulated contaminant fate and transport—described in Faye (2008)—were imposed on the active modeled area (Figure I1).

1. A mass loading rate for PCE of 1,200 grams/day (g/d) was assigned to the MT3DMS model cell corresponding to layer 1, row 47, and column 170 and was applied continuously during stress periods 25 (January 1953) to 408 (December 1984). This loading rate was derived through the use of field data and the model calibration process described in the Chapter E (Faye and Green 2007) and Chapter F (Faye 2008) reports. Prior to January 1953 and after December 1984, a mass loading rate of 0.0 g/d was assigned to the cell.
2. A specified dispersive flux of 0.0 (Neuman type II boundary condition) was assumed to exist along the eastern, western, northern, and southern perimeters of the active model domain for all model layers.

Contaminant fate and transport simulations were conducted using monthly stress periods of 28, 29, 30, or 31 days that corresponded to January 1951–December 1994 for a total of 528 stress periods (Appendix I1). Calibrated contaminant fate and transport model parameter values reported by Faye (2008) also are listed in Table I2. Calibration statistics are summarized in the Chapter A report (Maslia et al. 2007) and discussed in detail in the Chapter F report (Faye 2008).

Water-Distribution System

Since March 1987, the Holcomb Boulevard WTP has provided finished water to the Holcomb Boulevard and Tarawa Terrace water-distribution systems (Figure I3). Consequently, it was necessary to develop calibrated models for both water-distribution systems that were reflective of present-day conditions using field data collected during the period May–October 2004 (Maslia et al. 2004, 2005; Sautner et al. 2005, 2007). For the purpose of the Chapter I report, more emphasis and detail are given to the discussion of the Tarawa Terrace water-distribution system. The Chapter J report (Sautner et al. In press 2009) provides additional details for both the Tarawa Terrace and Holcomb Boulevard water-distribution systems.

The public domain water-distribution system model, EPANET 2 (Rossman 2000), was used to simulate hydraulics and water-quality dynamics of the Tarawa Terrace and Holcomb Boulevard water-distribution systems (Sautner et al. 2005, 2007, In press 2009). Table I3 lists information used to characterize the present-day (2004) Tarawa Terrace and Holcomb Boulevard water-distribution systems for EPANET 2 model simulations. As described above, since 1987, the Holcomb Boulevard WTP has provided finished water to Tarawa Terrace ground-storage tank STT-39 (Figure I3). From a modeling perspective, however, Tarawa Terrace ground-storage tank STT-39 was modeled as the source of finished water for the Tarawa Terrace water-distribution system.

Based on expert peer review of using the water-distribution system modeling approach to simulate spatially distributed PCE concentrations (Maslia 2005) and exhaustive reviews of historical data—including water-supply well and WTP operational data when available—study staff concluded that the Tarawa Terrace WTP and water-distribution system

Table I2. Calibrated groundwater-flow and contaminant fate and transport model parameters, Tarawa Terrace and vicinity, U.S. Marine Corps Base Camp Lejeune, North Carolina.[1]

[ft/d, foot per day; d, day; in/yr, inch per year; g/ft^3, gram per cubic foot; ft, foot; ft^3/g, cubic foot per gram; g/d, gram per day; ft^2/d, square foot per day]

Model parameter[2]	Calibrated value	Method of assigning values
Groundwater-flow model parameters[3]		
Horizontal hydraulic conductivity, Layer 1, K_H (ft/d)	12.2–53.4	Distributed by cell
Horizontal hydraulic conductivity, Layer 2, K_H (ft/d)	1.0	Distributed by cell
Horizontal hydraulic conductivity, Layer 3, K_H (ft/d)	4.3–20.0	Distributed by cell
Horizontal hydraulic conductivity, Layer 4, K_H (ft/d)	1.0	Distributed by cell
Horizontal hydraulic conductivity, Layer 5, K_H (ft/d)	6.4–9.0	Distributed by cell
Horizontal hydraulic conductivity, Layer 6, K_H (ft/d)	1.0	Distributed by cell
Horizontal hydraulic conductivity, Layer 7, K_H (ft/d)	5.0	Distributed by cell
Leakance, $K_z / \delta z$ (1/d)	3.6×10^{-3}–4.2×10^{-1}	Distributed by cell
Infiltration (recharge), I_R (in/yr)	6.6–19.3	Constant annual value for layer 1; annual value varied by year (every 12 stress periods)
Specific yield, S_y	0.05	Constant for layer 1
Storage coefficient, S	4.0×10^{-4}	Constant for layers 2–7
Contaminant fate and transport model parameters[4]		
Bulk density, ρ_b (g/ft^3)	77,112	Constant for model
Longitudinal dispersivity, α_L (ft)	25	Constant for model
Distribution coefficient, K_d (ft^3/g)	5.0×10^{-6}	Constant for model
Effective porosity, n_E	0.2	Constant for model
Mass-loading rate, $q_s C_s$ (g/d)	1,200	[5]Single cell, constant for stress periods 25 to 408
Molecular diffusion, D^* (ft^2/d)	8.5×10^{-4}	Constant for model
Reaction rate, r (1/d)	5.0×10^{-4}	Constant for model

[1]Refer to the Chapter C report (Faye and Valenzuela 2007) for a discussion of groundwater-flow simulation; refer to the Chapter F report (Faye 2008) for a discussion of contaminant fate and transport simulation

[2]Symbolic notation used to describe model parameters obtained from Chiang and Kinzelbach (2001)

[3]MODFLOW-96 model code (Harbaugh and McDonald 1996) used to conduct groundwater-flow simulations

[4]MT3DMS model code (Zheng and Wang 1999) used to conduct contaminant fate and transport simulations

[5]Refer to Appendix I1 for month and year corresponding to stress period

were not interconnected with other water-distribution systems at Camp Lejeune (for example, Holcomb Boulevard) for any substantial time periods (greater than 2 weeks) during the period of interest to this study (1968–1985).[11] All water arriving at the Tarawa Terrace WTP was assumed to originate solely from Tarawa Terrace water-supply wells (Faye and Valenzuela 2007) and to be completely and uniformly mixed prior to delivery to residences of Tarawa Terrace through the network of water-distribution system pipelines and storage tanks. Accordingly, study staff concluded that a simple mixing model approach, based on the principles of continuity and conservation of mass (Masters 1998, Maslia et al. 2007), would provide a sufficient level of detail and accuracy to estimate monthly PCE concentrations at Tarawa Terrace. To test the appropriateness of this assumption, results of a simulation for December 1984 conditions based on using the mixing model and water-distribution system model approaches are listed in Table I4. These results demonstrate that after 7 days, the mixing model and the spatially derived EPANET 2 concentrations of PCE are equivalent—even at the furthest extent of the water-distribution system (Montford Point area, Figure I3). These results confirmed the decision to use the simple mixing model approach for estimating PCE concentrations in finished water delivered to the Tarawa Terrace housing area.

[11] The term "interconnection" is defined in this study as the continuous flow of water in a pipeline from one water-distribution system to another for periods exceeding two weeks. Pipelines constructed in 1984 and 1986 to the Holcomb Boulevard and Montford Point water-distribution systems, respectively, did connect to the Tarawa Terrace water-distribution system (Maslia et al. 2007). However, information and operational data are not available to document the continuous flow of water to and from these water-distribution systems. Therefore, the Holcomb Boulevard, Tarawa Terrace, and Montford Point water-distribution systems were assumed not to be interconnected for the purposes of the present study.

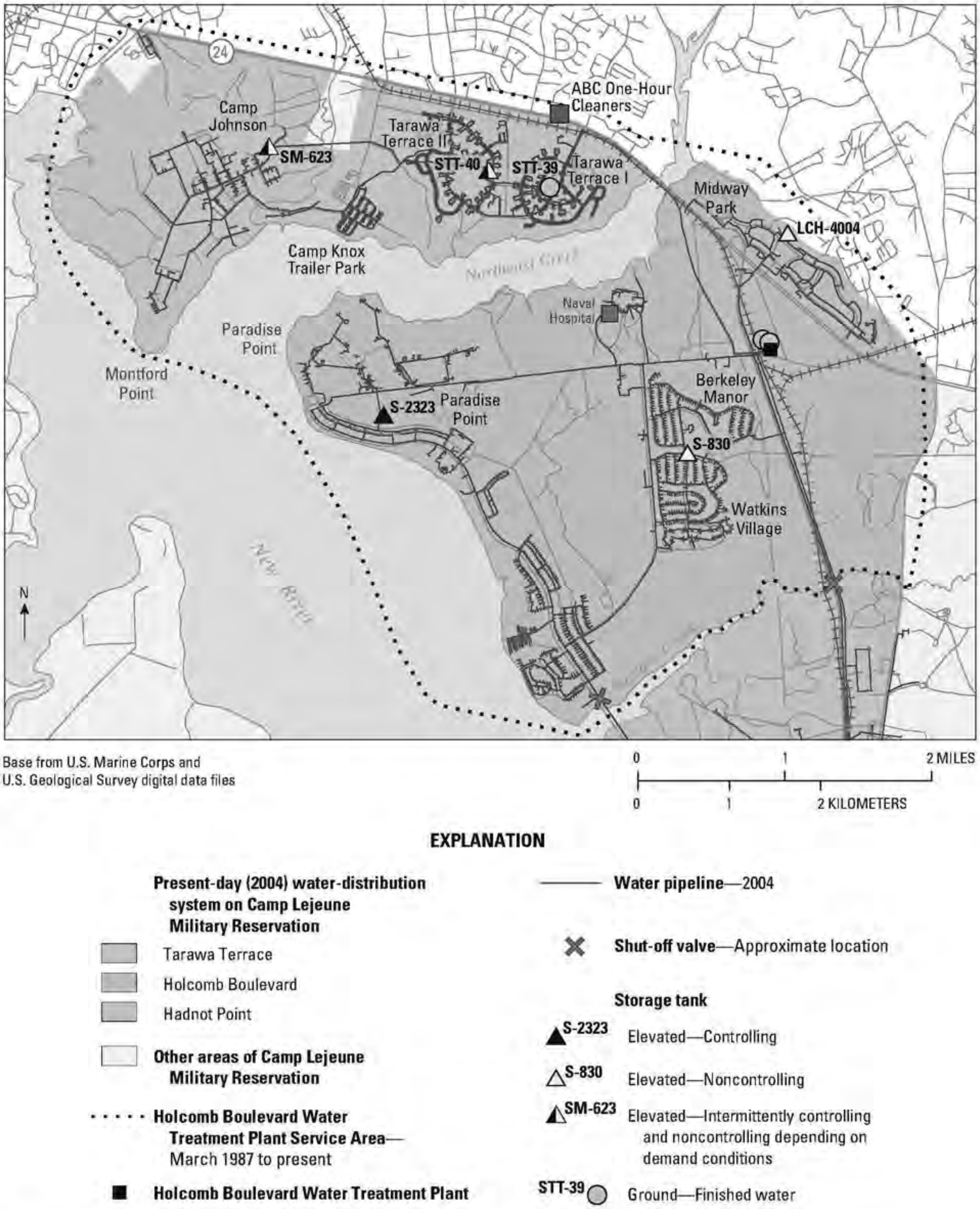

Figure I3. Location of present-day (2004) Tarawa Terrace and Holcomb Boulevard water-distribution systems, U.S. Marine Corps Base Camp Lejeune, North Carolina (modified from Maslia et al. 2007).

Table I3. Characterization of the Tarawa Terrace and Holcomb Boulevard present-day (2004) water-distribution systems for EPANET 2 model simulations, U.S. Marine Corps Base Camp Lejeune, North Carolina.[1, 2]

[ft, foot; mi, mile; PVC, polyvinyl chloride; %, percent; CI, cast iron; CU, copper; DI, ductile iron; AC, asbestos cement; gal, gallon; —, not applicable; WTP, water treatment plant]

Component	Water-distribution system	
	Tarawa Terrace	Holcomb Boulevard
Number of junctions or nodes	6,186	4,782
Number of pipelines	6,327	4,909
Total pipeline length	269,360 ft (51.0 mi)	386,813 ft (73.3 mi)
Pipeline diameter range	0.75–12 inches	0.75–24 inches
Pipeline material (percent of total length)	PVC (66.7%), CI (29.5%), CU (3.6%), DI (0.2%)	CI (67.3%), CU (20.8%), AC (7.1%), PVC (2.5%), DI (2.3%)
Number of storage tanks, type, and capacity[3]	3	[4]3
STT-39	ground; 250,000 gal	—
STT-40	elevated; 250,000 gal	—
SM-623	elevated; 150,000 gal	—
LCH-4004	—	elevated; 200,000 gal
S-830	—	elevated; 300,000 gal
S-2323	—	elevated; 200,000 gal

[1]See Figure I3 for water-distribution system locations

[2]EPANET 2 water-distribution system model (Rossman 2000)

[3]Storage tank STT-39 is supplied with finished water from the Holcomb Boulevard WTP and is modeled as the source water for the Tarawa Terrace water-distribution system

[4]Holcomb Boulevard finished water ground tanks are not modeled as part of the Holcomb Boulevard water-distribution system

Table I4. Simulated concentrations of tetrachloroethylene (PCE), derived from a mixing model and the EPANET 2 water-distribution system model, December 1984 conditions, Tarawa Terrace and vicinity, U.S. Marine Corps Base Camp Lejeune, North Carolina.[1]

[WTP, water treatment plant; TT, Tarawa Terrace]

Simulated PCE concentration, in micrograms per liter					
Mixing model[2] Tarawa Terrace WTP December 1984	EPANET 2 water-distribution system model[3]				
	Simulation time (days after 0:00 hours, December 1, 1984)	STT-40 (TT-II housing area)[4]	SM-623 (Camp Johnson)[4]	Camp Knox (trailer park housing area)	Montford Point area
173.0	0.25	173.0	0.0	0.0	0.0
	0.5	173.0	0.0	0.0	0.0
	0.75	173.0	172.0	0.0	0.0
	1	173.0	173.0	0.0	0.0
	2	173.0	173.0	159.8	23.7
	3	173.0	173.0	172.9	162.9
	4	173.0	173.0	173.0	167.9
	5	173.0	173.0	173.0	168.6
	6	173.0	173.0	173.0	172.4
	7	173.0	173.0	173.0	173.0
	14	173.0	173.0	173.0	173.0
	21	173.0	173.0	173.0	173.0
	28	173.0	173.0	173.0	173.0

[1]See Figure I3 for water-distribution system location

[2]Mixing model based on principles of continuity and conservation of mass (Masters 1998, Maslia et al. 2007); mixing model assumes constant concentration value on a monthly basis

[3]EPANET 2 water-distribution system model (Rossman 2000)

[4]STT-40 and SM-623 are the Tarawa Terrace and Camp Johnson elevated storage tanks, respectively

Sensitivity Analyses

Sensitivity analysis is a method used to ascertain the dependency of a given model output (for example, water level, hydraulic head, or concentration) upon model input parameters (for example, hydraulic conductivity, pumping rate, or mass loading rate). Thus, sensitivity analysis is the study of how the variations in the output of a model can be apportioned, qualitatively or quantitatively, to different sources of variation. Numerous methods are described in the literature for conducting a sensitivity analysis. One such method, referred to as the one-at-a-time design or experiment, is conducted by changing the values of input parameters of a calibrated model, one at a time; then, the variation of the output is measured (Saltelli et al. 2000). Results of sensitivity analyses are commonly reported as a metric such as an average measure of an output parameter difference; for example, the change in average PCE concentration at a particular location due to a 10-percent (%) change in the calibrated value of porosity. Another common metric is the root-mean-square, or *RMS*, which can be defined as the mean deviation of an output parameter (for example, PCE concentration) from the calibrated output parameter value by perturbing or modifying an input parameter value (for example, horizontal hydraulic conductivity). Because the calibrated model is assumed to be a reliable predictor of a given condition, quantifying model sensitivity to changes in certain parameters will help to assess the robustness of the model. Although sensitivity analysis has the limitation of weakly assessing the effect of simultaneous changes in input parameters, it is an important tool that can be used to identify essential parameters to be analyzed for a probabilistic analysis (Cullen and Frey 1999).

Groundwater-Flow and Contaminant Fate and Transport Models

For Tarawa Terrace groundwater-flow and contaminant fate and transport models, the following sensitivity analyses were conducted (Figure I2):

- input parameter sensitivity analysis,
- cell-size sensitivity analysis, and
- time-step size sensitivity analysis.

Input Parameter Sensitivity Analysis

For the Tarawa Terrace groundwater-flow and contaminant fate and transport models (Faye and Valenzuela 2007, Faye 2008), 18 input parameters were subjected to input parameter sensitivity analysis. The groundwater-flow model sensitivity analysis included 11 input parameters. These parameters were: horizontal hydraulic conductivity (K_H) for model layers 1–7, leakance ($K_Z/\Delta z$), infiltration (I_R), specific yield (S_y), and storage coefficient (S; Table I2).[12] Seven parameters were included in the sensitivity analysis of the contaminant fate and transport model. These were: bulk density (ρ_b), longitudinal dispersivity (α_L), distribution coefficient (K_d), effective porosity (n_E), mass-loading rate ($q_s C_s$), molecular diffusion coefficient (D^*), and reaction rate (r). For definitions of specific parameters relative to the groundwater-flow and contaminant fate and transport models, readers should refer to Harbaugh and McDonald (1996), Zheng and Wang (1999), Chiang and Kinzelbach (2001), Faye and Valenzuela (2007), and Faye (2008).

Five metrics were used to assess the sensitivity of groundwater-flow and contaminant fate and transport model parameters (Table I5): (1) relative change in duration (R_D) when finished water at the Tarawa Terrace WTP exceeded the current maximum contaminant level[13] (MCL) for PCE (5 micrograms per liter [μg/L]), (2) relative change in maximum concentration (R_C) when finished water at the Tarawa Terrace WTP exceeded the current MCL for PCE, (3) root-mean-square of concentration difference at water-supply wells and the WTP (*RMS*), (4) absolute mean relative change ($\overline{R}$), and (5) standard deviation of absolute mean relative change ($\sigma_{\overline{R}}$).[14] For the input parameter sensitivity analysis, the bases for all computations are the calibrated parameter values and resulting calibrated PCE concentrations in water-supply well TT-26 or the PCE concentration of finished water at the Tarawa Terrace WTP described in the Chapter A (Maslia et al. 2007), Chapter C (Faye and Valenzuela 2007), and Chapter F (Faye 2008) reports. Mathematical formulae and definitions for the aforementioned five metrics used to assess the sensitivity of model input parameters are listed in Table I5.

The perturbed duration (D_I^P) refers to the duration in months that finished water at the Tarawa Terrace WTP exceeded the current MCL for PCE of 5 μg/L. The perturbed

[12] Symbolic notation used to describe model parameters was obtained from PMWIN by Chiang and Kinzelbach (2001); leakance, identified as *VCONT* in PMWIN, is defined as follows:

$$VCONT = \frac{2}{\dfrac{\Delta v_k}{(K_Z)_{k,i,j}} + \dfrac{\Delta v_{k+1}}{(K_Z)_{k+1,i,j}}},$$

where $(K_Z)_{k,i,j}$ and $(K_Z)_{k+1,i,j}$ are the vertical hydraulic conductivity values of layers K and K+1, respectively, and Δv_k and Δv_{k+1} are the thicknesses of layers K and K+1, respectively.

[13] The maximum contaminant level (MCL) is a legal threshold limit set by the U.S. Environmental Protection Agency on the amount of a hazardous substance that is allowed in drinking water under the Safe Drinking Water Act; usually expressed as a concentration in milligrams or micrograms per liter. Effective dates for MCLs are as follows: trichloroethylene (TCE) and vinyl chloride (VC), January 9, 1989; tetrachloroethylene (PCE) and *trans*-1,2-dichloroethylene (1,2-tDCE), July 6, 1992 (40 CFR, Section 141.60, Effective Dates, July 1, 2002, ed.).

[14] The fourth and fifth metrics listed in Table I5, the absolute mean relative change ($\overline{R}$) and the standard deviation of absolute mean relative change ($\sigma_{\overline{R}}$), will be discussed in the "Probabilistic Analysis of Groundwater Flow and Contaminant Fate and Transport" section of this report.

Table I5. Mathematical formulae and definitions of metrics used to assess sensitivity of model parameters, Tarawa Terrace and vicinity, U.S. Marine Corps Base Camp Lejeune, North Carolina.

[WTP, water treatment plant; MCL, maximum contaminant level; PCE, tetracholorethylene; μg/L, microgram per liter]

Metric name and symbol	Mathematical formula	Definition of variables	Notes
Relative change in duration, in percent, R_D	$R_D=\frac{D_i^p-D_i^{cal}}{D_i^{cal}}\times 100\%$	D_i^p = perturbed duration in months using varied parameter i; D_i^{cal} = calibrated duration in months using calibrated parameter i	Duration refers to the number of months finished water at the WTP exceeded the MCL for PCE of 5 μg/L.
Relative change in maximum concentration, in percent, R_C	$R_C=\frac{C_i^p-C_i^{cal}}{C_i^{cal}}\times 100\%$	C_i^p = perturbed maximum concentration using varied parameter i; C_i^{cal} = calibrated maximum concentration using calibrated parameter i	Concentration refers to maximum simulated concentration of PCE in finished water at the WTP.
Root-mean-square of concentration difference, in μg/L, *RMS*	$RMS=\left[\frac{\sum_{i=1}^{N_{SP}}\left(C_{t_i}^p-C_{t_i}^{cal}\right)^2}{N_{SP}}\right]^{1/2}$	$C_{t_i}^p$ = perturbed concentration for stress period i; $C_{t_i}^{cal}$ = calibrated concentration for stress period i; N_{SP} = number of stress periods used to calculate *RMS*	Concentration refers to simulated concentration of PCE in finished water at the WTP. Number of stress periods (N_{SP}) equals 352 (November 1957–February 1987).
Absolute mean relative change, in percent, $\overline{R}$	$\overline{R}=\frac{\sum_{i=1}^{N_{SP}}\left\lvert\frac{C_{t_i}^p-C_{t_i}^{cal}}{C_{t_i}^{cal}}\right\rvert}{N_{SP}}\times 100\%$	$C_{t_i}^p$ = perturbed concentration for stress period i; $C_{t_i}^{cal}$ = calibrated concentration for stress period i; N_{SP} = number of stress periods used to calculate $\overline{R}$	Concentration refers to simulated concentration of PCE in finished water at the WTP. Number of stress periods (N_{SP}) equals 201 (January 1968–January 1985).[1]
Standard deviation of absolute mean relative change, in percent, $\sigma_{\overline{R}}$	$\sigma_{\overline{R}}=\left[\frac{\sum_{i=1}^{N_{SP}}\left(R_{C_i}-\overline{R}\right)^2}{N_{SP}-1}\right]^{1/2}$	R_{C_i} = relative change in concentration for stress period i, in percent; $\overline{R}$ = absolute mean relative change, in percent; N_{SP} = number of stress periods used to calculate $\sigma_{\overline{R}}$	Concentration refers to simulated concentration of PCE in finished water at the WTP. Number of stress periods (N_{SP}) equals 201 (January 1968–January 1985).[1]

[1]Number of stress periods excludes times when water-supply well TT-26 was not in service—July–August 1980 (stress periods 355–356) and January–February 1983 (stress periods 385–386)

duration was determined by using a model input parameter that was modified from the calibrated value of that parameter. (Refer to Table I2 for a listing of calibrated model input parameters and their values.) Similarly, the perturbed concentration (C_i^p) refers to the simulated maximum concentration in finished water at the Tarawa Terrace WTP that is in excess of the current MCL. Also note that the metric identified as the *RMS*, or root-mean-square, of concentration difference is referred to by some in the literature as the root-mean-square of error (Anderson and Woessner 1992). As used in the current analysis, the *RMS* provides an indication of the mean or average deviation from calibrated finished water concentrations. The smaller the deviation (that is, the closer the *RMS* value is to 0), the closer the value of the perturbed parameter is to the calibrated parameter value.

Table I6 is a list of results of the sensitivity analysis conducted using the relative change in duration and concentration metrics (R_D and R_C, respectively, in Table I5) for calibrated Tarawa Terrace groundwater-flow and contaminant fate and transport models. Results were obtained using the one-at-a-time method. Calibrated model parameters—with the exception of pumpage[15]—were multiplied by factors ranging from about 50% to 200% of their calibrated values. For example, horizontal hydraulic conductivity (K_H) for model layers 1–7 was varied by 90, 110, 150, and 250% of calibrated values; longitudinal dispersivity (α_L) was varied by 50, 90, 110, 200, and 400% of calibrated values. Thus, for example, for a calibrated

[15] Sensitivity to changes in pumpage values (that is, uncertainty and variation in the scheduling and operations of water-supply wells) is discussed in the "Probabilistic Analysis of Groundwater Flow and Contaminant Fate and Transport" section of this report and in the Chapter H report (Wang and Aral 2008).

Table I6. Relative change in duration and concentration metrics (R_D and R_C) computed as part of the sensitivity analysis of groundwater-flow and contaminant fate and transport model parameters, Tarawa Terrace and vicinity, U.S. Marine Corps Base Camp Lejeune, North Carolina.

[MCL, maximum contaminant level; µg/L, microgram per liter; ft/d, foot per day; —, not applicable; d, day; in/yr, inch per year; ft³/g, cubic foot per gram; ft, foot; g/ft³, gram per cubic foot; g/d, gram per day; ft²/d, square foot per day]

Model parameter[1]	Calibrated value	Ratio of varied to calibrated parameter value	Simulated tetrachloroethylene (PCE) concentrations in finished water at the water treatment plant[2]				
			Date first exceeding MCL[3]	Duration exceeding MCL, in months	Relative change in duration, in percent[4]	Maximum concentration, in µg/L[5]	Relative change in concentration, in percent[6]
Groundwater-flow model parameters							
Horizontal hydraulic conductivity, all layers, K_H (ft/d)	1.0–53.4	0.9	—[7]	—[7]	—[7]	—[7]	—[7]
		1.1	Sept. 1957	350	1.2	189	3.4
		1.5	Feb. 1957	359	3.8	202	10.2
		2.5	Apr. 1956	371	7.2	186	1.6
Horizontal hydraulic conductivity, layer 1, K_H (ft/d)	12.2–53.4	0.9	—[7]	—[7]	—[7]	—[7]	—[7]
		1.1	Aug. 1957	351	1.4	196	7.0
		1.5	Oct. 1956	365	5.5	223	22.0
		2.5	Oct. 1955	377	9.0	209	14.1
Horizontal hydraulic conductivity, layer 2, K_H (ft/d)	1.0	0.9	Nov. 1957	346	0.0	183	–0.1
		1.1	Nov. 1957	346	0.0	183	0.1
		1.5	Nov. 1957	346	0.0	184	0.4
		2.5	Oct. 1957	347	0.3	186	1.6
Horizontal hydraulic conductivity, layer 3, K_H (ft/d)	4.3–20.0	0.9	Oct. 1957	348	0.6	184	0.5
		1.1	Nov. 1957	345	–0.3	182	–0.5
		1.5	Feb. 1958	341	–1.4	179	–2.3
		2.5	July 1958	339	–2.0	187	2.1
Horizontal hydraulic conductivity, layer 4, K_H (ft/d)	1.0	0.9	Nov. 1957	346	0.0	183	0.3
		1.1	Nov. 1957	346	0.0	183	–0.3
		1.5	Nov. 1957	345	–0.3	181	–1.2
		2.5	Dec. 1957	343	–0.9	176	–3.6
Horizontal hydraulic conductivity, layer 5, K_H (ft/d)	6.4–9.0	0.9	Oct. 1957	347	0.3	185	1.2
		1.1	Nov. 1957	346	0.0	181	–1.0
		1.5	Jan. 1958	343	–0.9	176	–4.0
		2.5	Apr. 1958	339	–2.0	169	–7.9
Horizontal hydraulic conductivity, layer 6, K_H (ft/d)	1.0	0.9	Nov. 1957	346	0.0	183	0.0
		1.1	Nov. 1957	346	0.0	183	0.0
		1.5	Nov. 1957	346	0.0	183	–0.1
		2.5	Nov. 1957	346	0.0	182	–0.3
Horizontal hydraulic conductivity, layer 7, K_H (ft/d)	5.0	0.9	Nov. 1957	346	0.0	183	–0.1
		1.1	Nov. 1957	346	0.0	183	0.1
		1.5	Nov. 1957	345	–0.3	184	0.5
		2.5	Nov. 1957	345	–0.3	185	1.2
Leakance, $K_Z / \Delta z$ (1/d)	3.6×10^{-3}–4.2×10^{-1}	0.9	Nov. 1957	346	0.0	182	–0.3
		1.1	Oct. 1957	347	0.3	183	0.2
Infiltration (recharge), I_R (in/yr)	6.6–19.3	0.75	—[7]	—[7]	—[7]	—[7]	—[7]
		0.9	Nov. 1957	347	0.3	186	1.5
		1.1	Nov. 1957	345	–0.3	195	6.5
		1.25	Dec. 1957	343	–0.9	210	14.8
Specific yield, S_y	0.05	0.9	Nov. 1957	346	0.0	183	0.1
		1.1	Nov. 1957	346	0.0	183	0.0
		2.5	Nov. 1957	345	–0.3	183	–0.3
		5.0	Nov. 1957	344	–0.6	183	–0.1
		10.0	Nov. 1957	342	–1.2	182	–0.6
		20.0	Nov. 1957	338	–2.3	178	–2.6
Storage coefficient, S	4.0×10^{-4}	0.9	Nov. 1957	346	0.0	183	0.0
		1.1	Nov. 1957	346	0.0	183	0.0
		2.5	Nov. 1957	346	0.0	183	0.0
		5.0	Nov. 1957	346	0.0	183	–0.1
		10.0	Nov. 1957	346	0.0	183	–0.2
		20.0	Nov. 1957	346	0.0	182	–0.3

Table I6. Relative change in duration and concentration metrics (R_D and R_C) computed as part of the sensitivity analysis of groundwater-flow and contaminant fate and transport model parameters, Tarawa Terrace and vicinity, U.S. Marine Corps Base Camp Lejeune, North Carolina.—Continued

[MCL, maximum contaminant level; µg/L, micrograms per liter; ft/d, feet per day; in/yr, inch per year; ft³/g, cubic feet per gram; ft, feet; d, day; g/ft³, grams per cubic foot; g/d, grams per day; ft²/d, feet squared per day; —, not applicable]

Model parameter[1]	Calibrated value	Ratio of varied to calibrated parameter value	Simulated tetrachloroethylene (PCE) concentrations in finished water at the water treatment plant[2]				
			Date first exceeding MCL[3]	Duration exceeding MCL, in months	Relative change in duration, in percent[4]	Maximum concentration, in µg/L[5]	Relative change in concentration, in percent[6]
Contaminant fate and transport model parameters							
Distribution coefficient, K_d (ft³/g)	5.0x10⁻⁶	0.5	Apr. 1956	371	7.2	214	16.7
		0.9	July 1957	352	1.7	191	4.2
		1.1	Mar. 1958	338	–2.3	180	–1.8
		1.5	June 1959	310	–10.4	165	–10.0
		2.0	Dec. 1960	286	–17.3	143	–21.8
		4.0	Nov. 1972	143	–58.7	61	–66.5
Bulk density, ρ_b (g/ft³)	77,112	0.9	July 1957	352	1.7	191	4.2
		1.1	Mar. 1958	338	–2.3	180	–1.8
Effective porosity, n_E	0.2	0.5	Dec. 1956	363	4.9	349	90.9
		0.9	Sept. 1957	349	0.9	205	11.9
		1.1	Jan. 1958	340	–1.7	169	–7.7
		1.5	Oct. 1958	318	–8.1	124	–32.1
		2.0	Sept. 1959	301	–13.0	86	–53.0
Reaction rate, r (d⁻¹)	5.0x10⁻⁴	0.5	Oct. 1957	349	0.9	294	60.4
		0.9	Nov. 1957	347	0.3	199	8.6
		1.1	Nov. 1957	344	–0.6	171	–6.8
		1.5	Dec. 1957	335	–3.2	130	–29.1
		2.0	Jan. 1958	326	–5.8	94	–48.7
		4.0	July 1958	315	–9.0	30	–83.7
Mass-loading rate, $q_S C_S$ (g/d)[5]	1,200	0.5	May 1958	329	–4.9	92	–50.0
		0.9	Dec. 1957	343	–0.9	165	–10.0
		1.1	Oct. 1957	348	0.6	201	10.0
		1.5	Aug. 1957	351	1.4	275	50.0
		2.0	June 1957	353	2.0	366	100.0
Longitudinal dispersivity, α_L (ft)	25	0.5	Apr. 1958	337	–2.6	184	0.3
		0.9	Dec. 1957	344	–0.6	183	0.1
		1.1	Oct. 1957	348	0.6	183	–0.1
		2.0	Mar. 1957	356	2.9	181	–1.0
		4.0	June 1956	367	6.1	176	–3.7
Molecular diffusion coefficient, D^* (ft²/d)	8.5x10⁻⁴	0.9	Nov. 1957	346	0.0	183	0.0
		1.1	Nov. 1957	346	0.0	183	0.0
		5.0	Nov. 1957	346	0.0	183	–0.1
		10.0	Nov. 1957	346	0.0	183	–0.1
		20.0	Nov. 1957	346	0.0	182	–0.3

[1]Symbolic notation used to describe model parameters obtained from Chiang and Kinzelbach (2001)

[2]For calibrated model, date finished water at water treatment plant exceeded MCL for PCE is November 1957, duration of exceeding MCL is 346 months, and maximum PCE concentration is 183 µg/L—see Maslia et al. (2007, Table A12 and Appendix A2)

[3]Maximum contaminant level (MCL) for PCE is 5 µg/L

[4]Refer to Table I5 for mathematical formula and definition of relative change in duration (R_D)

[5]Concentration values rounded to three significant digits for reporting purposes; simulations conducted with concentration values containing six significant digits

[6]Refer to Table I5 for mathematical formula and definition of relative change in concentration (R_C)

[7]Dry wells simulated for this sensitivity analysis

value of K_H of 20 feet per day (ft/d) for model layer 1, a value used for the sensitivity analysis of 30 ft/d would yield a ratio of varied to calibrated K_H for model layer 1 of 30 ft/d divided by 20 ft/d, or 1.5 (Table I6).[16]

Measures of the effect of varying the groundwater-flow and contaminant fate and transport model parameters were quantified in terms of five computations listed in Table I6: (1) the date (month and year) when finished drinking water at the Tarawa Terrace WTP first exceeded the current MCL for PCE (5 μg/L), (2) the duration (in months) that finished drinking water at the WTP exceeded the current MCL, (3) the relative change in these durations (percent) caused by varying the calibrated parameter values (R_D in Table I5), (4) the maximum PCE concentration in finished water at the Tarawa Terrace WTP, and (5) the relative change (percent) in the maximum concentration (R_C in Table I5). For calibrated model input parameters, the date that the PCE in finished water at the WTP first exceeded the current MCL was simulated as November 1957; the duration that finished water exceeded the MCL for PCE was 346 months; and the maximum concentration of PCE was 183 μg/L (Maslia et al. 2007, Figure A18 and Table A12; Faye 2008). Results of the sensitivity analysis show that some parameters are insensitive to change, even when varied by factors of 10 and 20. For example, large changes in specific yield (S_y), storage coefficient (S), and molecular diffusion (D^*) (ratios of 10:1 and 20:1, Table I6) resulted in very little change in simulated results—less than 3% change in relative duration or concentration. Changes in other parameters, such as horizontal hydraulic conductivity (K_H) for model layer 1 and infiltration (I_R), that were less than the calibrated value (for example, a ratio of varied to calibrated value of 0.9) resulted in wells going dry during the groundwater-flow simulation process.[17] Generally, increasing or decreasing a calibrated parameter value by 10% (ratio of varied to calibrated parameter value of 0.9–1.1) resulted in changes of 6 months or less to the date that finished water first exceeded the MCL for PCE (5 μg/L).

Results of selected sensitivity analyses listed in Table I6 also are shown graphically in Figure I4. Results are shown in terms of date on the abscissa and simulated PCE concentrations at water-supply well TT-26 or in finished water at the Tarawa Terrace WTP on the ordinate. Review of the graphical sensitivity analysis results indicates that horizontal hydraulic conductivity (K_H) for model layer 1 is the most sensitive groundwater-flow model input parameter and that reaction rate (r) is the most sensitive contaminant fate and transport model input parameter. Other model input parameters, such as those for the contaminant fate and transport model—effective porosity (n_E), mass-loading rate ($q_S C_S$), and distribution coefficient (K_d)—also show significant sensitivity (also refer to Table I6). Using the graphs in Figure I4 to make qualitative comparisons between the groundwater-flow and contaminant fate and transport model parameters, the following observations can be made:

- overall, simulated results of the contaminant fate and transport model are significantly more sensitive to changes in parameter values relative to calibrated values than simulated results of the groundwater-flow model, and
- sensitivity of groundwater-flow model parameters appears to be greater during early years of simulation (prior to about 1960) compared to the sensitivity of fate and transport model parameters which appear to indicate greater sensitivity subsequent to 1960.

The diminished sensitivity of groundwater-flow model simulation results compared to corresponding results of the contaminant fate and transport model is possibly related to the number and temporal distribution of field data used for model calibration. Although limited, field data for K_H, I_R, pumpage, and water levels were available for groundwater-flow model development and calibration. By comparison, parameter values assigned to the contaminant fate and transport model were obtained largely from literature-reported values, and concentration data were sparse and available only between 1985 and 1991 (Faye 2008, Table F13). Thus, part of the contaminant fate and transport model sensitivity may be attributed strictly to numerical properties because input parameter values were not specifically calibrated against measured field-derived or laboratory-derived properties unique to Tarawa Terrace and vicinity.

The *RMS* computations of concentration differences are listed in Table I7. Results of the sensitivity analysis using the *RMS* metric were computed using simulated concentrations during the period November 1957–February 1987 (stress periods 83–434, or 352 stress periods; Appendix I1). November 1957 represents the date when the concentration of finished water at the Tarawa Terrace WTP first exceeded the current MCL for PCE of 5 μg/L, based on calibrated model simulations (Maslia et al. 2007, Faye 2008). February 1987 represents the date when all Tarawa Terrace water-supply wells were removed from continuous operation (Faye and Valenzuela 2007, Maslia et al. 2007). The *RMS* metric provides additional confirmation that horizontal hydraulic conductivity (K_H) for model layer 1 and infiltration (I_R) are by far the most sensitive groundwater-flow model input parameters. Note that as the sensitivity of a model input parameter increases, its deviation from an *RMS* value of 0.0 also increases. Furthermore, the sensitivity of the groundwater-flow model to changes in K_H for all model layers is primarily driven by the sensitivity to the change in the K_H value for model layer 1. For example, an increase of 10% from the calibrated

[16] The terms factor, ratio, and percent may be used inconsistently in the literature. For the purposes of this report, they are defined according to the following example: a calibrated value of 10 and a perturbed value of 15 are related by a factor of 1.5, a ratio of 1.5:1, 150%, or an increase of 50%.

[17] When a well goes dry during a groundwater-flow simulation, the simulation process is halted and concentrations cannot be computed from that time forward. As a consequence, sensitivity analysis metrics also cannot be computed (Table I6).

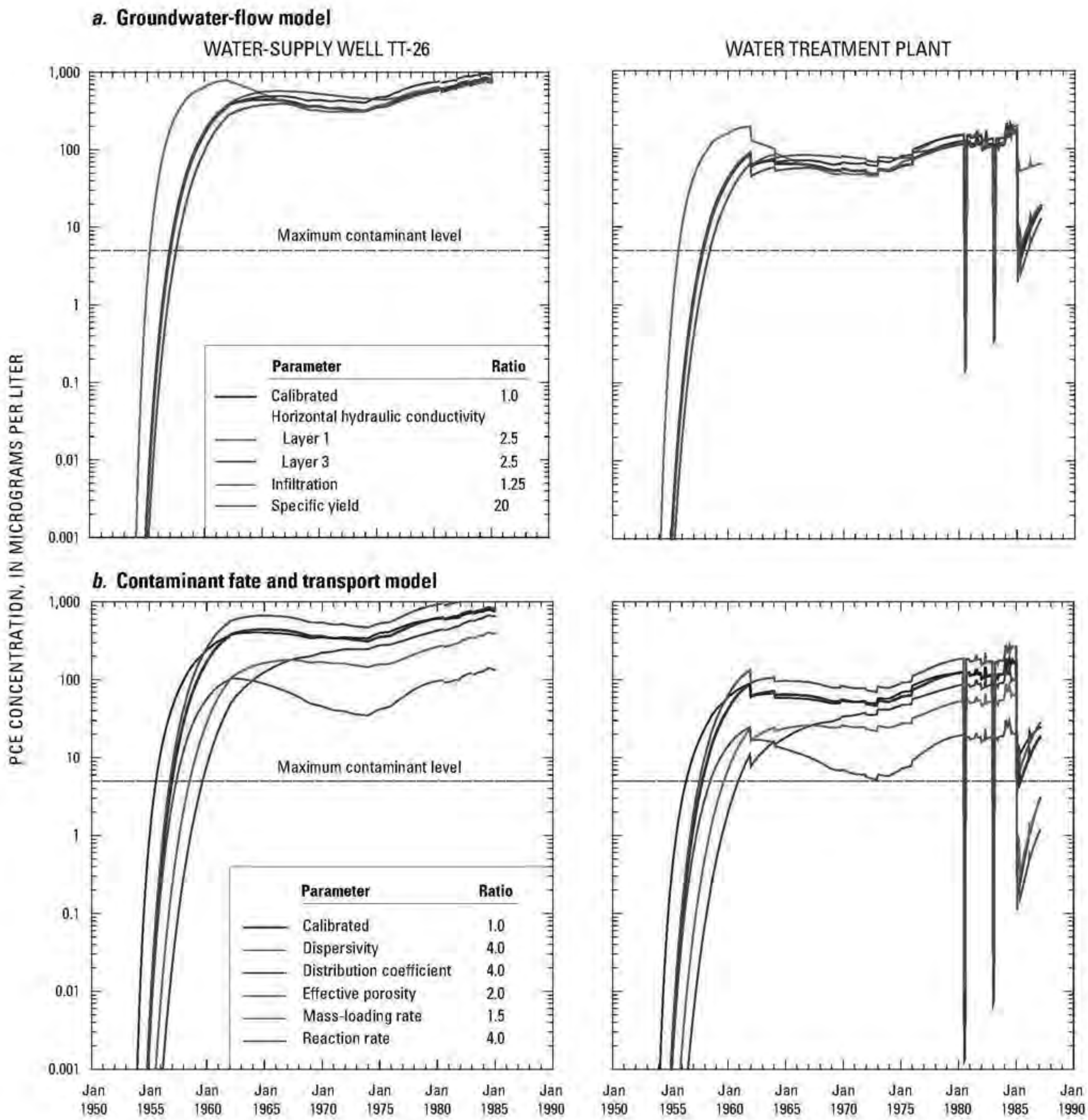

Figure I4. Sensitivity of simulated tetrachloroethylene concentration to changes in model parameter values: *(a)* groundwater-flow model and *(b)* contaminant fate and transport model, Tarawa Terrace, U.S. Marine Corps Base Camp Lejeune, North Carolina. [PCE, tetrachloroethylene]

Table I7. Root-mean-square of concentration difference in finished water at the water treatment plant computed as part of sensitivity analysis of groundwater-flow and contaminant fate and transport model parameters, Tarawa Terrace and vicinity, U.S. Marine Corps Base Camp Lejeune, North Carolina.[1]

[*RMS*, root-mean-square; μg/L[3], microgram per cubic liter; ft/d, foot per day; —, not applicable; d, day; in/yr, inch per year; g/ft³, gram per cubic foot; ft, foot; ft³/g, cubic foot per gram; g/d, gram per day; ft²/d, square foot per day]

Model parameter[2]	Ratio of varied to calibrated parameter value	*RMS* difference, in μg/L[3]
Horizontal hydraulic conductivity, all layers, K_H (ft/d)	0.9	—[4]
	1.1	3.312
	1.5	13.99
	2.5	26.87
Horizontal hydraulic conductivity, layer 1, K_H (ft/d)	0.9	—[4]
	1.1	5.184
	1.5	22.34
	2.5	47.72
Horizontal hydraulic conductivity, layer 2, K_H (ft/d)	0.9	0.062
	1.1	0.060
	1.5	0.294
	2.5	1.587
Horizontal hydraulic conductivity, layer 3, K_H (ft/d)	0.9	0.888
	1.1	0.847
	1.5	3.861
	2.5	9.378
Horizontal hydraulic conductivity, layer 4, K_H (ft/d)	0.9	0.227
	1.1	0.225
	1.5	1.108
	2.5	3.203
Horizontal hydraulic conductivity, layer 5, K_H (ft/d)	0.9	1.110
	1.1	0.983
	1.5	4.054
	2.5	8.847
Horizontal hydraulic conductivity, layer 6, K_H (ft/d)	0.9	0.042
	1.1	0.043
	1.5	0.207
	2.5	0.597
Horizontal hydraulic conductivity, layer 7, K_H (ft/d)	0.9	0.240
	1.1	0.232
	1.5	1.087
	2.5	2.719
Leakance, $K_z/\Delta z$ (1/d)	0.9	0.814
	1.1	0.689
Infiltration (recharge), I_R (in/yr)	0.75	—[4]
	0.9	6.466
	1.1	6.306
	1.25	15.17
Specific yield, S_y	0.9	0.089
	1.1	0.088
	2.5	1.261
	5.0	3.251
	10.0	7.1025
	20.0	14.53
Storage coefficient, S	0.9	0.003
	1.1	0.004
	2.5	0.049
	5.0	0.130
	10.0	0.289
	20.0	0.602
Bulk density, ρ_b (g/ft³)	0.9	5.358
	1.1	4.953
Longitudinal dispersivity, α_L (ft)	0.5	2.589
	0.9	0.463
	1.1	0.440
	1.5	2.000
	2.0	3.596
	4.0	7.754
Distribution coefficient, K_d (ft³/g)	0.5	30.16
	0.9	5.358
	1.1	4.953
	1.5	21.00
	2.0	34.77
	4.0	64.70
Effective porosity, n_E	0.5	52.15
	0.9	8.017
	1.1	7.151
	1.5	29.11
	2.0	46.54
Mass-loading rate, q_sC_s (g/d)	0.5	39.38
	0.9	7.877
	1.1	7.877
	1.5	39.38
Molecular diffusion, D^* (ft²/d)	0.9	1.7×10^{-3}
	1.1	1.8×10^{-4}
	1.5	8.7×10^{-3}
	5	6.9×10^{-2}
	10	1.6×10^{-1}
	20	3.3×10^{-1}
Reaction rate, r (d^{-1})	0.5	35.54
	0.9	5.905
	1.1	5.419
	1.5	23.09
	2.0	38.59
	4.0	66.13

[1] *RMS* metric computed for simulation period of November 1957–February 1987 (stress periods 83–434; total of 352 stress periods)

[2] Symbolic notations used to describe model parameters obtained from Chiang and Kinzelbach (2001)

[3] Refer to Table I5 for mathematical formula and definition of root-mean-square of concentration difference

[4] Dry wells simulated for this sensitivity analysis

value of K_H (that is, a ratio of 1.1) results in an *RMS* value of about 5.2 µg/L for model layer 1 and 3.3 µg/L for all model layers combined. This result is compared to an *RMS* value of less than 1 for all other individual model layers. With the exception of the aforementioned model parameters of K_H and I_R, groundwater-flow model input parameters are relatively insensitive to changes from their calibrated values.

The *RMS* metric computed for contaminant fate and transport model parameters indicates that the reaction rate (r), distribution coefficient (K_d), effective porosity (n_E), and mass-loading rate ($q_S C_S$) are most sensitive to changes in calibrated parameter values with calculated *RMS* values exceeding 20 µg/L for a varied to calibrated input parameter ratio of 1.5. The *RMS* values for other contaminant fate and transport model parameters (for example, α_L and D^*) are much lower, and some are near a value of 0.0.

Selected sensitivity analysis results computed using the *RMS* of concentration differences metric (Table I7) are shown graphically in Figures I5 and I6. The value of 100% on the abscissa and a value of 0 on the ordinate of these figures indicate the calibrated model parameter value (Table I6). Figure I5 shows the sensitivity for changes in horizontal hydraulic conductivity (K_H) for all model layers combined and for each model layer modified independently. Results indicate a high degree of sensitivity to changes in K_H for model layer 1. In addition, the sensitivity to change in K_H for model layer 1 apparently accounts for the overall sensitivity to K_H for all layers combined. Furthermore, results shown in Figure I5 indicate that the groundwater-flow model is insensitive to input parameter value changes in K_H for model layers 2, 4, 6, and 7. Note, for K_H values of less than 100% of calibrated values, water-supply wells were simulated as dry (also see Tables I6 and I7). Simulations were halted once a water-supply well was simulated as dry, and subsequent concentrations were not simulated.

Figure I6 shows *RMS* concentration differences plotted for selected groundwater-flow (other than K_H) and contaminant fate and transport model parameters as they were varied from calibrated values (*RMS* = 0 and percentage of calibrated value = 100%). Groundwater-flow and contaminant fate and transport model input parameters indicating less sensitivity to

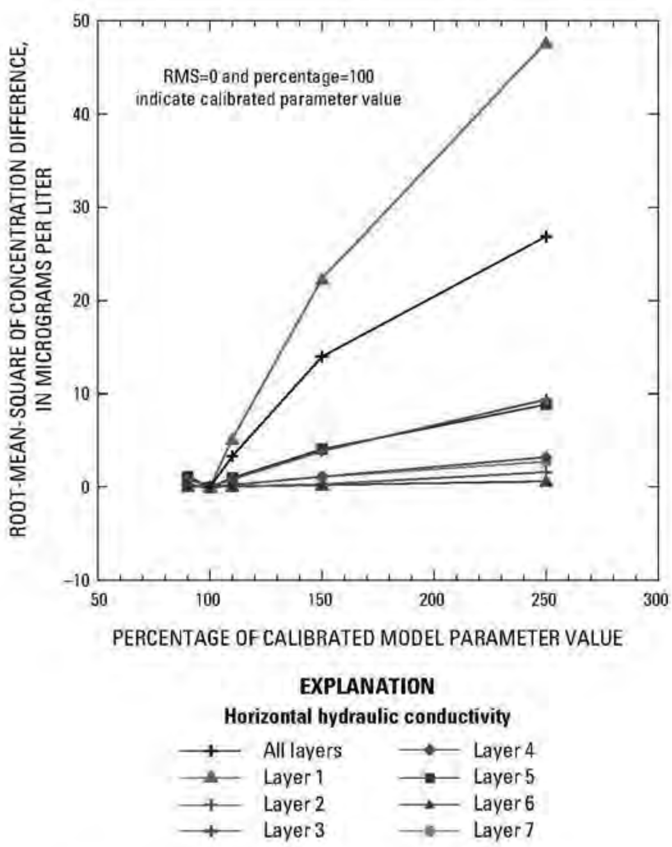

Figure I5. Sensitivity analysis results for horizontal hydraulic conductivity for all model layers in terms of root-mean-square (*RMS*) of concentration difference in finished water at the water treatment plant, Tarawa Terrace, U.S. Marine Corps Base Camp Lejeune, North Carolina.

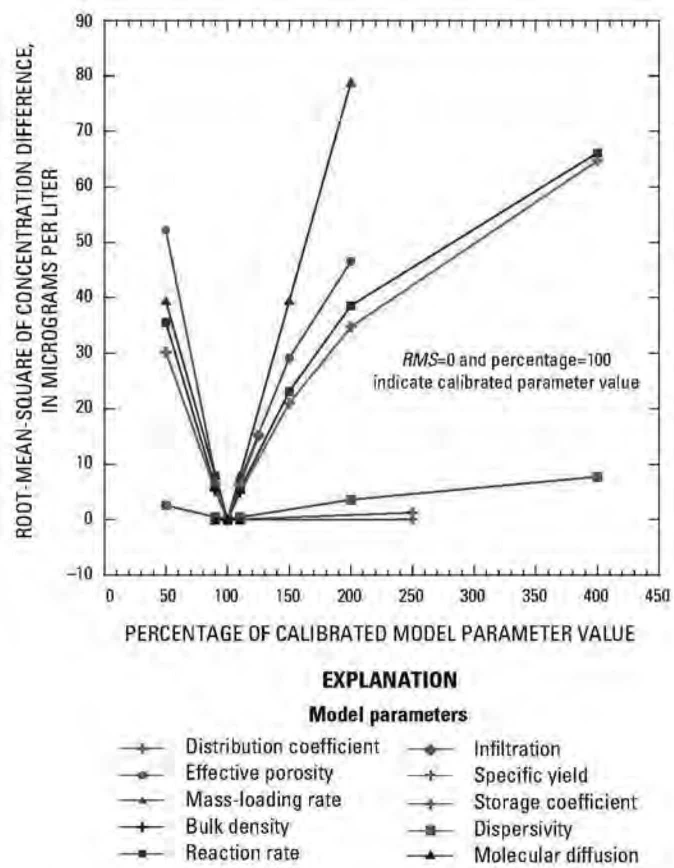

Figure I6. Sensitivity analysis results for groundwater-flow and contaminant fate and transport model parameters in terms of root-mean-square (*RMS*) of concentration difference in finished water at the water treatment plant, Tarawa Terrace, U.S. Marine Corps Base Camp Lejeune, North Carolina.

change from calibrated values are storage coefficient (S), specific yield (S_y), longitudinal dispersivity (α_L), and molecular diffusion (D^*). Parameters indicating a relatively high degree of sensitivity to change from calibrated values are distribution coefficient (K_d), reaction rate (r), effective porosity (n_E), and mass-loading rate (q_sC_s).

In summary, the aforementioned one-at-a-time sensitivity analyses are limited with respect to assessing the effect of simultaneous changes in multiple model input parameters. However, the sensitivity analysis did identify essential parameters that should be included in enhanced analyses (K_H, I_R, K_d, n_E, r, and q_sC_s). The variability and uncertainty of these and other model input parameters (pumpage, ρ_b, and α_L) are described in detail in the "Probabilistic Analysis of Groundwater Flow and Contaminant Fate and Transport" section of this report.

Cell-Size Sensitivity Analysis

A sensitivity analysis was conducted to determine if the finite difference cell size of 50 ft per side, which was used for the calibrated groundwater-flow and contaminant fate and transport models (Faye and Valenzuela 2007, Faye 2008), was appropriate in terms of simulating the water level in a pumping well when compared to a smaller cell size. For this analysis, a refined model grid consisting of a smaller cell size was used in the areas surrounding water-supply wells and the contaminant source (Figure I7). The cell dimensions of the refined grid were 25 ft along each cell side. Figure I7 shows the location of the calibrated model grid (50-ft cells) and the refined model grid (25-ft cells). The refined model grid is located within the rectangular area bounded by cells at row and column coordinates 36 and 151, respectively, and 112 and 191, respectively.[18] Water levels simulated using the refined model grid (25-ft cells) were compared to simulated water levels in well TT-26 using the grid of the calibrated model (50-ft cells). Comparisons were made for January 1952, November 1957, January 1968, and March 1987 (Figure I8). The graphs in Figure I8 show that water levels simulated using the refined and calibrated model grids (50-ft and 25-ft cells, respectively) are nearly identical. For example, during January 1952, the simulated water level in well TT-26 using the calibrated model grid was –18.3 ft (Faye and Valenzuela 2007); for the refined model grid, the simulated water level was –14.6 ft (Figure I8*a*). Thus, sensitivity to a 50% reduction in cell dimension (75% reduction in cell area) throughout much of the active model domain is apparent only at cells where pumpage is assigned. The difference in simulated water levels at these cells is small compared to total simulated drawdown. Simulated differences (maximum of 3.7 ft [Figure I8]) are well within the transient model calibration target range of ±12 ft (Faye and Valenzuela 2007).

[18] Cell coordinates are defined by a row, column designation for each model layer. In this case, coordinates for two cells that bound a rectangular area of 25-ft cells have been defined as follows (Figure I7): upper left or northwestern corner, row 36, column 151; lower right or southeastern corner, row 112, column 191.

Time-Step Size Sensitivity Analysis

When conducting fate and transport simulations, numerical instability related to inappropriate temporal discretization (that is, time-step size) is minimized when the Courant number (C) equals 1.0 or less. The Courant number is defined as:

$$C = \frac{V\Delta t}{\Delta l}, \tag{1}$$

where

C = Courant number, [L^0];
V = simulated groundwater-flow velocity, [LT^{-1}];
Δt = stress-period length or time-step size, [T]; and
Δl = a characteristic length, [L].[19]

The characteristic length of finite-difference numerical models is typically related to grid cell dimensions. The MODFLOW-96 and MT3DMS models applied to Tarawa Terrace and vicinity are uniform at 50 ft per side (Faye and Valenzuela 2007, Faye 2008). Therefore, the characteristic length, Δl, becomes the length of the cell side or the distance between two adjacent cell centroids (50 ft). To minimize and control oscillations of the numerical solution resulting from the temporal discretization, Daus and Frind (1985) indicate that the Courant number (C) should be less than or equal to 1. For the Tarawa Terrace models, the stress periods were equal to the number of days in a month (that is, 28, 29, 30, or 31). Except in the immediate vicinity of water-supply wells, groundwater-flow velocities ranged between 0.01 and 1.0 ft/d (Faye and Valenzuela 2007, Faye 2008). Thus, applying Equation 1 to the Tarawa Terrace models yields the following values for Courant numbers:

$$\begin{gathered} \frac{0.01 \times 28}{50} \le C \le \frac{1.0 \times 31}{50} \\ 0.006 \le C \le 0.6 \end{gathered} \tag{2}$$

This demonstrates that for the Tarawa Terrace models, the Courant number was less than 1 throughout the entire active model domain except in the immediate vicinity of operating water-supply wells.

In the immediate vicinity of operating water-supply wells, velocities were simulated as great as 8 ft/d (Faye and Valenzuela 2007, Faye 2008). Substituting this value of velocity into Equations 1 and 2 results in a maximum-value Courant number of about 5; this number could cause numerical oscillations leading to inaccurate simulated concentrations. To assess the effect of numerical oscillations caused by an inappropriate time discretization (that is, too large of a time step), contaminant fate and transport simulations were conducted by assigning 1-day stress periods ($\Delta t = 1$) to the calibrated Tarawa Terrace contaminant fate and transport

[19] L represents length units; T represents time units; L^0 indicates a dimensionless variable.

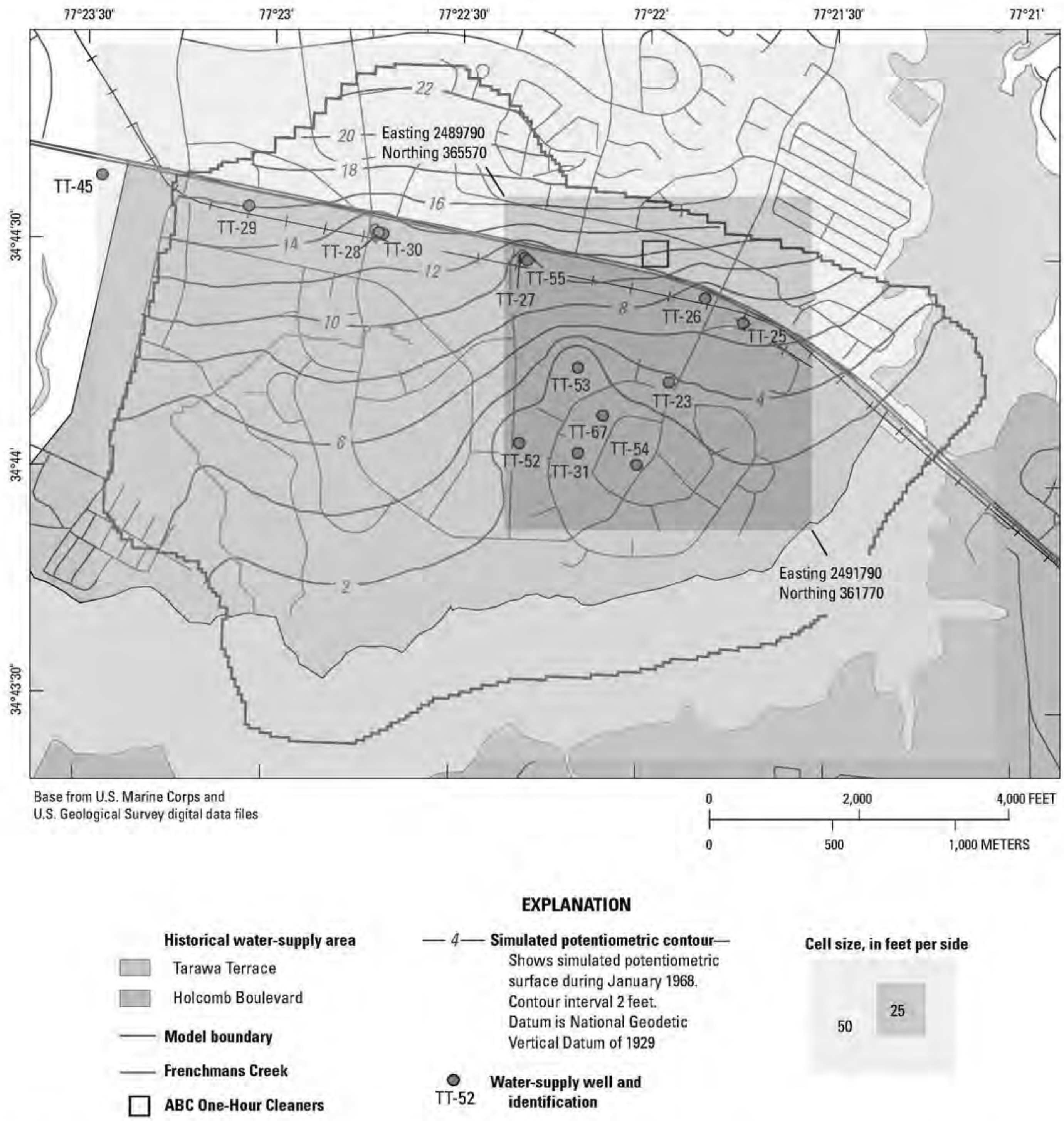

Figure I7. Location of model grids containing cell dimensions of 50 feet per side and 25 feet per side used to conduct cell-size sensitivity analysis, Tarawa Terrace and vicinity, U.S. Marine Corps Base Camp Lejeune, North Carolina.

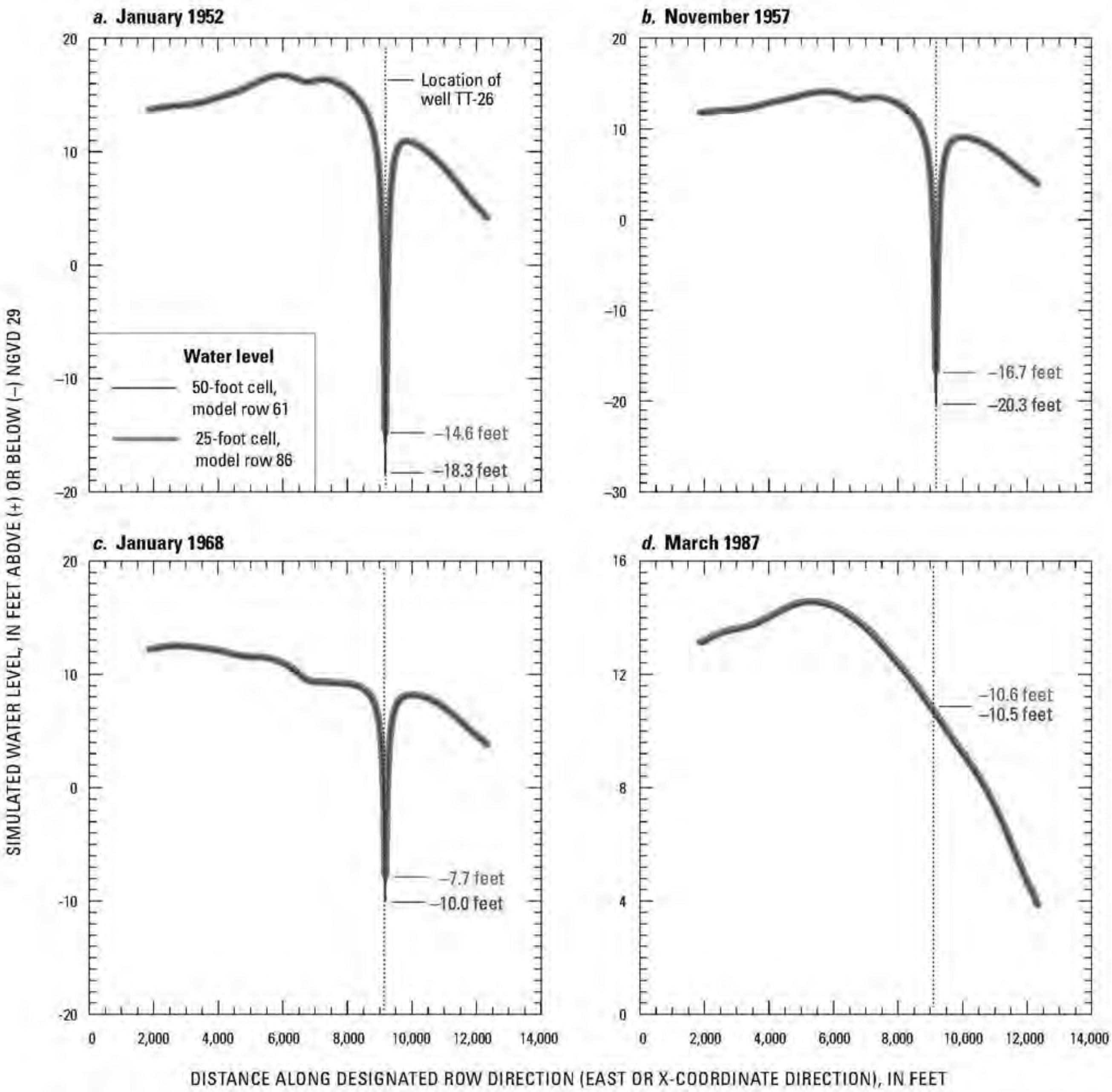

Figure I8. Simulated water levels along designated model row containing water-supply well TT-26 using finite-difference cell dimensions of 50 feet per side and 25 feet per side during: *(a)* January 1952, *(b)* November 1957, *(c)* January 1968, and *(d)* March 1987, Tarawa Terrace and vicinity, U.S. Marine Corps Base Camp Lejeune, North Carolina. [NGVD 29, National Geodetic Vertical Datum of 1929]

model from November 1, 1984 to January 31, 1985. Pumpage assigned to these months in the calibrated model (Faye and Valenzuela 2007) was assigned to every day of each respective month for the time-step sensitivity analysis. Comparisons of calibrated (30- and 31-day time steps) and simulated (1-day time step) concentrations of PCE for the days of November 30, 1984, December 31, 1984, and January 31, 1985 for water-supply wells TT-23 and TT-26 are listed in Table I8. These results show that the relative absolute difference in simulated PCE concentrations at water-supply wells TT-23 and TT-26 between the 1-day time step and the 30- and 31-day time steps is typically less than a tenth of 1 percent and that simulated concentrations at these wells are similar to three or four significant digits. Thus, PCE concentrations simulated by the Tarawa Terrace contaminant fate and transport model were clearly unaffected by numerical oscillations caused by inappropriate temporal discretization.

Water-Distribution System Model

Calibration of the Tarawa Terrace and Holcomb Boulevard water-distribution system models was accomplished in two stages: (1) a trial-and-error stage wherein model parameters were changed within reasonable limits and simulation results were compared to field data (hydraulic heads and tracer concentrations) and (2) a parameter estimation stage using the advanced parameter estimation tool PEST (Doherty 2005). Final calibration was achieved using parameter estimation to test the sensitivity of simulated hydraulic heads to several model input model parameters. Details of the modeling effort and the collection of field data used to support model calibration are described in Sautner et al. (2005, 2007), Grayman et al. (2006), and in Chapter J of the Tarawa Terrace report series (Sautner et al. In press 2009). The locations of pipelines, storage tanks, and field-test monitoring equipment for the Tarawa Terrace and Holcomb Boulevard water-distribution systems are shown in Figure I9.

During the trial-and-error stage, simulated results varied depending on: (1) which storage-tank model was used to account for mixing within storage tanks (see section on "Storage-Tank Mixing"), (2) the friction factor assigned to pipes with the distribution network (C-factor value), and (3) the pattern of demand imposed on the water-distribution system by water users. These model inputs, individually and in combination, significantly affected the heads simulated in several storage tanks located within the Tarawa Terrace and Holcomb Boulevard water-distribution systems (see Figure I9 for location of storage tanks STT-40, S-2323, S-830, and LCH-4004). Heads simulated in the storage tanks determine, to a large degree, the distribution of hydraulic head within the network and thus, the quality of calibration of the water-distribution system models. Sensitivity tests using parameter estimation methods were used to determine the optimum combination of tank mixing model, C-factors, and demand patterns that minimized the difference between simulated and observed hydraulic head.

Table I8. Comparisons of calibrated groundwater concentrations of tetrachloroethylene (PCE) using 30- and 31-day time steps with simulated groundwater concentrations using a 1-day time step, Tarawa Terrace and vicinity, U.S. Marine Corps Base Camp Lejeune, North Carolina.

Site name	Stress period	Date	Simulated elapsed time, in days	Simulated PCE, in grams per cubic foot[1]		Simulated PCE, in micrograms per liter[1]		Absolute relative difference, in percent[2]
				$\Delta t = 30$ or 31 days	$\Delta t = 1$ day	$\Delta t = 30$ or 31 days	$\Delta t = 1$ day	
TT-23	407	Nov. 30, 1984	12,388	0.0071823	0.0071840	253.3	253.4	0.02
	408	Dec. 31, 1984	12,419	0.0072117	0.0072149	254.4	254.5	0.04
	409	Jan. 31, 1985	12,450	0.0072000	0.0071987	254.0	253.9	0.02
TT-26	407	Nov. 30, 1984	12,388	0.0229735	0.0229851	810.4	810.8	0.05
	408	Dec. 31, 1984	12,419	0.0227652	0.0227989	803.0	804.2	0.15
	409	Jan. 31, 1985	12,450	0.0227541	0.0227619	802.6	802.9	0.03

[1]Simulated PCE concentrations for $\Delta t = 30$ or $\Delta t = 31$ days are from calibrated fate and transport model described in Faye (2008)

[2]Absolute relative difference ($|R_c|$) of simulated PCE concentration at water-supply wells defined as:

$$|R_C| = \frac{C_{cal} - C_{\Delta t=1}}{C_{\Delta t=1}} \times 100\%,$$

where C_{cal} is the calibrated PCE concentration simulated using a time-step size of 30 or 31 days and $C_{\Delta t=1}$ is the PCE concentration simulated using a time-step size of 1 day

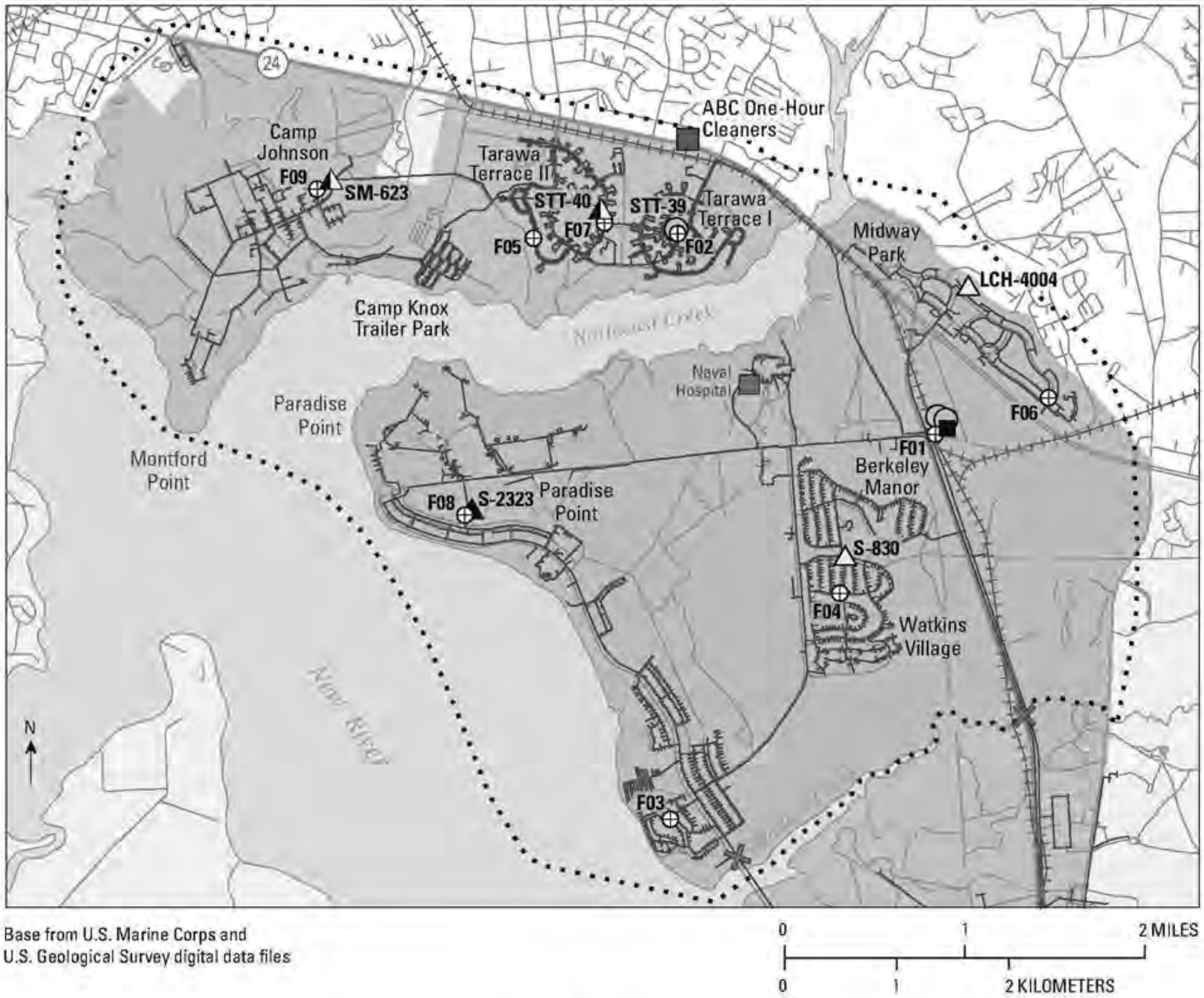

Base from U.S. Marine Corps and
U.S. Geological Survey digital data files

EXPLANATION

Present-day (2004) water-distribution system on Camp Lejeune Military Reservation
- Tarawa Terrace
- Holcomb Boulevard
- Hadnot Point

Other areas of Camp Lejeune Military Reservation

Holcomb Boulevard water treatment plant service area—March 1987 to present

Holcomb Boulevard water treatment plant

Water pipeline—2004

Shut-off valve—Approximate location

F03 **Fluoride logger and number**—CRWQME

Storage tank
- S-2323 Elevated—Controlling
- S-830 Elevated—Noncontrolling
- SM-623 Elevated—Intermittently controlling and noncontrolling depending on demand conditions
- STT-39 Ground—Finished water

Figure I9. Locations of continuous recording water-quality monitoring equipment (CRWQME; F01–F09) and present-day (2004) Tarawa Terrace and Holcomb Boulevard water-distribution systems used for conducting a fluoride tracer test, September 22–October 12, 2004, U.S. Marine Corps Base Camp Lejeune, North Carolina (from Maslia et al. 2007).

Storage-Tank Mixing[20]

Storage tanks and reservoirs commonly are used in water-distribution systems to provide emergency water supply for fire fighting and pumping outages in addition to equalizing pumping requirements and operating pressures. Poor mixing in finished water tanks can worsen water-quality conditions in a distribution system. Studies of storage tanks can generally be grouped into three areas: (1) monitoring and sampling, (2) physical-scale modeling, and (3) mathematical modeling. For the purpose of the current study, a subset of mathematical models—simplified input/output representations, referred to as "system models"—were used. Detailed discussions of the different classifications of storage tanks, field-test methods, experimental methods, and analyses can be found in the following references: Grayman and Clark (1993), Kennedy et al. (1993), Boulos et al. (1996), Grayman et al. (1996), Rossman and Grayman (1999), Roberts and Tian (2002), Grayman et al. (2004), Roberts et al. (2005), and Sautner et al. (2007).

When applied to water-distribution systems, system models use highly conceptual empirical relationships to represent mixing in tanks and reservoirs. These system models have been used to represent tanks that operate in the fill-and-drain mode or with continuous inflow and outflow and include complete mixing (CSTR), multi-compartment models, such as two-compartment mixing (2-COMP), first-in, first-out (FIFO) plug flow, and last-in, first-out (LIFO) plug flow. System models are typically used to simulate substances that are conservative or decay according to first-order functions. Water age also can be simulated with system models. System models are easily integrated into hydraulic and water-quality models of distribution systems such as EPANET 2. The four storage-tank mixing models are described in detail by Clark and Grayman (1998) and in the EPANET 2 Users Manual (Rossman 2000). Conceptual diagrams of the four EPANET 2 storage-tank mixing models are shown in Figure I10.

To characterize and understand water-supply areas and the water-distribution systems serving base housing at Camp Lejeune, ATSDR conducted a series of field tests during 2004. These tests were hydraulic (pressure and flow) and water-quality (tracer) tests. Tracer tests consisted of injecting calcium chloride and sodium fluoride into the distribution system and turning WTP fluoride feeds off and on. Test details are described in Maslia et al. (2004, 2005) and Sautner et al. (2005, In press 2009). During initial tracer injection activities (May 2004), water in some storage tanks apparently did not mix completely or uniformly. It was not logistically possible to monitor the internal mixing patterns of the Camp Lejeune storage tanks. Therefore, in subsequent field tests, controlling storage tanks (Figure I9) were equipped with continuous recording water-quality monitoring equipment (CRWQME). The CRWQME was connected to the inlet and outlet of the storage tanks, so that fill and drain patterns of the storage tanks could be continuously recorded and monitored. Storage-tank monitoring occurred at 15-minute (min) intervals. A schematic diagram and photographs showing a typical CRWQME installation at a controlling storage tank is shown in Figure I11. Based on this storage-tank field monitoring design, the CRWQME was expected to capture continuous fill and drain sequences of the storage tank during the tracer test.

[20] Assessment of storage-tank mixing models was originally published by Sautner et al. (2007).

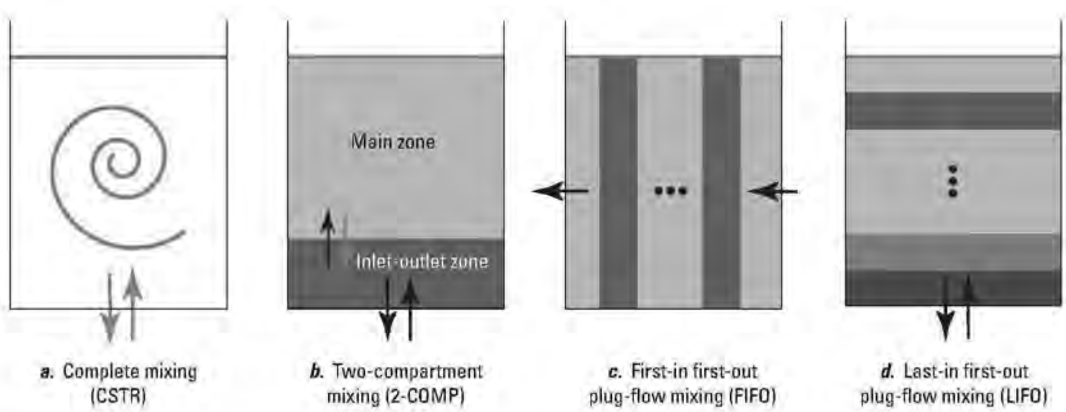

Figure I10. Storage-tank mixing models analyzed using test data gathered during a tracer test of the Tarawa Terrace and Holcomb Boulevard water-distribution systems, September 22–October 12, 2004, U.S. Marine Corps Base Camp Lejeune, North Carolina. [Storage-tank mixing models from Rossman 2000]

Hydraulic and water-quality extended period simulations (EPS) of tracer tests were accomplished using the EPANET 2 water-distribution system model software. Detailed descriptions of tracer-test methodology and the tracer tests conducted on the Tarawa Terrace and Holcomb Boulevard water-distribution systems are provided in Maslia et al. (2004, 2005) and Sautner et al. (2005, 2007, In press 2009). Four types of storage-tank mixing models were analyzed using the tracer-test data and the EPANET 2 software. These were: CSTR, 2-COMP, FIFO, and LIFO. A sensitivity analysis approach was used to assess which of the conceptual system storage-tank models was most appropriate for conceptualizing mixing in the Tarawa Terrace and Holcomb Boulevard storage tanks based on data gathered during the tracer test of September 22–October 12, 2004.

Water-quality simulations were conducted by using the collected tracer-test data for source locations (F01 and F02, Figure I9) and the four mixing model options contained in EPANET 2 (Figure I10). The simulations were used to assess characteristics of mixing models and their effect on water-quality dynamics during the simulation. For the Tarawa Terrace water-distribution system, simulation results compared with measured data for controlling storage tank SM-623 (Camp Johnson tank, monitoring location F09; Figure I9) are shown in Figure I12. The four graphs show EPANET 2 simulations using the four storage-tank mixing model types—CSTR, 2-COMP, FIFO, and LIFO—and measured fluoride tracer data. For all simulations, hydraulic and water-quality simulation time steps were 5 and 2 minutes, respectively. For the two-compartment mixing model (2-COMP), it was assumed that the ratio of the first compartment to total tank volume was 1:10 (0.1).

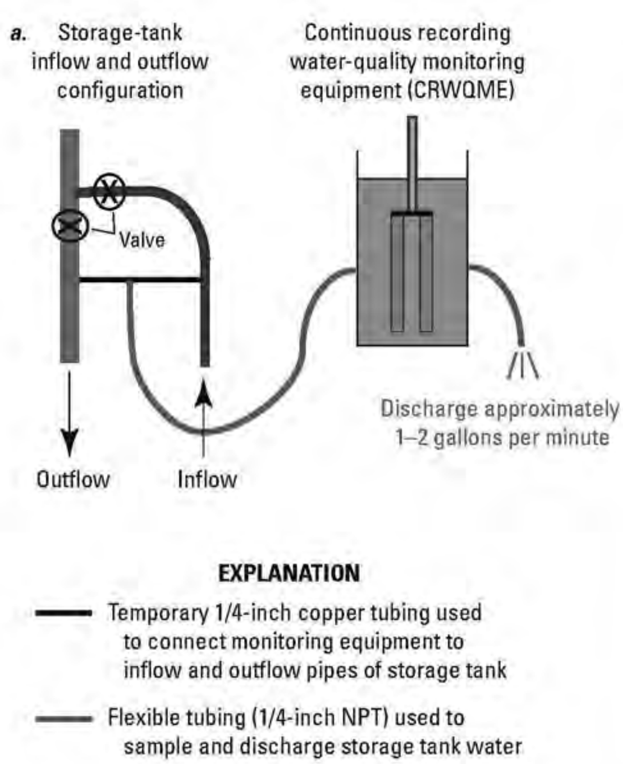

b.

c.

Figure I11. Method of connecting CRWQME to controlling storage tank: *(a)* schematic diagram, *(b)* photograph of connection to elevated storage tank SM-623, and *(c)* photograph of housing containing CRWQME and discharge tube, and staff person from U.S. Marine Corps Environmental Management Division. [See Figure I9 for location of storage tank SM-623; from Sautner et al. 2007; NPT, National Pipe Thread]

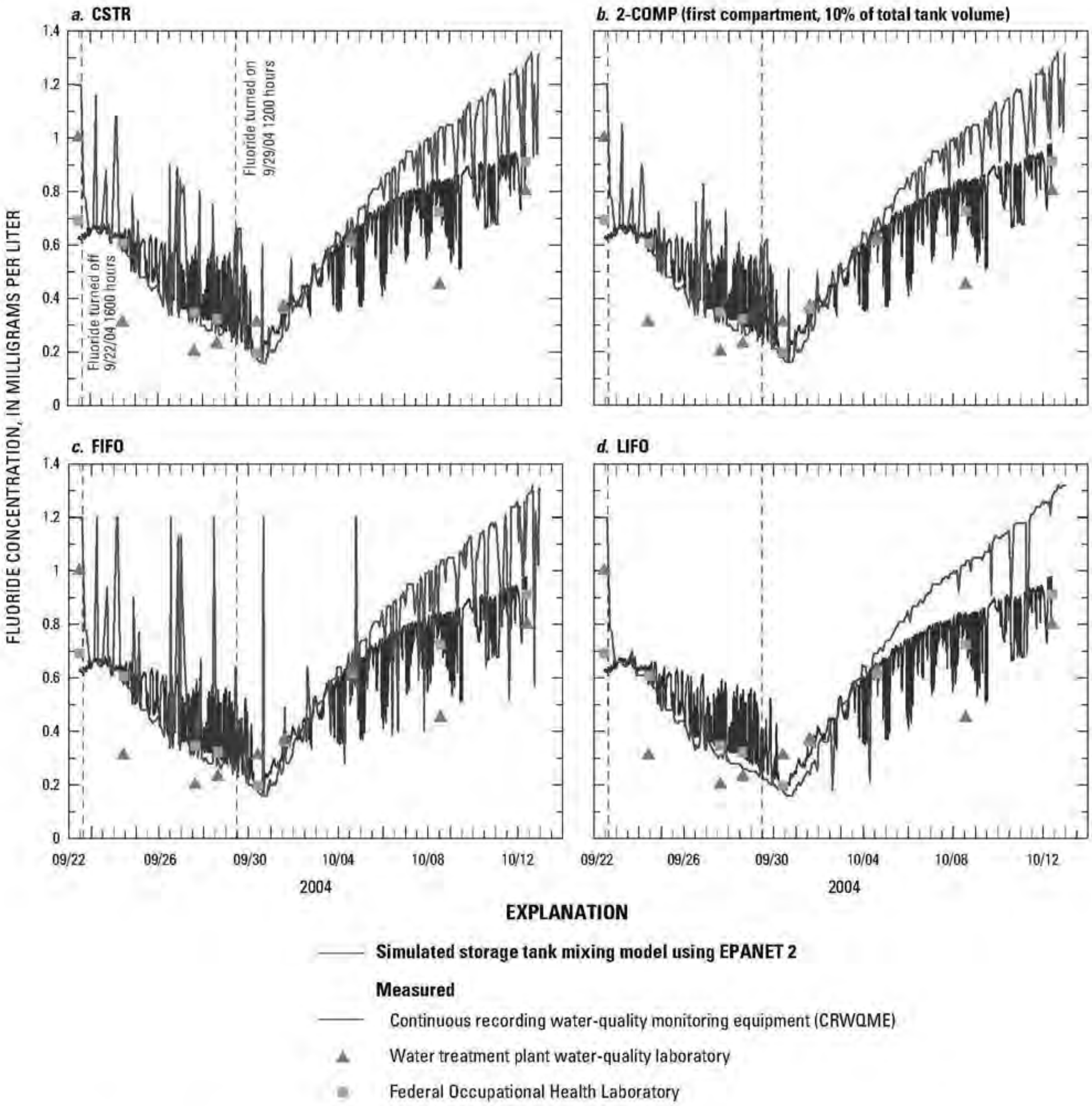

Figure I12. Storage-tank mixing model simulated fluoride concentrations and measured data for storage tank SM-623 (Camp Johnson elevated): *(a)* complete mixing (CSTR), *(b)* two-compartment (2-COMP), *(c)* first-in, first-out plug flow (FIFO), and *(d)* last-in, first-out plug flow (LIFO), September 22–October 12, 2004, Tarawa Terrace water-distribution system, U.S. Marine Corps Base Camp Lejeune, North Carolina. [Refer to Figure I9 for location of storage tank SM-623]

For the Holcomb Boulevard water-distribution system, simulation results compared with measured data for controlling tank S-2323 (Paradise Point tank, monitoring location F08; Figure I9) are shown in Figure I13. The four graphs also show EPANET 2 simulations using the four mixing model types and measured fluoride tracer data. The same hydraulic and water-quality time and storage-tank parameters used for the Tarawa Terrace simulation were used for the Holcomb Boulevard simulation.

The sensitivity analysis results shown in Figures I12 and I13, using the EPANET 2 results comparing the four storage-tank models—CSTR, 2-COMP, FIFO, and LIFO—with measured data indicate that the choice of mixing model does make a difference. For example, at both elevated storage tanks (SM-623 and S-2323), the FIFO model results show very sharp "spikes" indicating—unrealistically—that mixing is not occurring during the simulation. Alternatively, the LIFO models seem to "dampen out" the fluctuations in

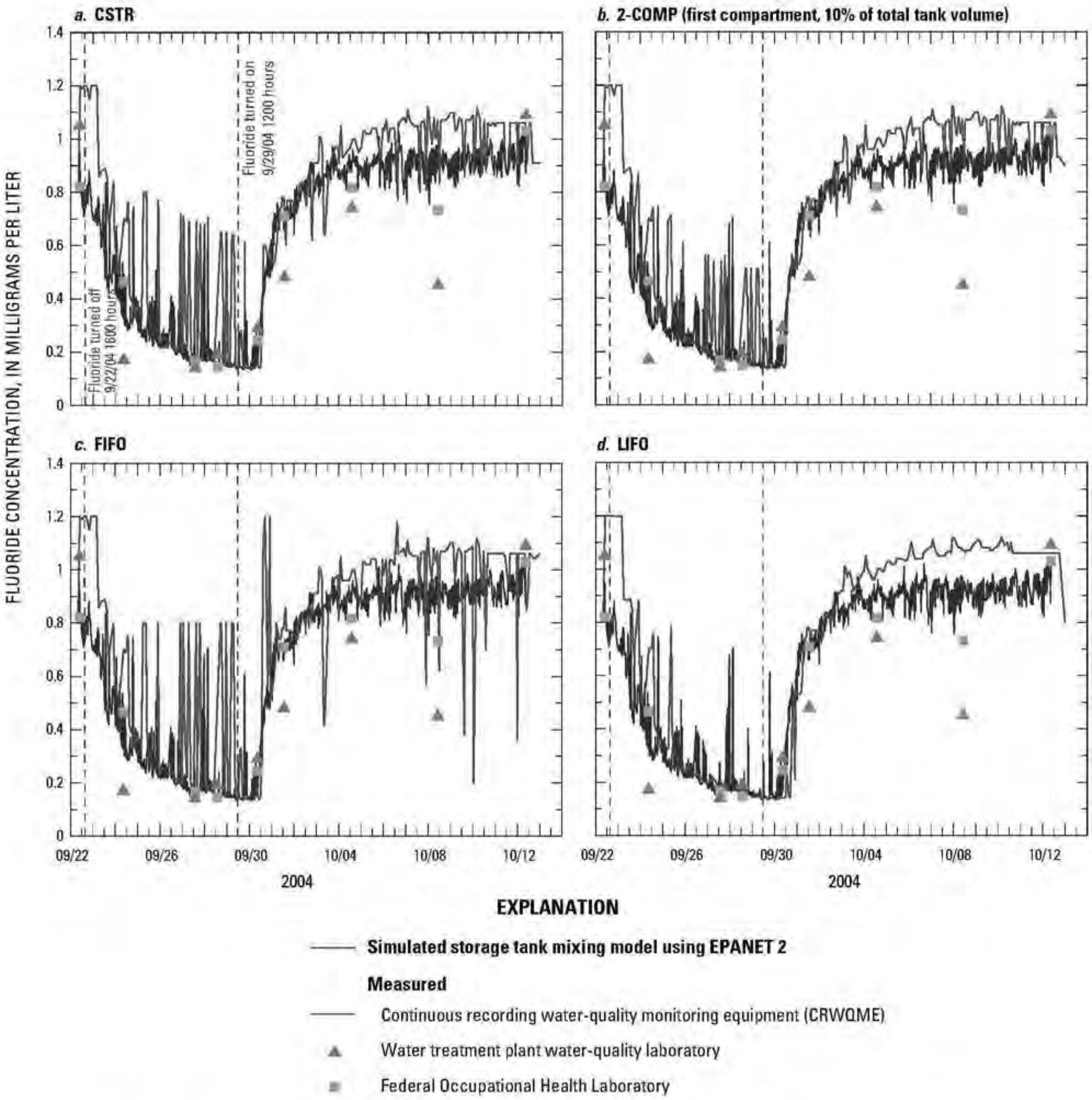

Figure I13. Storage-tank mixing model simulated fluoride concentrations and measured data for storage tank S-2323 (Paradise Point elevated): *(a)* complete mixing (CSTR), *(b)* two-compartment (2-COMP), *(c)* first-in first-out plug flow (FIFO), and *(d)* last-in first-out plug flow (LIFO), September 22–October 12, 2004, Holcomb Boulevard water-distribution system, U.S. Marine Corps Base Camp Lejeune, North Carolina. [Refer to Figure I9 for location of storage tank S-2323]

fluoride concentration. Based on these analyses and recorded and measured data, the LIFO storage-tank mixing model was used to represent storage-tank mixing in the calibrated Tarawa Terrace and Holcomb Boulevard water-distribution systems.

Finally, comparison of simulation results and CRWQME data at both of the aforementioned elevated storage tanks indicate that better overall matches are achieved for the Paradise Point storage tank (S-2323, location F08 in Figure I9) than for the Camp Johnson storage tank (SM-623, location F09 in Figure I9). One reason may be the water-quality dynamics associated with the monitoring location identified as the source condition for each water-distribution system. Monitoring data for the Holcomb Boulevard source (location F01 in Figure I9) indicate a significantly sharper front than do data for the Tarawa Terrace source (location F02 in Figure I9), which are characterized by a more subdued and attenuated concentration (fluoride tracer) front.

Parameter Estimation and Sensitivity Analysis Using PEST

Numerous methods have been developed to assess the sensitivity of a model to a set of input parameters. Examples of such approaches are the one-at-a-time approach, which is used for testing sensitivity of groundwater-flow and contaminant fate and transport model input parameters, and the alternative conceptual model approach, which is used to assess the effect of selecting different storage-tank model conceptualizations for water-distribution systems. Another method for estimating and assessing the sensitivity of model parameters is referred to as linear and nonlinear parameter estimation. This approach allows for more complex parameterizations than would be possible using trial-and-error calibration and the one-at-a-time sensitivity analysis. Additional information describing linear and nonlinear parameter estimation is provided in Cooley (1977, 1979, 1985) and Hill and Tiedman (2007). One of the most advanced parameter estimation packages (models) available for environmental simulation is called PEST—an acronym for Parameter ESTimation (Doherty 2005). The advantage of using this modeling package is that PEST, a nonlinear parameter estimator, exists independently of any specific model (for example, EPANET 2, MODFLOW-96, or MT3DMS), yet can be used to estimate parameters of interest for any model whether it is a simple analytical model or a complex numerical code. PEST accomplishes this by taking control of an existing model code (for example, EPANET 2) and running it many times until an optimal set of parameters is obtained that minimizes the differences between model-generated numbers and corresponding measured data (for example, simulated and measured hydraulic head). Thus, PEST was chosen to assist with the calibration and sensitivity analysis of parameters contained in the EPANET 2 model that was applied to the Tarawa Terrace and Holcomb Boulevard water-distribution systems. Details relative to parameter values and the calibration procedure for the EPANET 2 model applied to the Tarawa Terrace and Holcomb Boulevard water-distribution system are provided in Chapter J of the Tarawa Terrace report series (Sautner et al. In press 2009).

Two groups of model input parameters were analyzed using the PEST code: (1) pipe material roughness coefficients (C-factors) and (2) demand-pattern factors. PEST, in combination with EPANET 2, was used to assess which parameters required adjustment during the calibration process and to automate the calibration of the water-distribution models for Tarawa Terrace and Holcomb Boulevard (instead of using a manual trial-and-error method for model calibration). The objective function minimized by PEST is the sum of the squared differences between measured and simulated storage-tank hydraulic head. Definitions of the aforementioned model input parameters and of hydraulic head are provided below.

- Pipe material roughness coefficient (C-factor)—also known as the Hazen-Williams C-factor; represents a pipe carrying capacity. Higher C-factors represent smoother pipes (for example, polyvinyl chloride [PVC]), and lower C-factors represent rougher pipes (for example, cast iron [CI]) (Walski et al. 2001).
- Demand-pattern factor—a set of multipliers that scale base demand (consumption) distributed at locations throughout the water-distribution system network (Boulos et al. 2006). For a 24-hour diurnal pattern, a demand-pattern factor is generally assigned to each hour of the 24-hour pattern.
- Storage-tank hydraulic head—the sum of the water level in a storage tank and the elevation of the bottom of the storage tank. Water levels in storage tanks are recorded at certain time intervals (for example, 15 min), most often using a supervisory control and data acquisition (SCADA) system. Thus, as part of the calibration process for the water-distribution system model, an attempt is made to minimize the difference between measured and simulated storage-tank hydraulic head.

The PEST model requires three types of input files: (1) template files, identified with the suffix *ptf*, (2) instruction files, identified with the suffix *pinsf*, and (3) a control file, identified with the suffix *pst*. Using these three file types, PEST generates additional files during the course of a simulation. All of these files are provided on the compact disc read-only memory (CD–ROM) containing the PEST files for the Tarawa Terrace and Holcomb Boulevard simulations included with this report. For details pertaining to the construction of the PEST file types and running the PEST model, readers should refer to the PEST users manual (Doherty 2005).

Pipe material roughness coefficient, or Hazen-Williams C-factor value, varies depending on parameters and conditions such as pipe material, age, roughness, and diameter. Typical values for C-factors are provided in numerous water-distribution system modeling texts such as Walski (1992) and Cesario (1995). For the Tarawa Terrace and Holcomb Boulevard water-distribution systems, initial C-factor values for CI and PVC pipes were estimated as 94 and 145, respectively (Table I9). These values were obtained from typical C-factor values provided in Walski (1992) and Cesario (1995) for CI and PVC pipe. The result of the PEST simulation produced similar C-factor values for CI and PVC pipe of 83 and 149, respectively (Table I9). The PEST analysis for C-factor also indicates that the water-distribution system model is relatively insensitive to C-factor, with PEST-computed sensitivities in the range of 10^{-4} to 10^{-5}. The *RMS* of hydraulic head difference also was computed by PEST using measured water levels from storage tank STT-40. In this situation, the *RMS* was computed to be 0.06 ft using initial C-factor values and also using values derived from the PEST analysis. Based on the small PEST-computed sensitivities and no change in *RMS* of hydraulic head difference, the initial estimates for values of C-factor—94 for CI pipe and 145 for PVC pipe—were used in all EPANET 2 model simulations.

The PEST results summarized in Table I9 also indicate that the model is about an order of magnitude more sensitive

Table I9. Initial estimates and PEST-derived C-factor values, Tarawa Terrace water-distribution system, U.S. Marine Corps Base Camp Lejeune, North Carolina.

[C-factor, pipe material roughness coefficient]

Pipe material	C-factor (initial estimate)[1]	PEST-derived values[2]			
		C-factor	95-percent confidence interval	Sensitivity	Relative sensitivity
Cast iron (CI)	94	83	78–88	5.365×10^{-5}	4.442×10^{-3}
Polyvinyl chloride (PVC)	145	149	147–151	1.564×10^{-4}	2.335×10^{-2}

[1]Inital C-factor values derived from water-balance analysis and values described in Walski (1992) and Cesario (1995) for CI and PVC pipes

[2]See PEST Users Manual (Doherty 2005) for details pertaining to use and implementation of the PEST model

to C-factor value for pipes constructed of PVC than for pipes constructed of CI—computed relative sensitivities of about 2.3×10^{-2} for PVC pipe C-factor and about 4.4×10^{-3} for CI pipe C-factor. To further emphasize this finding, a series of simulations were conducted for the Tarawa Terrace water-distribution system using C-factors for PVC pipe that varied from 120 to 180, while keeping the C-factor for CI pipe constant at a value of 94. Another series of simulations were conducted using C-factors for CI pipe that varied from 70 to 120, while keeping the C-factor for PVC pipe constant at a value of 145.[21] Results of these simulations are shown in Figure I14 by plotting C-factor value versus the sum of hydraulic head difference squared for storage tank STT-40. These results clearly demonstrate that the water-distribution system model is significantly more sensitive to changes in PVC pipe C-factor value than to changes in CI pipe C-factor value. For the Tarawa Terrace water-distribution system, total length of PVC pipe is 179,747 ft compared with a total length of CI pipe of 79,405 ft.

The Tarawa Terrace and Holcomb Boulevard water-distribution system models were initially constructed using a single (or global) demand pattern that was determined from a water-balance analysis derived from information and data contained in a water-conservation analysis conducted by ECG, Inc. (1999). Examples of the initial estimated demand factors for a 4-day period—September 23–26, 2004—from a tracer test conducted September 22–October 12, 2004, are shown in Figure I15.[22] A complete hourly listing of the numerical values of the initial demand-pattern factors for the duration of the tracer test (September 22–October 12, 2004) is provided in Appendix I2. PEST was used to derive optimized demand-pattern factors using information and data from the aforementioned tracer test of the Tarawa Terrace and Holcomb Boulevard water-distribution systems. To derive the optimized demand-pattern factors, measured water levels in storage tanks STT-40, S-830, S-2323, and LCH-4004 (Figure I9) were obtained from the Camp Lejeune SCADA system. These water levels were used to compute hydraulic heads from which comparisons were made against simulated hydraulic heads (Figure I16). Simulated hydraulic heads were derived by using the EPANET 2 water-distribution system modeling software.

In PEST, the objective function to be minimized is the sum of the squared differences between measured and simulated hydraulic head. Table I10 lists the *RMS* and correlation coefficient for simulated hydraulic heads derived from the water-balance analysis and from PEST for the four aforementioned storage tanks. Overall, the PEST-derived

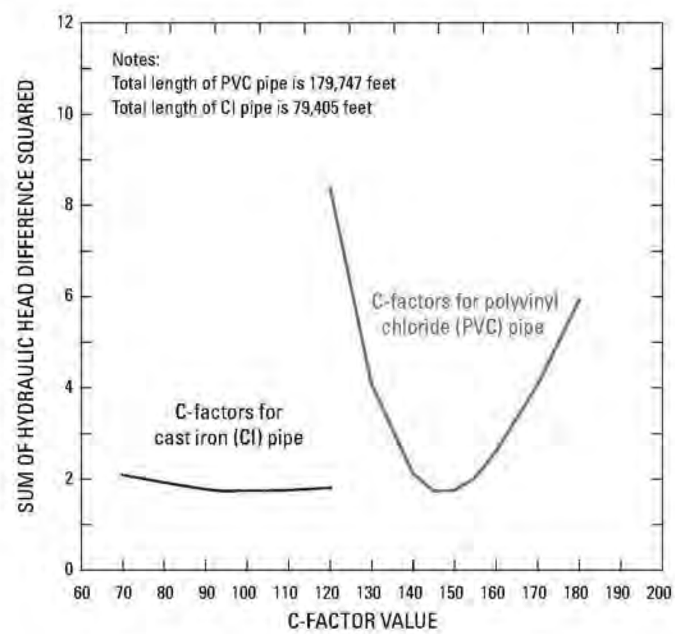

Figure I14. Sensitivity of hydraulic head to C-factor value at storage tank STT-40, Tarawa Terrace water-distribution system, U.S. Marine Corps Base Camp Lejeune, North Carolina. [See Figure I9 for storage tank location]

[21] This is another example of the application of the one-at-a-time design sensitivity analysis (Saltelli 2000), previously presented. In this application, however, the one-at-a-time sensitivity analysis was automated by using the PEST model.

[22] The examples provided in this discussion are derived from a fluoride tracer test of the Holcomb Boulevard and Tarawa Terrace water-distribution systems that was conducted September 22–October 12, 2004. Refer to the Chapter J report (Sautner et al. In press 2009) for details relative to the tracer test.

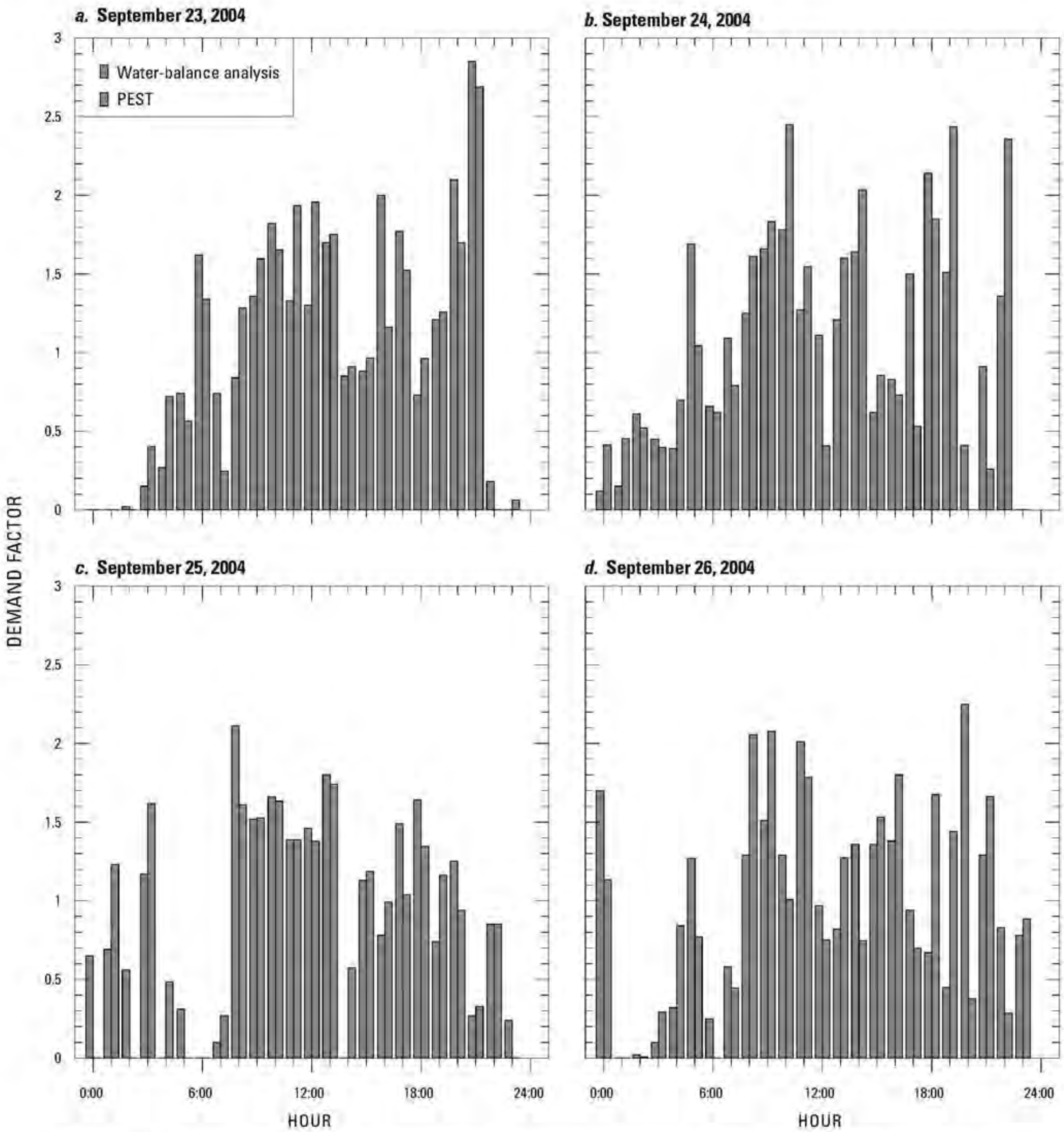

Figure I15. Demand-pattern factors estimated from water-balance analysis and derived from PEST simulation, September 23–26, 2004, Tarawa Terrace and Holcomb Boulevard water-distribution systems, U.S. Marine Corps Base Camp Lejeune, North Carolina. [PEST, parameter estimation model developed by Doherty (2005); missing bar indicates demand factor value of 0.0]

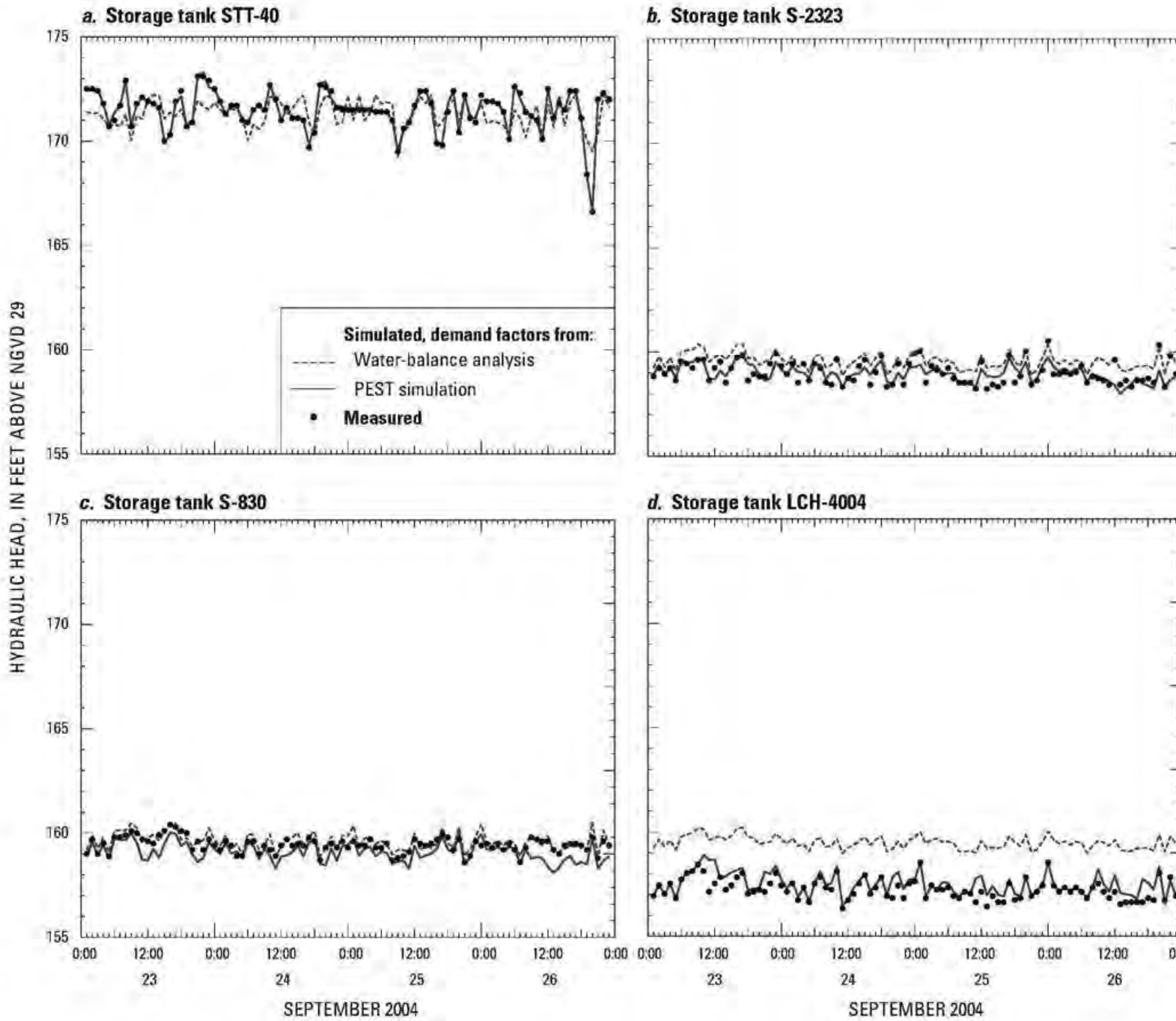

Figure I16. Measured and simulated hydraulic head for storage tanks: *(a)* STT-40, *(b)* S-2323, *(c)* S-830, and *(d)* LCH-4004, September 23–26, 2004, Tarawa Terrace and Holcomb Boulevard water-distribution systems, U.S. Marine Corps Base Camp Lejeune, North Carolina. [PEST, parameter estimation model developed by Doherty (2005); NGVD 29, National Geodetic Vertical Datum of 1929; see Figure I9 for storage tank locations]

demand-pattern factors resulted in lower *RMS* values, greater correlation coefficients (Table I10), and closer matches between measured and simulated hydraulic heads in the storage tanks (Figure I16). For storage tanks STT-40, S-2323, and LCH-4004, the PEST-derived demand-pattern factors (Figure I15) result in much closer agreement between measured and simulated hydraulic head than do the initial demand-pattern factors. At storage tank S-830, little improvement is seen between measured and simulated hydraulic head, regardless of the choice of demand-pattern factor—initial or PEST-derived (Figure I16).

In summary, therefore, the PEST-derived demand-pattern factors were used as input for EPANET 2 in constructing the calibrated Tarawa Terrace and Holcomb Boulevard water-distribution system models (Sautner et al. In press 2009). The EPANET 2 input files and typical PEST input and simulation files are also provided on the CD–ROM included with this report.

Table I10. Root-mean-square and correlation coefficient for varying demand factors, Tarawa Terrace and Holcomb Boulevard water-distribution systems, U.S. Marine Corps Base Camp Lejeune, North Carolina.

[2]Storage-tank identification	[1]Source of demand factors			
	Water-balance analysis		PEST simulation	
	[3]Root-mean-square of hydraulic head difference, in feet	Correlation coefficient	[3]Root-mean-square of hydraulic head difference, in feet	Correlation coefficient
Tarawa Terrace water-distribution system				
STT-40	0.70	0.63	0.06	0.99
Holcomb Boulevard water-distribution system				
S-2323	0.57	0.82	0.41	0.63
S-830	0.34	0.80	0.43	0.70
LCH-4004	2.22	0.79	0.35	0.83

[1] Water-balance analysis derived from information and data contained in the water-conservation analysis conducted by ECG, Inc. (1999); PEST, parameter estimation model developed by Doherty (2005)

[2] See Figure I9 for storage-tank locations

[3] Root-mean-square of difference between measured hydraulic head in storage tank derived from SCADA (supervisory control and data acquisition) system data and EPANET 2 simulated hydraulic head in storage tank

Probabilistic Analysis of Groundwater Flow and Contaminant Fate and Transport

A probabilistic analysis can be defined as an analysis in which frequency or probability distributions are assigned to represent uncertainty or variability in model parameters; the output of a probabilistic analysis is a probability distribution (Cullen and Frey 1999). A probabilistic analysis is used to generate uncertainties in model inputs (for example, hydraulic conductivity or contaminant-source mass-loading rate) in order to estimate uncertainties of model outputs (for example, water level or PCE concentration in groundwater). Although the sensitivity analyses provide some insight into the relative importance of selected model parameters, a probabilistic analysis provides a quantitative range and likelihood (probability) of model outputs. Probabilistic analysis is frequently used to understand and quantify variability and uncertainty of model output (Cullen and Frey 1999). Several methods are available for conducting a probabilistic analysis (that is, for propagating distributions or the moments of distributions through models) and those most commonly used are listed in Table I11. These methods are grouped as follows: (1) analytical solutions for moments, (2) analytical solutions for distributions, (3) approximation methods for moments, and (4) numerical methods. The probabilistic analysis used to characterize uncertainty and variability of Tarawa Terrace model output is a numerical method—Monte Carlo (MC) simulation. General and theoretical discussions of probabilistic analysis methods, and in particular MC simulation, are found in U.S. Environmental Protection Agency (USEPA; 1997), Deutsch and Journel (1998), Cullen and Frey (1999), Zhang (2002), Doherty (2005), and Tung and Yen (2005).

It is important to understand the conceptual difference between the deterministic modeling analysis approach used to calibrate model parameter values, described in Faye and Valenzuela (2007) and Faye (2008), and a probabilistic analysis. As described in Maslia and Aral (2004), with respect to the approach referred to as a deterministic modeling analysis, single-point values are specified for model input parameters and results are obtained in terms of single-valued output, for example, the concentration of PCE. This approach is shown conceptually in Figure I17*a*. In a probabilistic analysis, input parameters (all or a selected subset) of a particular model (for example, contaminant fate and transport) are characterized in terms of statistical distributions that can be generated using the MC simulation method (USEPA 1997, Tung and Yen 2005) or a sequential Gaussian (SG) simulation method (Deutsch and Journel 1998, Doherty 2005). Results are obtained in terms of distributed-value output that can be used to assess model uncertainty and parameter variability as part of the probabilistic analysis (Figure I17*b*).

MC simulation is a computer-based (numerical) method of analysis that uses statistical sampling techniques to obtain a probabilistic approximation to the solution of a mathematical equation or model (USEPA 1997). The MC simulation method is used to simulate probability density functions (PDFs). PDFs are mathematical functions that express the probability of a random variable (variant or model input) falling within some

Table I11. Classification of common probabilistic methods for propagating moments of distributions through models.[1]

Analytical Solutions for Moments	
	Central limit theorems
	Properties of the mean and variance
Analytical Solutions for Distributions	
	Transformation of variables
Approximation Methods for Moments	
	First-order methods
	Taylor series expansions
Numerical Methods	
	Monte Carlo simulation
	Latin hypercube sampling
	Importance sampling
	Fourier amplitude sensitivity test
	Others

[1]From Cullen and Frey (1999)

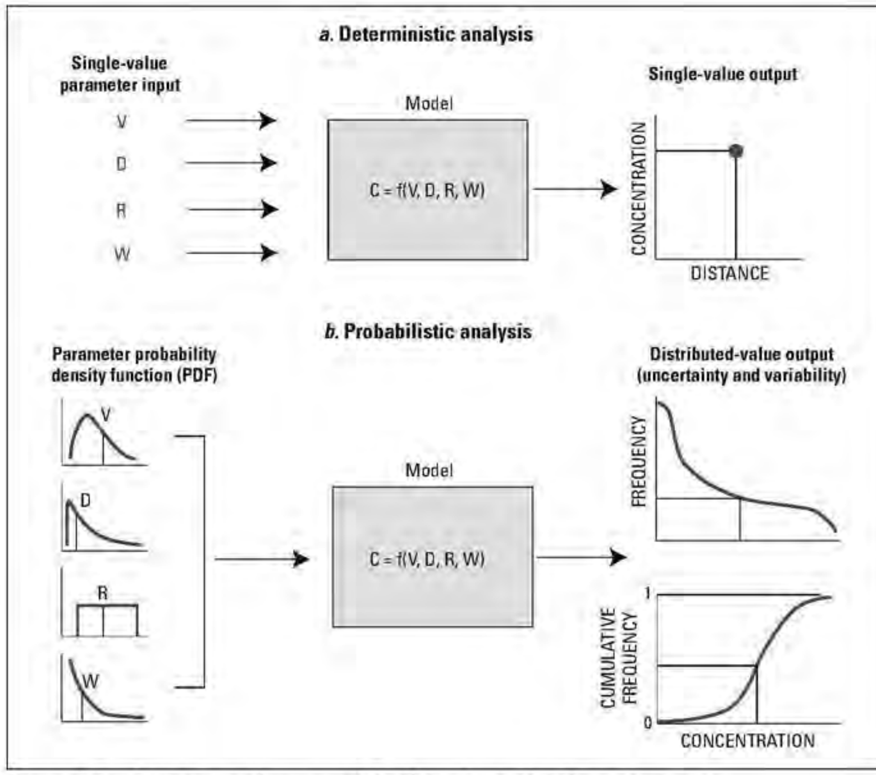

Figure I17. Conceptual framework for *(a)* a deterministic analysis and *(b)* a probabilistic analysis (from Maslia and Aral 2004).

interval. SG simulation is a process in which a field of values (such as horizontal hydraulic conductivity) is obtained multiple times, assuming the spatially interpolated values follow a Gaussian (normal) distribution. Additional details pertaining to the SG simulation methodology are provided in Deutsch and Journel (1998) and Doherty (2005).

The process used to incorporate MC and SG simulation into the Tarawa Terrace groundwater-flow and contaminant fate and transport models is shown in Figure I18. Monte Carlo analysis was used in a two-stage approach. In stage 1, random values were generated to approximate the PDF of a model's input parameter (for example, infiltration). In stage 2, the model was run (for example, MT3DMS) using input values generated during stage 1. The MC simulation procedure shown in Figure I18 can be explained as follows.

1. Select the most sensitive and uncertain parameters to be included in the probabilistic analysis (Monte Carlo analysis) using results from the sensitivity analyses.
2. Generate statistically defined random values for uncertain input parameters (variants) of the groundwater-flow and contaminant fate and transport models using pseudo-random number generators (PRNGs). Examples are PDFs for infiltration and longitudinal dispersivity and random fields of horizontal hydraulic conductivity generated using SG simulation. Each set of uncertain parameter values is referred to as a realization.
3. Run the groundwater-flow model (MODFLOW-2000) code[23] for each realization using a filter to discard physically implausible realizations. The filter compares the potentiometric head values for 13 Tarawa Terrace water-supply wells and 16 other locations of interest against specific model criteria—dry wells and potentiometric heads. Simulations that do not meet these criteria are discarded. Table I12 lists the criteria used by the filter to identify physically implausible solutions.
4. If the MODFLOW-2000 simulation is physically plausible (that is, a simulation that is not discarded by the filter), then run the contaminant fate and transport model (MT3DMS).

[23] MODFLOW-96 was the code used in Faye and Valenzuela (2007) to calibrate the Tarawa Terrace groundwater-flow model. Because of programming requirements associated with conducting the MC simulation, it was programmatically more efficient to use the MODFLOW-2000 model code (Harbaugh et al. 2000). MODFLOW-2000, developed by the U.S. Geological Survey, is an updated version of the MODFLOW-96 model code. Model parameter values for MODFLOW-2000 were identical and equivalent to the calibrated model parameter values derived using MODFLOW-96 (Table I2; Faye and Valenzuela 2007). Groundwater-flow simulation results were identical for both MODFLOW-96 and MODFLOW-2000.

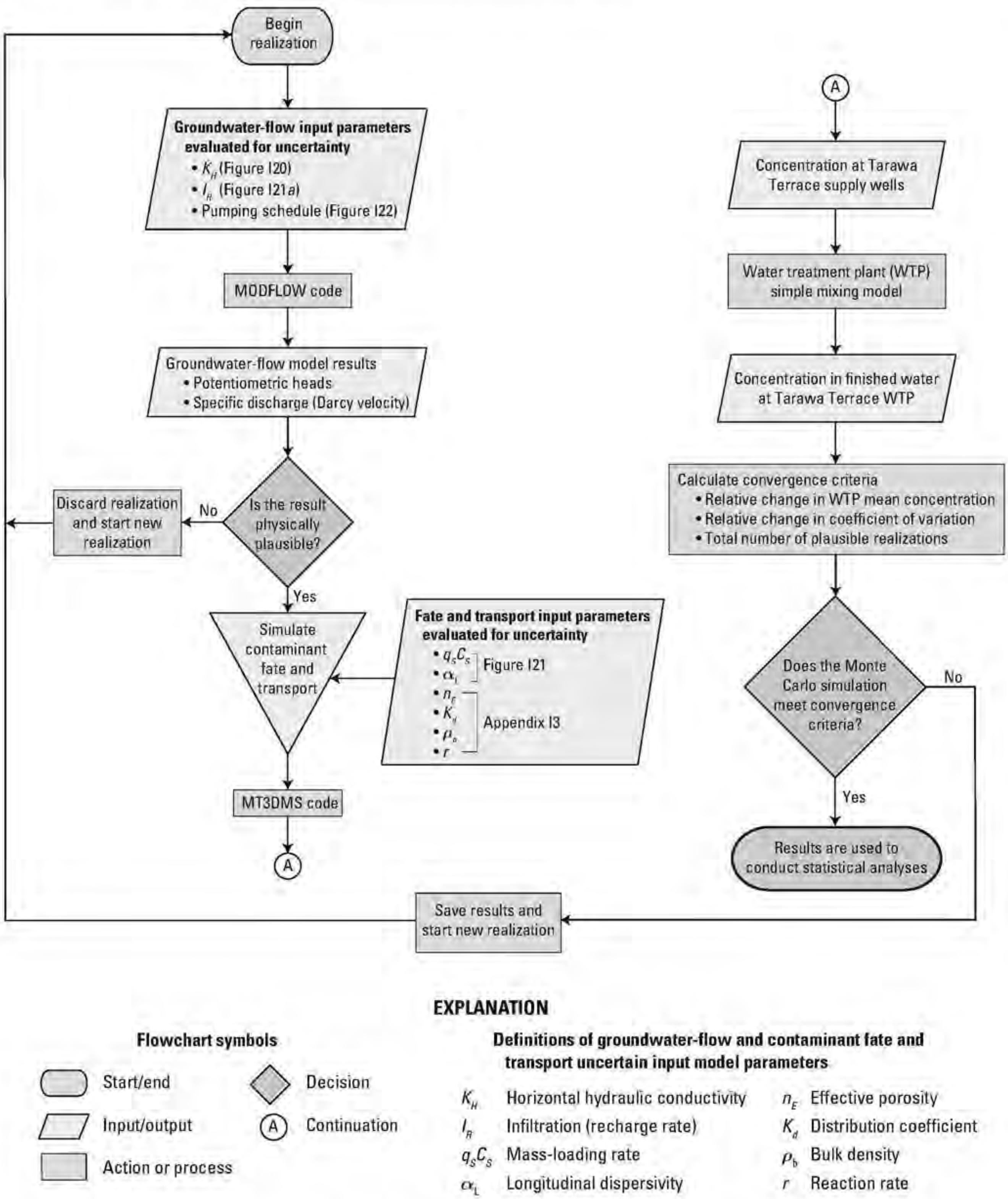

Figure I18. Flowchart for incorporating Monte Carlo simulation into groundwater-flow and contaminant fate and transport models, Tarawa Terrace and vicinity, U.S. Marine Corps Base Camp Lejeune, North Carolina.

Table I12. Identification of water-supply wells, control points, and criteria used to determine physically implausible realizations for Monte Carlo simulations of groundwater-flow and contaminant fate and transport, Tarawa Terrace and vicinity, U.S. Marine Corps Base Camp Lejeune, North Carolina.

[ft, feet; NGVD 29, National Geodetic Vertical Datum of 1929]

Site name	Groundwater-flow model location[1]			Criteria for a physically implausible solution
	Layer	Row	Column	
Water-supply wells				
TT-23	3	84	175	
TT-25	3	67	194	
TT-26	3	61	184	
TT-27	3	52	135	
TT-28	3	47	96	
TT-29	3	41	61	Water-supply well goes dry for any stress period; simulation is halted.
TT-30	3	47	97	
TT-31	1	104	152	
TT-52	1	101	136	
TT-53	1	81	151	
TT-54	1	106	167	
TT-55	1	53	136	
TT-67	3	93	158	
Control points				
CP-1	1	12	108	
CP-2	1	78	61	
CP-3	1	83	96	
CP-4	1	74	119	
CP-5	1	111	61	
CP-6	1	120	38	
CP-7	1	111	91	Potentiometric head is less than 24 ft below (–24 ft) or greater than 28 ft above (+28 ft) NGVD 29; simulation is halted.
CP 8	1	134	69	
CP-9	1	166	81	
CP-10	1	141	122	
CP-11	1	137	154	
CP-12	1	132	190	
CP-13	1	112	213	
CP-14	1	97	198	
CP-15	1	75	237	
CP-16	1	46	159	

[1]Refer to Faye and Valenzuela (2007) for details describing groundwater-flow model grid

5. Extract model-simulated concentrations at Tarawa Terrace water-supply wells and use these concentrations with a simple mixing model (Maslia et al. 2007, Faye 2008) to obtain the concentration in finished water at the Tarawa Terrace WTP.
6. Compute statistics of arithmetic mean ($\overline{C}$), standard deviation (σ_C), and coefficient of variation of change (C_v) in the finished water concentration at Tarawa Terrace WTP for every new realization.
7. If computed statistics in Step 6 indicate less than a 0.25% change (between two successive realizations) and the total number of physically plausible realizations exceeds 500 realizations, the MC simulation has converged and the process is stopped; otherwise, begin a new realization.

Step 6 lists three statistical quantities—the arithmetic mean ($\overline{C}$), standard deviation (σ_C), and coefficient of variation (C_v)—that are used in step 7 to compute stopping criteria for the MC simulation process. These statistics all use and reference the simulated PCE concentration in finished water at the Tarawa Terrace WTP. The mathematical formulae defining these statistical metrics and the formulae used to compute changes in the three statistical quantities for comparison with the MC simulation stopping criteria are listed in Table I13.

In Step 7, convergence is defined as the point where it is reasonable to assume that samples are truly representative of the underlying stationary distribution (Cowles and Carlin 1996). At the converging point, the output distributions do not change markedly by including additional samples. Some metrics usually used as a measure of convergence are sample mean versus true mean, skewness, percentile probabilities, or other statistics (Palisade 2008). For the Tarawa Terrace MC simulations, convergence criteria were needed to determine when the number of samples (realizations) sufficiently represented the underlying distribution. It is important to note, however, that results of an MC simulation do not directly provide a distribution, but rather, a sample of the distribution (Cowles and Carlin 1996).

The MC simulation procedure shown in Figure I18 and described above was incorporated into the Tarawa Terrace groundwater-flow and contaminant fate and transport models using a series of customized computer codes. A description of these codes and how they were implemented in the MC simulation process follows.

1. Subroutines from the IMSL™ FORTRAN numerical libraries (IMSL 2003) were used to generate the PRNG for model input parameter PDFs (for example, PDFs for infiltration, mass-loading rate, etc.).

2. FIELDGEN (Doherty 2005), a computer code developed for conducting SG simulation, was used to generate multiple realizations of the horizontal hydraulic conductivity fields for model layers 1, 3, and 5.

3. A customized FORTRAN 77 code, compiled using the Absoft® (2005) FORTRAN compiler, was developed to generate values from input parameter PDFs and the random horizontal hydraulic conductivity field in the required model input format for the groundwater-flow (MODFLOW-2000) and contaminant fate and transport (MT3DMS) models.

Simulations were conducted using six Dell Precision 690 workstations configured with Windows® XP Professional x64 edition operating system and 8 gigabytes of random access memory. For the Tarawa Terrace models, two sets of probabilistic analyses were conducted: (1) MC simulations excluding pumping schedule uncertainty and (2) MC simulations including pumping schedule uncertainty (Figure I2).

Table I13. Mathematical formulae and definitions of metrics used to compute stopping criteria for Monte Carlo simulations, Tarawa Terrace and vicinity, U.S. Marine Corps Base Camp Lejeune, North Carolina.

[µg/L, microgram per liter; WTP, water treatment plant; PCE, tetrachloroethylene]

Metric name and symbol	Mathematical formula	Definition of variables
Arithmetic mean of concentration, $\overline{C}$, in µg/L	$\overline{C}=\frac{\sum_{i=1}^{N_{SP}} C_i^{WTP}}{N_{SP}}$	C_i^{WTP} = finished water concentration of PCE at the WTP for stress period i; N_{SP} = number of stress periods[1]
Relative change in arithmetic mean of concentration, $\Delta\overline{C}$, in percent	$\Delta\overline{C}=\frac{\frac{\sum_{j=2}^{N_R}\overline{C_j}}{j}-\frac{\sum_{j=2}^{N_R}\overline{C_{j-1}}}{j-1}}{\frac{\sum_{j=2}^{N_R}\overline{C_{j-1}}}{j-1}}\times 100\%$	$\overline{C}_j$ = arithmetic mean of concentration for realization j; N_R = number of Monte Carlo realizations
Standard deviation of concentration, σ_C, in µg/L	$\sigma_C=\left[\frac{\sum_{i=1}^{N_{SP}}\left(C_i^{WTP}-\overline{C}\right)^2}{N_{SP}-1}\right]^{1/2}$	C_i^{WTP} = finished water concentration at the WTP for stress period i; $\overline{C}$ = arithmetic mean of concentration; N_{SP} = number of stress periods[1]
Relative change in standard deviation of concentration, $\Delta\sigma_C$, in percent	$\Delta\sigma_C=\frac{\frac{\sum_{j=2}^{N_R}\sigma_{C,j}}{j}-\frac{\sum_{j=2}^{N_R}\sigma_{C,j-1}}{j-1}}{\frac{\sum_{j=2}^{N_R}\sigma_{C,j-1}}{j-1}}\times 100\%$	$\sigma_{C,j}$ = standard deviation of concentration for realization j; N_R = number of Monte Carlo realizations
Coefficient of variation of concentration, C_v	$C_v=\sigma_C/\overline{C}$	$\overline{C}$ = arithmetic mean of concentration; σ_C = standard deviation of concentration
Relative change in coefficient of variation, ΔC_v, in percent	$\Delta C_v=\frac{\frac{\sum_{j=2}^{N_R}C_{v,j}}{j}-\frac{\sum_{j=2}^{N_R}C_{v,j-1}}{j-1}}{\frac{\sum_{j=2}^{N_R}C_{v,j-1}}{j-1}}\times 100\%$	$C_{v,j}$ = coefficient of variation of concentration for realization j; N_R = number of Monte Carlo realizations

[1] The number of stress periods, N_{SP}, is 528 (Faye and Valenzuela 2007, Faye 2008)

Selection of Uncertain Input Parameters

The uncertain model input parameters that were included in MC simulations were selected based on results of the sensitivity analyses described previously (refer to the "Sensitivity Analyses" section of this report). Table I14 lists results for sensitivity analyses expressed in terms of the absolute mean relative change, $\overline{R}$, and the standard deviation of the absolute mean relative change, $\sigma_{\overline{R}}$, computed for model parameters increased and decreased by 10% from calibrated values (refer to Table I5 for mathematical formulae defining $\overline{R}$ and $\sigma_{\overline{R}}$). According to these results, during the period January 1968–January 1985, the two most sensitive groundwater-flow parameters were horizontal hydraulic conductivity (K_H) for model layer 1 and infiltration (I_R). K_H for model layer 1 was considered sensitive to change because a 10% decrease from its calibrated value resulted in water-supply wells drying out (Table I14). Infiltration (I_R) was considered sensitive to change because varying its calibrated value by ±10% resulted in an $\overline{R}$ value of about 9.5% and a $\sigma_{\overline{R}}$ value of about 2%—the maximum values for $\overline{R}$ and $\sigma_{\overline{R}}$ of any of the parameters listed in Table I14. The least sensitive groundwater-flow parameters ($\overline{R} \leq 0.02\%$) were horizontal hydraulic conductivity (K_H) for model layer 6, specific yield (S_y), and storage coefficient (S). For the contaminant fate and transport model input parameters, five of seven fate and transport parameters—bulk density (ρ_b), distribution coefficient (K_d), effective porosity (n_E), mass-loading rate (q_sC_s), and reaction rate (r)—had $\overline{R}$ values exceeding 2% for changes in calibrated values of ±10%. Based on the aforementioned sensitivity analysis, all model input parameters with computed $\overline{R}$ values exceeding 1% were included as uncertain parameters in the probabilistic analysis. In addition to these model input parameters, K_H for model layers 3 and 5 also was included because K_H is used to derive groundwater velocity which is critical to the simulation of contaminant transport. Longitudinal dispersivity (α_L), although showing less sensitivity to change than other fate and transport parameters (Table I14), also was included as an uncertain parameter in the probabilistic analysis because it is a characteristic aquifer property and represents the effect of aquifer heterogeneity on the spreading of a dissolved contaminant mass (Schwartz and Zhang 2003).

As summarized in Chapter A (Maslia et al. 2007) and described in detail in Chapter H (Wang and Aral 2008), pumping schedule variation and uncertainty can cause changes in the arrival times of PCE at water-supply wells and the Tarawa Terrace WTP and, in turn, possibly affect the ensuing epidemiological study. For completeness, therefore, pumpage uncertainty and variation were included in the probabilistic analysis. For the Tarawa Terrace models, two scenarios of MC simulations were conducted. In scenario 1, pumpage was not considered uncertain, and in scenario 2, pumpage was considered uncertain (Figure I2). For the scenario where pumpage was considered an uncertain model parameter (scenario 2), the generation of uncertain and variable pumpage values is described in this report in the section on "Generation of Uncertain Input Parameters."

To summarize, the following 10 model input parameters were considered uncertain and were included in all probabilistic analyses using MC simulation: horizontal hydraulic conductivity (K_H) for model layers 1, 3, and 5, infiltration (I_R), bulk density (ρ_b), longitudinal dispersivity (α_L), distribution coefficient (K_d), effective porosity (n_E), mass-loading rate (q_sC_s), and reaction rate (r). Calibrated values of pumpage (Q) were not varied in one set of MC simulations (scenario 1) and were considered uncertain in a second set of MC simulations (scenario 2).[24]

Generation of Uncertain Input Parameters

Three procedures were used to generate uncertain model input parameters: (1) SG simulation, used to generate random fields of horizontal hydraulic conductivity, (2) PRNGs, used to generate parameter PDFs (for example, infiltration), and (3) statistical analysis of historical pumping variation, used to generate pumping realizations through the application of MC simulation. The process and procedures used to generate the uncertain input parameters are described below.

Sequential Gaussian Simulation

SG simulation is a process in which a field of values (such as K_H) is obtained multiple times assuming the spatially interpolated values follow a Gaussian (normal) distribution (Deutsch and Journel 1998, Doherty 2005).[25] Because of the availability of field values of K_H, spatial distributions of K_H were generated using the SG simulation method. Point values for K_H were derived from aquifer-test analyses described in Faye (2007) and Faye and Valenzuela (2007). A total of 36 K_H values were available for the Tarawa Terrace groundwater-flow model: 13 values for model layer 1; 14 values for model layer 3; and 9 values for model layer 5. Ranges for calibrated K_H values were 12.2–53.4 ft/d for model layer 1, 4.3–20.0 ft/d for model layer 3, and 6.4–9.0 ft/d for model layer 5 (Table I14). The SG simulation method was implemented through the application of the computer code FIELDGEN (Doherty 2005)—a two-dimensional stochastic field generator. The SG simulation method is similar to other interpolating techniques such as kriging (Davis 1973); the distinction is that multiple fields (spatial distributions) of a parameter can be obtained with SG simulation. The SG simulation method can be explained in three steps.

[24] Leakance, defined in PMWIN (Chiang and Kinzelbach 2001) as VCONT, is a function of vertical hydraulic conductivity (K_Z), which is a scaled factor of K_H. Although leakance was not varied or considered uncertain independently, when K_H is uncertain and varied in MC simulations, leakance also varies because it is a function of a scaled value of K_H.

[25] The Tarawa Terrace analyses assume the spatially interpolated K_H values follow a Gaussian distribution. Additional research and field data would be required to determine if other statistical distributions could or should be used to describe spatially interpolated field values of K_H and other model parameters.

Table I14. Sensitivity analysis metrics used for selecting uncertain parameters for conducting probabilistic analysis, Tarawa Terrace and vicinity, U.S. Marine Corps Base Camp Lejeune, North Carolina.

[ft/d, foot per day; —, not applicable; d, day; in/yr, inch per year; g/ft³, gram per cubic foot; ft, foot; ft³/g, cubic foot per gram]

Model parameter[1]	Calibrated value	Ratio of varied to calibrated parameter value	Absolute value of mean relative change ($\overline{R}$), in percent[2,3]	Standard deviation of mean relative change ($\sigma_{\overline{R}}$), in percent[3]
Groundwater-flow model parameters				
Horizontal hydraulic conductivity, all layers, K_H (ft/d)	1.0–53.4	0.9	—[4]	—[4]
		1.1	0.51	0.75
Horizontal hydraulic conductivity, layer 1, K_H (ft/d)	12.2–53.4	0.9	—[4]	—
		1.1	1.13	1.32
Horizontal hydraulic conductivity, layer 2, K_H (ft/d)	1.0	0.9	0.09	0.02
		1.1	0.08	0.01
Horizontal hydraulic conductivity, layer 3, K_H (ft/d)	4.3–20.0	0.9	0.40	0.29
		1.1	0.37	0.26
Horizontal hydraulic conductivity, layer 4, K_H (ft/d)	1.0	0.9	0.27	0.04
		1.1	0.26	0.04
Horizontal hydraulic conductivity, layer 5, K_H (ft/d)	6.4–9.0	0.9	0.75	0.41
		1.1	0.60	0.39
Horizontal hydraulic conductivity, layer 6, K_H (ft/d)	1.0	0.9	0.02	0.02
		1.1	0.02	0.02
Horizontal hydraulic conductivity, layer 7, K_H (ft/d)	5.0	0.9	0.33	0.15
		1.1	0.32	0.15
Leakance, K_Z/d_Z (1/d)	3.6×10^{-3}–4.2×10^{-1}	0.9	0.87	0.39
		1.1	0.74	0.34
Infiltration (recharge), I_R (in/yr)	6.6–19.3	0.9	9.59	2.06
		1.1	9.53	2.32
Specific yield, S_y	0.05	0.9	0.12	0.09
		1.1	0.11	0.09
Storage coefficient, S	4.00E–04	0.9	0.00	0.00
		1.1	0.01	0.00
Contaminant fate and transport model parameters				
Bulk density, ρ_b (g/ft³)	77,112	0.9	2.05	1.47
		1.1	2.20	1.24
Longitudinal dispersivity, α_L (ft)	25	0.9	0.32	0.26
		1.1	0.30	0.24
Distribution coefficient, K_d (ft³/g)	5.0×10^{-6}	0.9	2.05	1.47
		1.1	2.20	1.24
Effective porosity, n_E	0.2	0.9	9.11	0.95
		1.1	8.20	0.74
Mass-loading rate, $q_s C_s$ (g/d)	1,200	0.9	10.00	0.00
		1.1	10.00	0.00
Molecular diffusion, D^* (ft²/d)	8.5×10^{-4}	0.9	0.00	0.00
		1.1	0.00	0.00
Reaction rate, r (d⁻¹)	5.0×10^{-4}	0.9	7.86	0.51
		1.1	7.22	0.42

[1]Symbolic notation used to describe model parameters obtained from Chiang and Kinzelbach (2001)

[2]Refer to Table I5 for mathematical formula and definition of absolute value of mean relative change, $\overline{R}$, and standard deviation of mean relative change, $\sigma_{\overline{R}}$

[3]Calculated for January 1968–January 1985 (stress periods 205–409), not including periods when water-supply well TT-26 was out of service: July–August 1980 [stress periods 355–356] and January–February 1983 [stress periods 385–386]; TT-26 was permanently taken out of service after January 1985

[4]Water-supply wells simulated as dry for this sensitivity analysis

1. Using conditioning data and kriging, an expected field value and a field standard deviation are determined for a generic point.
2. Using the expected value and standard deviation, a random field value is generated based on the assumption of a Gaussian (normal) probability distribution.
3. Using this new value the same process is repeated for a new location.

To use the SG simulation method that is integrated into FIELDGEN, the structure of the kriging method has to be defined by way of variograms. A variogram, also known as a semivariogram, is a statistically-based (geostatistical), quantitative description of the spatial continuity or roughness of a dataset (Barnes 2003). Variograms for model layers 1, 3, and 5 were obtained and used in FIELDGEN. Initially during model calibration, K_H arrays were developed for the active model domain using the modified Sheperd's method (inverse distance method [Golden Software, Inc. 1999]). The 36 field measurements for K_H (Faye 2007, Faye and Valenzuela 2007) initially were used to generate variograms to apply to FIELDGEN. However, 36 field measurements of K_H alone were insufficient to accomplish the generation of multiple K_H fields representative of the calibrated K_H array; therefore, 100 random K_H values from each model layer were selected as conditioning points. Figure I19 shows the experimental and model variograms used within FIELDGEN. The variograms were constructed using the Surfer® software (Golden Software, Inc. 1999). Using the variograms shown in Figure I19, multiple K_H fields were generated by running FIELDGEN. Figure I20 shows examples of four generations of K_H fields from FIELDGEN for model layer 1. Also shown in Figure I20 are the measured K_H values reported by Faye (2007) and Faye and Valenzuela (2007) for model layer 1. Thus, for each MC realization, when a random field of K_H was required as input to MODFLOW-2000, a spatial distribution, exemplified by the K_H fields shown in Figure I20, was input to the model.

Pseudo-Random Number Generator

A PRNG is an algorithm for generating a sequence of numbers that approximates the properties of random numbers (Wikipedia 2008). Although not truly random, PRNGs have many significant statistical characteristics in common with true random numbers (Uner 2004); therefore, PRNGs can be used to approximate PDFs. Gaussian (normal) and lognormal PRNGs were used to approximate the PDFs of uncertain groundwater-flow and contaminant fate and transport model input parameters (also referred to as variants). Statistics associated with normal and lognormal PDFs for the uncertain model input parameters, such as the mean, minimum, maximum, and standard deviation, are listed in Table I15. The calibrated value associated with each variant—derived from model calibrations described in the Chapter C (Faye and Valenzuela 2007) and Chapter F reports (Faye 2008)—was assigned as the mean value of the distribution associated with each variant. Examples of PDFs generated for infiltration (recharge rate), mass-loading rate (source concentration), and longitudinal dispersivity compared with the appropriate theoretical distribution are shown in Figure I21. PDFs for all uncertain model input parameters derived from application of the PRNGs (I_R, K_d, ρ_b, n_E, r, q_sC_s, and α_L) are shown in Appendix I3. Details describing the generation of uncertain model input parameters using the PRNG method are described below:

Infiltration (recharge rate, I_R): The PRNG was defined based on the calibrated model approach for assigning infiltration (Faye and Valenzuela 2007). A single value for infiltration was assigned to the uppermost model layer—layer 1—for each simulation year (1951–1994). The arithmetic mean—hereafter referred to as mean—for the Gaussian PRNG was defined as the calibrated recharge rate for each respective year. The range of mean values for infiltration was 6.6–19.3 inches per year (in/yr) (Table I15). The minimum, maximum, and standard deviation values input to the PRNG were 4.4 in/yr, 21.9 in/yr, and 2.2 in/yr, respectively. An example of the infiltration PDF for 1984, derived using the PRNG, is shown in Figure I21*a*. Additional PDFs for infiltration characterizing a dry year (lower recharge) and a wet year (higher recharge) are shown in Appendix I3.

Distribution coefficient (K_d): For this variant, a Gaussian PRNG was used to assign cell-by-cell values of K_d using a mean value of 5.0×10^{-6} cubic feet per gram (ft³/g). The minimum, maximum, and standard deviation values input to the PRNG were 3.53×10^{-6}, 2.68×10^{-5}, and 1.77×10^{-6} ft³/g, respectively (Table I15). As a comparison, for PCE in a silt and sand environment, Hoffman (1995) reports a range of values for distribution coefficient of 7.4×10^{-6}–2.7×10^{-5} ft³/g.

Bulk density (ρ_b): This variant was defined with a Gaussian PRNG and assigned on a cell-by-cell basis using a mean value of 77,112 grams per cubic foot (g/ft³) and a standard deviation of 1,100 g/ft³ (Table I15). The Castle Hayne aquifer system is composed of fine, fossiliferous sand, limestone, and shell limestone (Faye 2007). Densities of silty soils reported by Morris and Johnson (1967) ranged from 69,943 to 79,004 g/ft³. The published range of density values was used to truncate the values obtained from the PRNG to account for silty limestones; that is, these values were used to represent the minimum and maximum values assigned to ρ_b.

Effective porosity (n_E): For this variant, a Gaussian PRNG was used to assign cell-by-cell values of n_E using a mean of 0.2 and a standard deviation of 0.05 (Table I15). For the fine, fossiliferous sand, limestone, and shell limestone of the Castle Hayne aquifer system (Faye 2007), the viable range for n_E was defined with a minimum value of 0.1 and a maximum value of 0.3. Field measurements were not available to determine n_E values in different areas of the model domain. Using the cell-by-cell approach for n_E, however, makes the modeling approach consistent because K_H was varied using a cell-by-cell approach, and both K_H and n_E are parameters that are used in the computation of groundwater velocity.

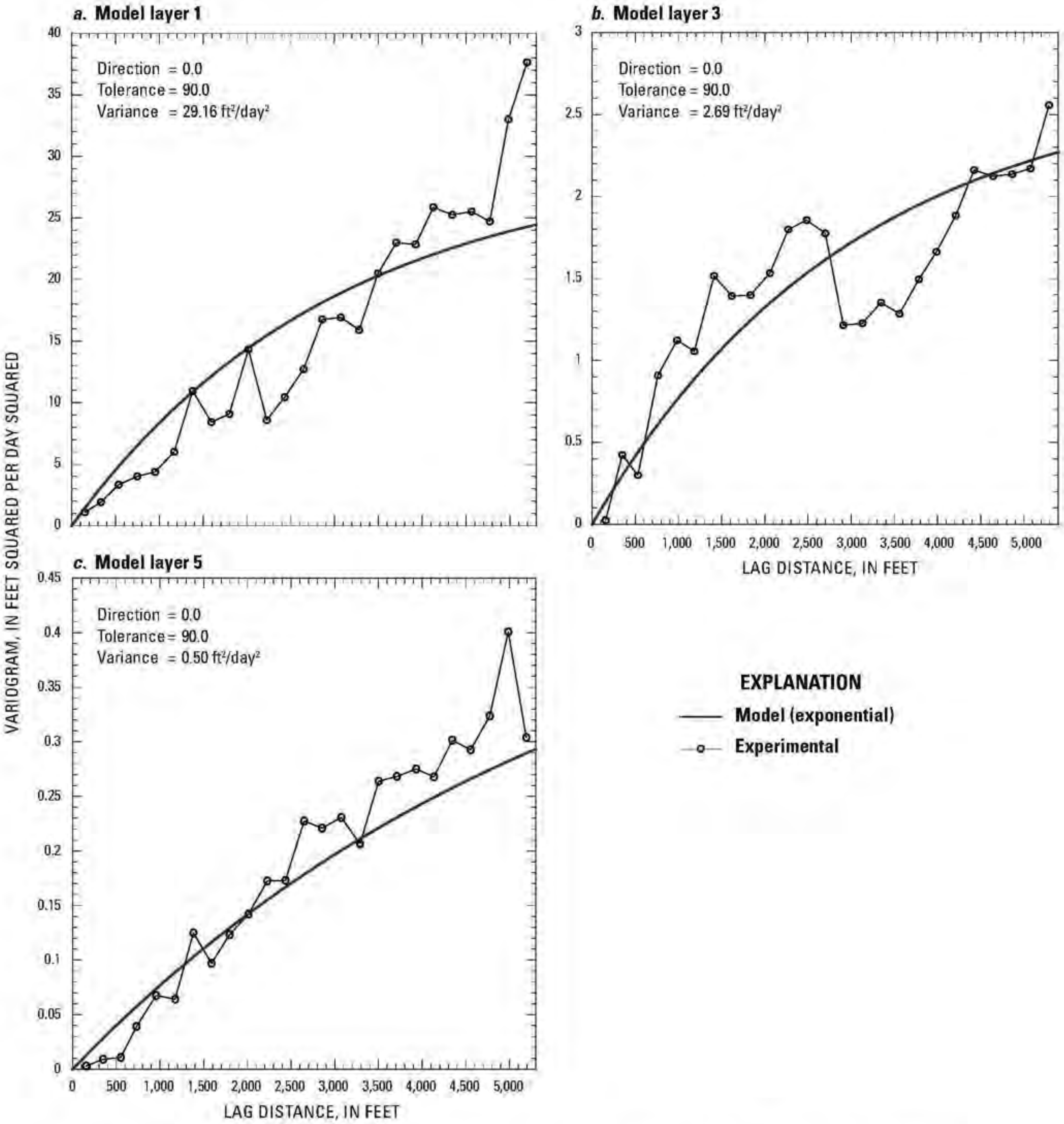

Figure I19. Variograms for horizontal hydraulic conductivity (K_H) for: *(a)* model layer 1, *(b)* model layer 3, and *(c)* model layer 5, Tarawa Terrace and vicinity, U.S. Marine Corps Base Camp Lejeune, North Carolina. [ft²/d², feet squared per day squared]

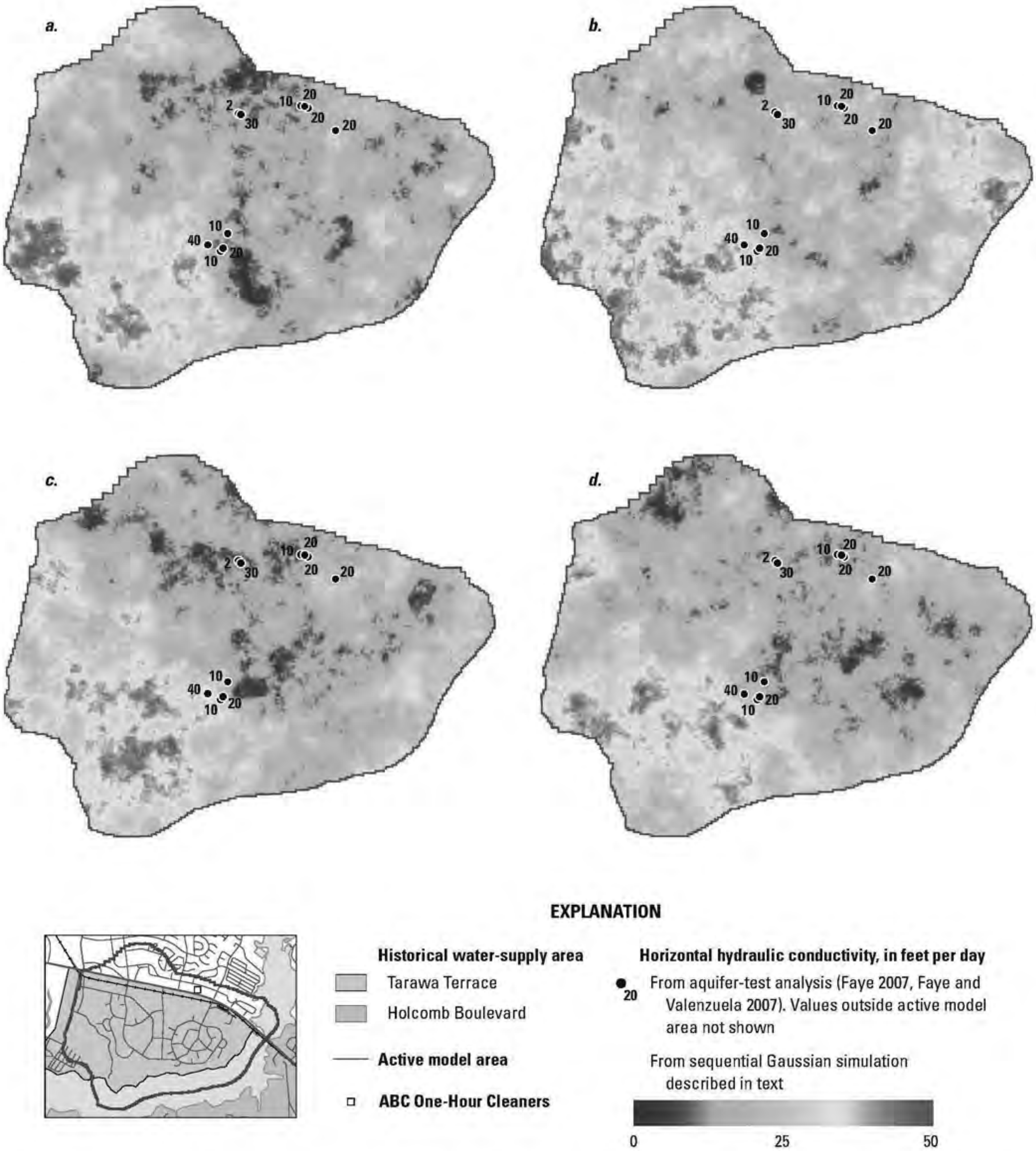

Figure I20. Horizontal hydraulic conductivity (K_H) fields for model layer 1 obtained from the FIELDGEN program: *(a)* generation 1, *(b)* generation 2, *(c)* generation 3, and *(d)* generation 4, Tarawa Terrace and vicinity, U.S. Marine Corps Base Camp Lejeune, North Carolina. [FIELDGEN from Doherty (2005); note: all hydraulic conductivity values are greater than 0 and less than 50 feet per day]

Table I15. Uncertain input parameters (variants) used in probabilistic analyses, Tarawa Terrace and vicinity, U.S. Marine Corps Base Camp Lejeune, North Carolina.

[ft/d, foot per day; —, not applicable; in/yr, inch per year; ft^3/g, cubic foot per gram; g/ft^3, gram per cubic foot; d, day; g/d, gram per day; ft, foot; SGS, sequential Gaussian simulation; MCS, Monte Carlo simulation; PDF, probability density function; ft^3/d, cubic foot per day]

Model parameter or variant[1,2]	Calibrated value	Statistical descriptions of probabilistic distributions				Method of generating uncertain input parameter	Method of assigning uncertain parameter in models
		Mean	Minimum	Maximum	Standard deviation		
Groundwater-flow model parameters							
Horizontal hydraulic conductivity, layer 1, K_H (ft/d)	12.2–53.4	[3]12.2–53.4	—	—	—	SGS used to generate random hydraulic conductivity field under a normal distribution[4]	Cell-by-cell distribution
Horizontal hydraulic conductivity, layer 3, K_H (ft/d)	4.3–20.0	[3]4.3–20.0	—	—	—	SGS used to generate random hydraulic conductivity field under a normal distribution[4]	Cell-by-cell distribution
Horizontal hydraulic conductivity, layer 5, K_H (ft/d)	6.4–9.0	[3]6.4–9.0	—	—	—	SGS used to generate random hydraulic conductivity field under a normal distribution[4]	Cell-by-cell distribution
Infiltration (recharge), I_R (in/yr), (ft/d)	6.6–19.3, 1.5×10^{-3}–4.4×10^{-3}	6.6–19.3, 1.5×10^{-3}–4.4×10^{-3}	4.4, 1.0×10^{-3}	21.9, 5.0×10^{-3}	2.2, 5.0×10^{-4}	MCS used to generate the PDF using a normal distribution; PDF generated for each stress period	Constant value assigned uppermost active cell (model layer 1), varied yearly
Pumpage, Q_K (ft^3/d)	See footnote 5						
Fate and transport model parameters							
Distribution coefficient, K_d (ft^3/g)	5.0×10^{-6}	5.0×10^{-6}	3.53×10^{-6}	2.68×10^{-5}	1.77×10^{-6}	MCS used to generate the PDF using a normal distribution	Cell-by-cell distribution
Bulk density, ρ_b (g/ft^3)	77,112	77,112	69,943	79,004	1,100	MCS used to generate the PDF using a normal distribution	Cell-by-cell distribution
Effective porosity, n_E	0.2	0.2	0.1	0.3	0.05	MCS used to generate the PDF using a normal distribution	Cell-by-cell distribution
Reaction rate, r (d^{-1})	5.0×10^{-4}	5.0×10^{-4}	2.30×10^{-4}	7.70×10^{-4}	1.35×10^{-4}	MCS used to generate the PDF using a normal distribution	Constant value assigned to entire model
Mass-loading rate, $q_S C_S$ (g/d)[5]	1,200	1,200	200	2,200	100	MCS used to generate the PDF using a normal distribution	Single value assigned to contaminant source cell[6]
Longitudinal dispersivity, α_L (ft)	25	3.2189	5	125	0.8047	MCS used to generate the PDF using a normal distribution[7]	Cell-by-cell spatial distribution

[1]Symbolic notation used to describe model parameters obtained from Chiang and Kinzelbach (2001)

[2]Statistical description of pumpage variation is described in the report section "Statistical Analysis of Historical Pumping Variation"

[3]For statistical descriptions of the mean, values were calculated using conditioning data obtained from the calibrated mean values

[4]The FIELDGEN model code described in Doherty (2005) was used to generate the random, spatially varying fields of hydraulic conductivity

[5]Pumpage varies by month, year, and model layer. Monte Carlo simulation was used to generate monthly pumpage variations based on statistical analyses of historical pumping. This approach is described in detail in the report section "Statistical Analyses of Historical Pumping Variation"

[6]Contaminant source cell is located in model layer 1, row 47, column 170 (Faye 2008)

[7]The mean value derived from Ln (25); standard deviation derived from Ln (5)/2, where Ln ( ) is the Naperian logarithm

***a.* Infiltration (I_R, recharge rate)**

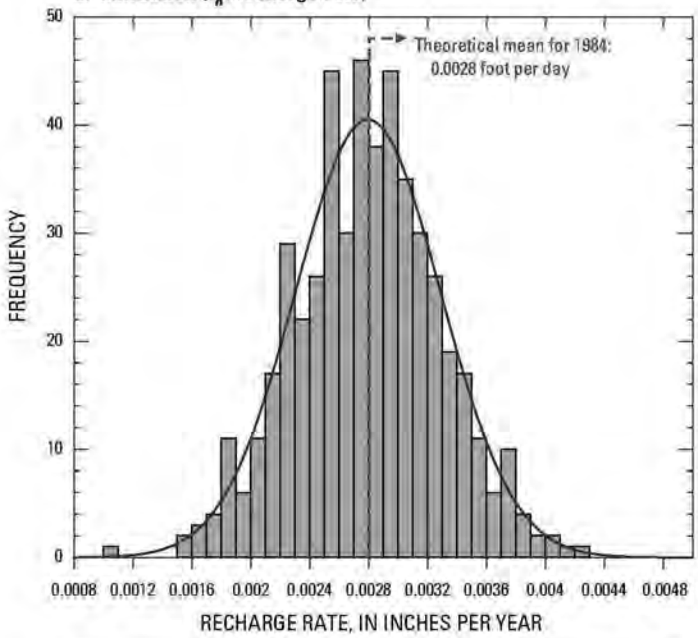

STATISTICS		
	Theoretical	Monte Carlo simulation
Distribution	Normal	Normal
Number of realizations	Not applicable	500
Minimum	– Infinity	0.001
Maximum	+ Infinity	0.005
Mean	0.00280	0.00280
Mode	0.00280	0.00260
Median	0.00280	0.00279
Standard deviation	0.00050	0.00049

***b.* Mass-loading rate ($q_s C_s$, source concentration)**

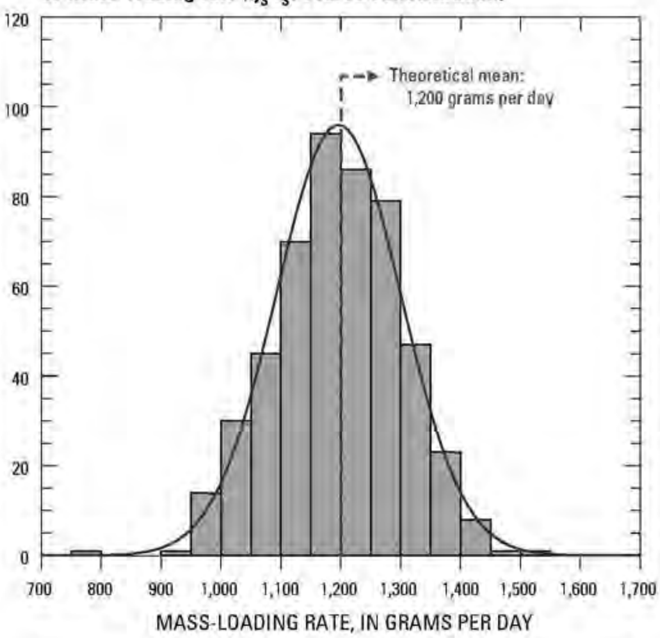

STATISTICS		
	Theoretical	Monte Carlo simulation
Distribution	Normal	Normal
Number of realizations	Not applicable	500
Minimum	– Infinity	200
Maximum	+ Infinity	2,200
Mean	1,200	1,196
Mode	1,200	1,257
Median	1,200	1,198
Standard deviation	100	104.0659

***c.* Longitudinal dispersivity (α_L)**

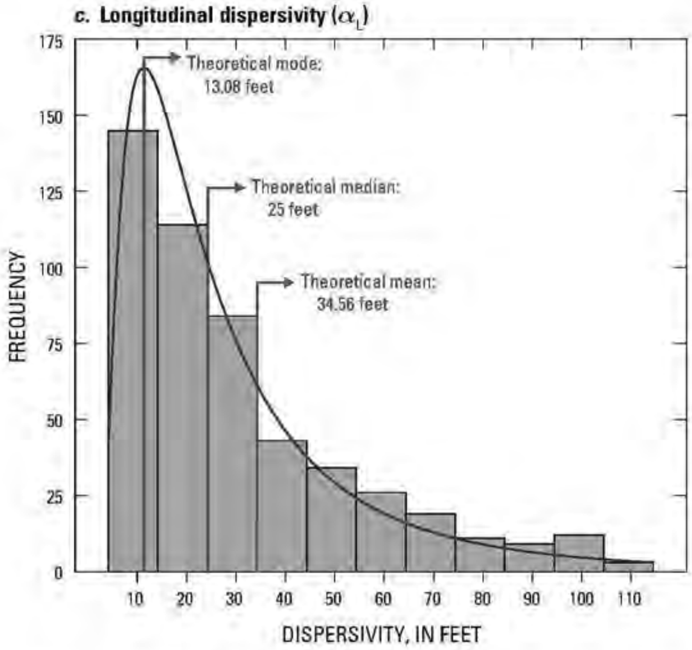

STATISTICS		
	Theoretical	Monte Carlo simulation
Distribution	Lognormal	Lognormal
Number of realizations	Not applicable	500
Minimum	0	5
Maximum	Infinity	125
Mean	34.56	31.32
Mode	13.08	N/A
Median	25	23.85
Standard deviation	32.98	23.59

Figure I21. Probability density functions for *(a)* infiltration (I_R, recharge rate), *(b)* mass-loading rate ($q_s C_s$, source concentration), and *(c)* longitudinal dispersivity (α_L) used to conduct probabilistic analyses, Tarawa Terrace and vicinity, U.S. Marine Corps Base Camp Lejeune, North Carolina. [–, minus; +, plus; N/A, not applicable]

Reaction rate (r): This variant was assigned uniformly—a single value for the entire model—because site information about reaction-driven or reaction-limited zones was not available. Reaction rate values were obtained using a Gaussian PRNG with a mean of 5.0×10^{-4} d^{-1} and a standard deviation of 1.35×10^{-4} d^{-1} (Table I15). The reaction rate range was defined with a minimum value of 2.30×10^{-4} d^{-1} (half-life of 8.3 years) and a maximum value of 7.70×10^{-4} d^{-1} (half-life of 2.5 years). This range corresponds to ± 2 times the standard deviation and was selected based on literature values and results from the sensitivity analyses. Howard et al. (1991) reported several values for aerobic and anaerobic biodegradation (that is, reaction rate) ranging from 6 months to 1 year for aerobic half-life and 98 days to 4.5 years for anaerobic half-life. They also report a half-life range for solutes in groundwater of 1–2 years. The reaction rate for the Tarawa Terrace site probably approximates anaerobic conditions; therefore, anaerobic half-life values are more appropriate than aerobic half-life values.

Mass-loading rate ($q_S C_S$): This variant was defined with a Gaussian PRNG assuming a month-to-month variation. The $q_S C_S$ value for PCE (the contaminant source) was assigned in the model to the grid cell that corresponded to the location of ABC One-Hour Cleaners' septic tank soil-adsorption system—layer 1, row 47, and column 170 (Faye 2008). The calibrated model used a constant value for $q_S C_S$ of 1,200 g/d that was applied as a continuous contaminant source during stress periods 25–408 (January 1953–December 1984). For the PRNG, the mean and standard deviation were assigned as 1,200 and 100 g/d, respectively (Table I15). Based on mass calculations using a shell methodology described by Pankow and Cherry (1996), a minimum mass-loading rate of about 230 g/d of PCE was calculated (Faye and Green 2007). Thus, a minimum to maximum range of 200–2,200 g/d was used for the PRNG. The PDF for mass-loading rate derived using the PRNG method and a comparison with the theoretical normal distribution are shown in Figure I21*b*.

Longitudinal dispersivity (α_L): This variant was defined with a log-normal PRNG and assigned in the model on a cell-by-cell basis. Site data for Tarawa Terrace were not available to estimate the range of plausible dispersivity values; however, field studies indicate that dispersivity can vary by orders of magnitude as the length of the plume increases (Gelhar et al. 1992). The calibrated value assigned to α_L is 25 ft as explained in Faye (2008), who also provides a detailed description as to how this value was derived for the Tarawa Terrace area. Because α_L was defined with a log-normal distribution, the mean value for the purposes of the probabilistic analysis is computed as the Naperian logarithm of 25 ft, which is 3.22 ft (Table I15). The minimum, maximum, and standard deviation values assigned to α_L are 5, 125, and 0.8047 ft, respectively, and these values were used to define the PRNG. The PDF for longitudinal dispersivity derived using the PRNG method and a comparison with the theoretical log-normal distribution are shown in Figure I21*c*.

Descriptive statistics for theoretical variants are shown in Figure I21 and in Appendix I3. For each variant, these statistics are compared to PDFs generated using PRNGs and MC simulation. The descriptive statistics for the PRNG-generated values show that 500 realizations (or MC simulations) produce similar statistics when compared with the theoretical statistics for each variant's PDF. For example, the descriptive statistics for mass-loading rate (Figure I21*b*) show a theoretical mean and standard deviation of 1,200 and 100 g/d, respectively. Comparing these values with the mean and standard deviation obtained from the MC simulation of 1,196 and 104 g/d, respectively, indicates that 500 realizations result in a PDF for this variant that is representative of the theoretical PDF for mass-loading rate.

Statistical Analysis of Historical Pumping Variation

The Chapter H report (Wang and Aral 2008) describes pumping schedule variations that result in different PCE arrival times at Tarawa Terrace water-supply wells and corresponding changes in concentration of PCE in finished water at the Tarawa Terrace WTP. Such variations could affect the results of the epidemiological study. Because historical pumping records are incomplete—pumping dates are recorded for 55 of 528 stress periods (Table I16)—the calibrated Tarawa Terrace models are based on uncertain and variable pumpage quantities. The effect of this uncertainty on modeling results was assessed using probabilistic techniques.

A statistical analysis procedure for analyzing historical pumping schedule variation was developed using available Tarawa Terrace pumpage data (Table I16). Results of the statistical analysis were then incorporated into a probabilistic analysis to account for historical pumping uncertainty (Figure I18). The method for incorporating the statistical analysis results into the MC simulation procedure is shown in a flowchart diagram in Figure I22.

Historical records for total groundwater withdrawals that supplied raw water to the Tarawa Terrace WTP are incomplete for the period covering model simulation (1951–1994). However, nearly complete monthly pumping records are available for 1978, 1980–1981, and 1983–1984 and were obtained from Henry Von Oesen and Associates, Inc. (1979) and various Camp Lejeune water documents (CLW 4436–4483) (Table I16). Using historical monthly pumpage data, ratios of monthly groundwater pumping rates ($Q_{monthly}$) to annual monthly mean pumping rates (Q_{mean}) were computed, and these ratios ($Q_{monthly}$ / Q_{mean}) are listed in Table I17. The $Q_{monthly}$ / Q_{mean} ratios were computed by dividing monthly total raw water delivered to the Tarawa Terrace WTP ($Q_{monthly}$; monthly entries listed in Table I16) by the annual monthly mean pumping rates (Q_{mean}; entries from last row in Table I16). Statistical analyses are summarized in Table I18 using the $Q_{monthly}$ / Q_{mean} ratios listed in Table I17 and also are shown graphically in Figure I23. The results of the statistical analysis indicate that pumping demand is higher in summer and early fall, and these results are representative of a realistic pumping demand pattern for North Carolina (North Carolina Rural Economic Development Center 2006). Note that during the

Table I16. Historical record of total monthly raw water (groundwater) delivered to the water treatment plant, Tarawa Terrace, U.S. Marine Corps Base Camp Lejeune, North Carolina.

[—, data not available]

Month	Monthly groundwater pumping demand ($Q_{monthly}$), in cubic feet per day[1]				
	1978	1980	1981	1983	1984
January	119,674	125,086	106,089	111,644	103,463
February	135,982	98,563	95,123	110,156	112,682
March	108,621	112,088	109,729	—	108,281
April	119,572	91,796	114,599	118,113	111,943
May	112,722	96,054	116,780	126,212	121,114
June	131,734	105,847	133,186	141,676	116,413
July	128,454	121,037	128,808	137,481	111,394
August	120,174	108,078	123,805	143,216	124,077
September	119,942	104,973	122,291	126,377	113,008
October	135,070	99,043	—	—	115,538
November	103,271	94,300	—	115,952	113,775
December	103,847	97,400	—	147,365	108,211
Annual total	**1,439,063**	**1,254,265**	**1,050,410**	**1,278,192**	**1,359,899**
Annual monthly mean (Q_{mean})	**119,921.9**	**104,522.1**	**116,712.2**	**127,819.2**	**113,324.9**

[1]1978 data from Henry Von Oesen and Associates, Inc. (1979); 1980–1981 and 1983–1984 data from CLW 4436–4483

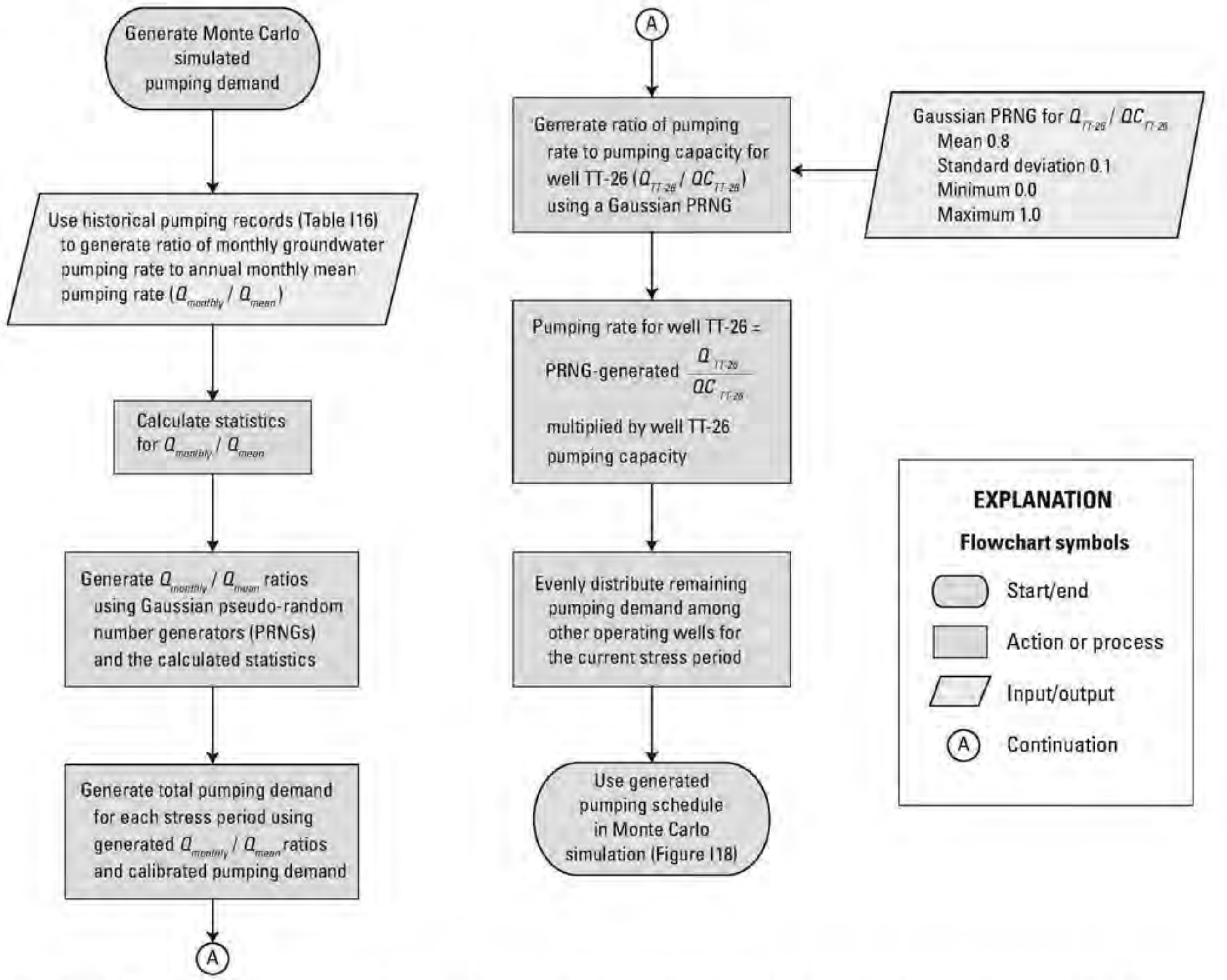

Figure I22. Flowchart for incorporating statistical analysis procedure used to assess historical pumping variation into Monte Carlo simulation, Tarawa Terrace and vicinity, U.S. Marine Corps Base Camp Lejeune, North Carolina.

12-month period shown in Figure I23, the mean value of the delivery of raw water to the Tarawa Terrace WTP (mean value of groundwater pumping demand) is indicated by a value for the ratio $Q_{monthly}$ / Q_{mean} of 1.0. During the months of June–October the yearly mean is exceeded; during the remaining months of the year, the $Q_{monthly}$ / Q_{mean} ratios are equal to or less than the yearly mean.

Results of the statistical analysis summarized in Tables I16–I18 and shown in Figure I23 were used to generate total pumping demand for each stress period (Figure I22) in which pumping occurred (stress periods 13–434 [January 1952–February 1987, respectively]). For each MC simulation, when pumping input data are required (Figure I18), the total pumping demand for 1978, 1980–1981, and 1983–1984 reflects the historical pumping demand data listed in Table I16 (annual total). For all other monthly stress periods, the yearly average pumping demand used for the calibrated model (Faye and Valenzuela 2007) was multiplied by the $Q_{monthly}$ / Q_{mean} ratios for each month of the year. The Gaussian PRNG procedure using the ratio-adjusted monthly pumping rates was then used to generate a pumping-demand schedule. This schedule was characterized with statistical properties of a mean and standard deviation based on the analyses of ratios listed in Table I18 and shown in Figure I23. An example of the statistically generated pumping demand used as input to MODFLOW-2000 for one MC simulation (realization) is shown in Figure I24.

After total pumping demand for each stress period was generated, it was assigned to all operating water-supply wells to create the well-package input data required by MODFLOW-2000.[26] Pumping rates for all operating Tarawa Terrace water-supply wells were calculated in accordance with the following procedure (Figure I22, middle column).

[26] A listing by stress period as to which water-supply wells were operating, for modeling purposes, is provided in the Chapter K report as supplemental information (Maslia et al. In press 2009).

Table I17. Ratios of historical monthly groundwater pumping rates to annual monthly mean pumping rates, ($Q_{monthly}$ / Q_{mean}), Tarawa Terrace, U.S. Marine Corps Base, Camp Lejeune, North Carolina.

[—, data not available]

Month	[1]Ratio of monthly groundwater pumping rate to annual monthly mean pumping rate ($Q_{monthly}$ / Q_{mean})				
	1978	1980	1981	1983	1984
January	0.997933	1.196742	0.908979	0.873453	0.912977
February	1.133921	0.942987	0.815022	0.861811	0.994327
March	0.905764	1.072386	0.940167	—	0.955492
April	0.997082	0.878245	0.981894	0.924063	0.987806
May	0.939962	0.918983	1.000581	0.987426	1.068732
June	1.098498	1.012676	1.141149	1.108409	1.027250
July	1.071147	1.158004	1.103638	1.075590	0.982961
August	1.002102	1.034021	1.060772	1.120458	1.094878
September	1.000167	1.004314	1.047799	0.988717	0.997203
October	1.126316	0.947580	—	—	1.019529
November	0.861152	0.902202	—	0.907156	1.003972
December	0.865955	0.931860	—	1.152918	0.954874

[1]Ratios of $Q_{monthly}$ / Q_{mean} computed by dividing monthly total raw water delivered to water treatment plant ($Q_{monthly}$) by annual monthly mean (Q_{mean}), listed in Table I16

Table I18. Statistical analyses of ratios of historical monthly groundwater pumping rates to annual monthly mean pumping rates, ($Q_{monthly}$ / Q_{mean}), Tarawa Terrace, U.S. Marine Corps Base, Camp Lejeune, North Carolina.[1]

Month	[2,3]Ratio of monthly groundwater pumping rate to mean annual monthly pumping rate ($Q_{T\text{-}monthly}$ / $Q_{T\text{-}mean}$)			
	Mean	Standard deviation	Minimum	Maximum
January	0.978017	0.130545	0.873453	1.196742
February	0.949614	0.124335	0.815022	1.133921
March	0.968452	0.072342	0.905764	1.072386
April	0.953818	0.051019	0.878245	0.997082
May	0.983137	0.058372	0.918983	1.068732
June	1.077596	0.055169	1.012676	1.141149
July	1.078268	0.063527	0.982961	1.158004
August	1.062446	0.047089	1.002102	1.120458
September	1.007640	0.023166	0.988717	1.047799
October	1.031142	0.089932	0.947580	1.126316
November	0.918620	0.060521	0.861152	1.003972
December	0.976402	0.123563	0.865955	1.152918

[1]Statistical analyses based on pumpage data for years 1978, 1980, 1981, 1983, and 1984—see Table I16.

[2]Ratios of $Q_{monthly}$ / Q_{mean} computed by dividing monthly total raw water delivered to water treatment plant ($Q_{monthly}$) by annual monthly mean (Q_{mean})—see Table I16.

[3]Mean, standard deviation, minimum, and maximum values derived from monthly $Q_{monthly}$ / Q_{mean} ratios—see Table I17.

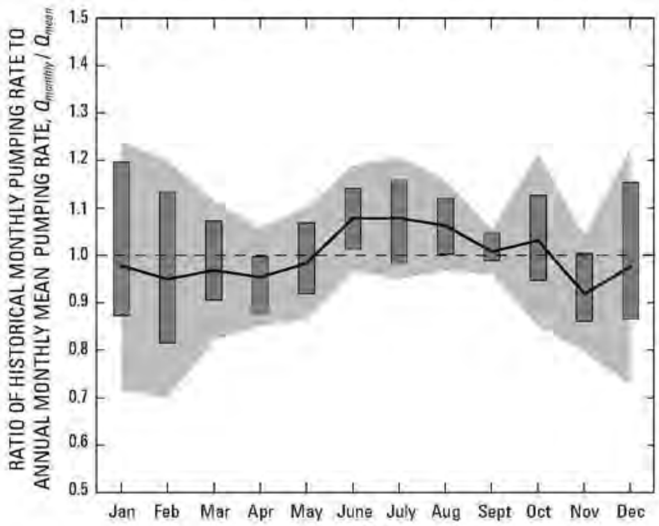

Figure I23. Results of statistical analysis of ratios of historical monthly pumping ($Q_{monthly}$) to annual monthly mean pumping (Q_{mean}), Tarawa Terrace and vicinity, U.S. Marine Corps Base Camp Lejeune, North Carolina. [Historical pumpage data sources: Henry Von Oesen and Associates, Inc. 1979; CLW 4436–4483]

1. A pumping rate to pumping capacity ratio for Tarawa Terrace water-supply well TT-26 ($Q_{TT\text{-}26} / QC_{TT\text{-}26}$) was generated using a Gaussian PRNG with a mean of 0.8 and a standard deviation of 0.1. For this ratio, the pumping rate is defined by the variable $Q_{TT\text{-}26}$, and the pumping capacity is defined by the variable $QC_{TT\text{-}26}$. The minimum and maximum values of the ratio are 0.0 and 1.0, respectively. By this definition, water-supply well TT-26 is pumping at approximately 80 percent of its capacity in a statistical sense.

2. The pumping rate assigned to water-supply well TT-26 is calculated using the statistically generated ratio $Q_{TT\text{-}26} / QC_{TT\text{-}26}$ and the known pumping capacity for water-supply well TT-26, which is 150 gallons per minute (Faye and Valenzuela 2007, Table C9).

3. The remaining pumping demand for all other Tarawa Terrace water-supply wells (total pumping demand minus pumping rate in well TT-26) is evenly distributed to all other operating water-supply wells for the stress period in question, based on each respective water-supply well's pumping capacity.

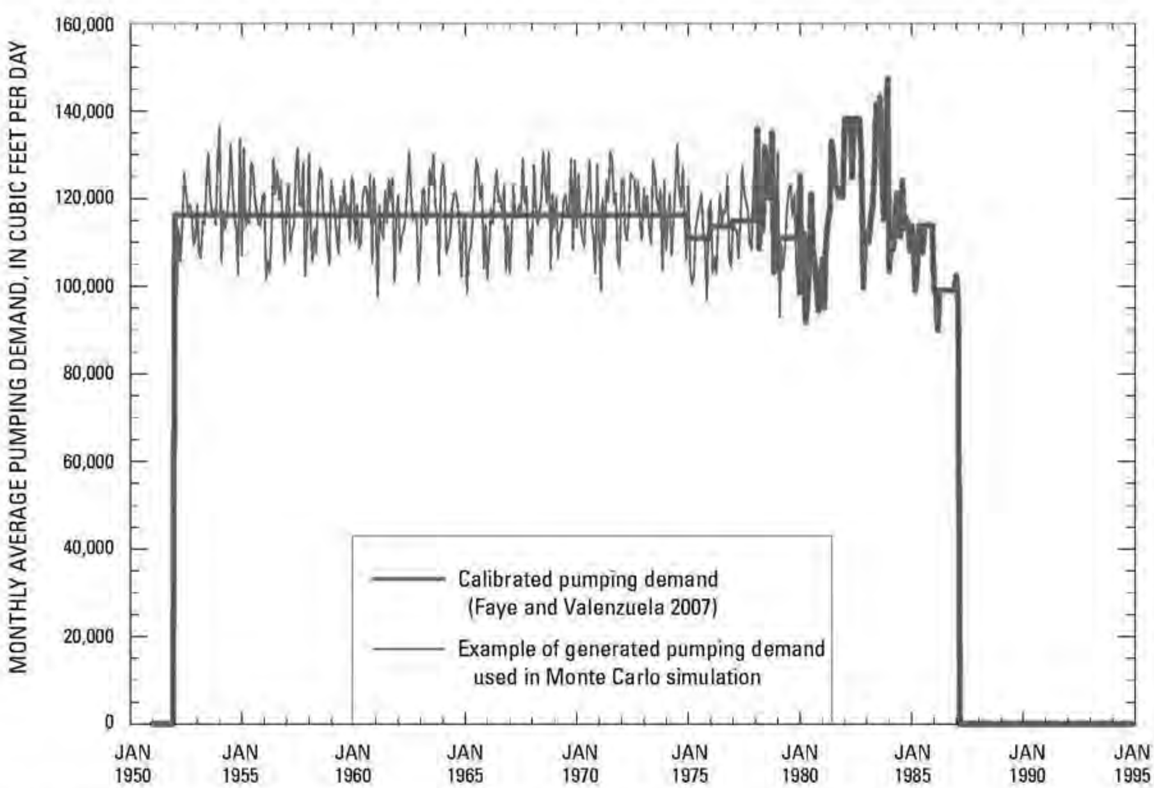

Figure I24. Comparison between calibrated pumping demand and Monte Carlo simulation generated pumping demand, Tarawa Terrace and vicinity, U.S. Marine Corps Base Camp Lejeune, North Carolina.

For the example of water-supply well TT-26, a plot of the ratio $Q_{TT\text{-}26} / QC_{TT\text{-}26}$ versus time is shown in Figure I25. Because the $Q_{TT\text{-}26} / QC_{TT\text{-}26}$ ratio was generated using a PRNG with a mean of 0.8 and a standard deviation of 0.1, the pumping rate in water-supply well TT-26 is close to 80% of its rated capacity in a statistical sense (that is, the mean value), and the rate varies from stress period to stress period. By comparison, for the calibrated model (Faye and Valenzuela 2007), the $Q_{TT\text{-}26} / QC_{TT\text{-}26}$ ratio for water-supply well TT-26 shows a mean of about 77% (Figure I25) and periods of no monthly variation.

In summary, information, data, methods, and analyses have been presented relative to three procedures that were used to generate uncertain input parameters: (1) SG simulation, used to generate random fields of horizontal hydraulic conductivity (K_H) (Figure I20); (2) PRNGs, used to generate parameter PDFs for infiltration (I_R), distribution coefficient (K_d), bulk density (ρ_b), effective porosity (n_E), reaction rate (r), mass-loading rate ($q_s C_s$), and longitudinal dispersivity (α_L) (Figure I21 and Appendix I3); and (3) statistical analysis of historical pumping variation used to generate pumping realizations through the application of a Gaussian PRNG and MC simulation (Figures I22 and I25).

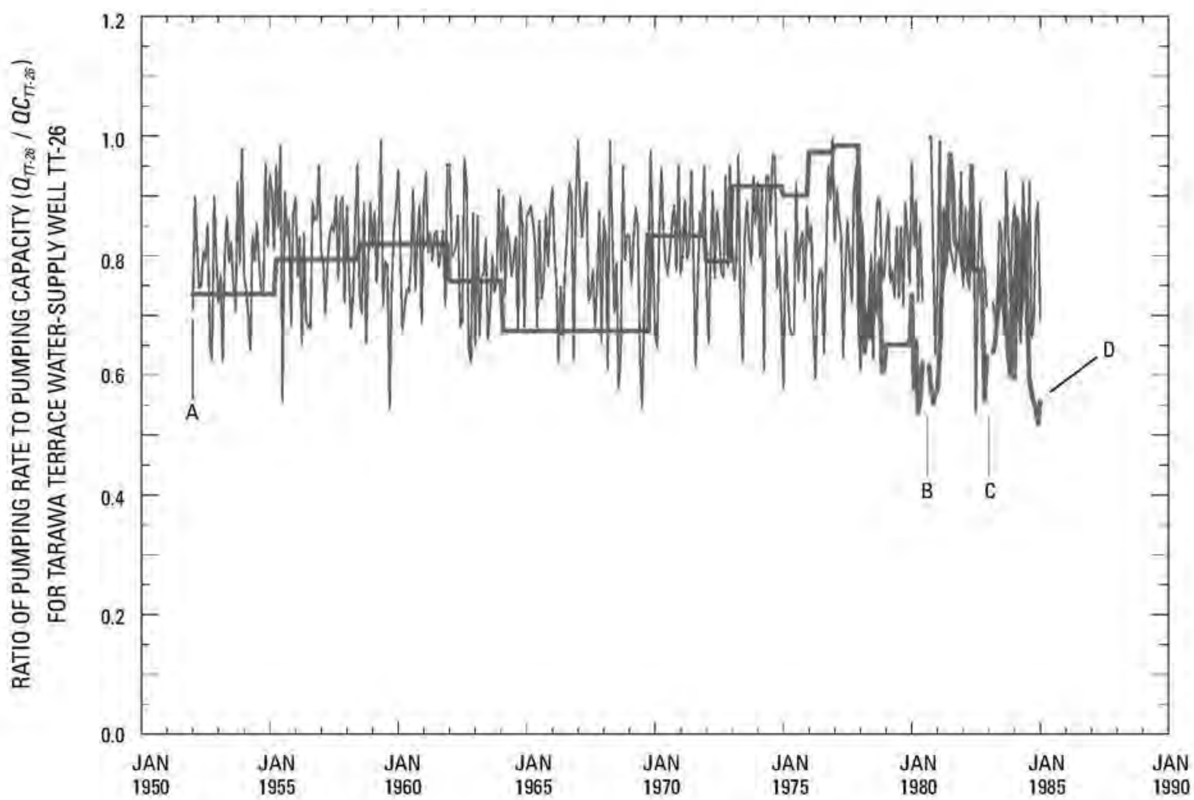

EXPLANATION

Simulation

Calibrated model (Faye and Valenzuela 2007)

Monte Carlo simulation

Well TT-26 operations

A January 1952, begin operations

B July–August 1980, not in service

C January–February 1983, not in service

D February 1985, shut down permanently

STATISTICS

	Calibrated model	Theoretical distribution	Monte Carlo simulation
Number of stress periods	393	393	393
Distribution	—	Normal	Normal
Mean	0.7722	0.8000	0.8008
Standard deviation	0.1001	0.1000	0.0963

Figure I25. Ratio of pumping rate to pumping capacity ($Q_{TT\text{-}26}$ / $QC_{TT\text{-}26}$) for water-supply well TT-26, calibrated model and Monte Carlo simulation, Tarawa Terrace, U.S. Marine Corps Base Camp Lejeune, North Carolina.

Monte Carlo Simulation

Once the uncertain input parameters (Table I15) were generated as previously described, they were applied sequentially to MODFLOW-2000 and MT3DMS groundwater-flow and contaminant fate and transport models, respectively. This probabilistic analysis process is shown conceptually in Figure I17*b*, and is shown algorithmically in a flow diagram format in Figure I18. Each MC simulation (realization) did not necessarily result in a physically plausible groundwater-flow solution based on constraints assigned to water-supply wells and selected potentiometric heads (Table I12). Realizations not resulting in physically plausible groundwater-flow solutions were discarded, in accordance with the procedure shown in the flowchart diagram (Figure I18).

Two probabilistic MC simulation scenarios were conducted (Figure I2). For scenario 1 (pumping uncertainty excluded), 840 MC simulations were initiated, and 510 realizations were successfully completed, which is a 61% success rate. For scenario 2 (pumping uncertainty included), 700 MC simulations were initiated, and 684 realizations were successfully completed, which is a 98% success rate. Determination of the total number of successful realizations was accomplished through the use of convergence or stopping criteria (Figures I18 and I26).

Three stopping criteria were used to halt the MC simulation: (1) relative change in the arithmetic mean of PCE concentration in finished water at the Tarawa Terrace WTP, $\Delta\overline{C}$; (2) relative change in the standard deviation of PCE concentration in finished water at the Tarawa Terrace WTP, $\Delta\sigma_C$; and (3) relative change in the coefficient of variation of PCE concentration in finished water at the Tarawa Terrace WTP, ΔC_V. Mathematical formulae and definitions of the aforementioned stopping criteria metrics are listed in Table I13. In applying the stopping criteria to the MC simulations, an upper and lower bound of ±0.25% was used for each metric (Figure I26). When the computed relative change ($\Delta\overline{C}$, $\Delta\sigma_C$, and ΔC_V) was within the aforementioned bounds and the total number of realizations was 500 or more, the MC simulation process was halted. As examples, the stopping criteria for each metric for scenario 1 simulations are shown graphically in Figure I26. Thus, for scenario 1—pumping uncertainty excluded—the MC simulations were halted after 510 realizations, and for scenario 2—pumping uncertainty included—the MC simulations were halted after 684 realizations. Results of the MC simulations and interpretation of the probabilistic analysis for each of the two simulation scenarios are discussed in subsequent sections of this report.

Probability of Occurrence

Probabilistic analysis results derived using MC simulation can be used to compare probabilities of occurrence. These probabilities, in turn, can be used to provide information on the probability of the occurrence of contaminated drinking water at specified concentrations (for example, the MCL). Several methods are available to derive the probabilities—mathematical, tabular, and graphical. The mathematical method refers to the analytical integration of the integral of the probability density function (Appendix I4). Analytical integration can be accomplished by the explicit solution of the integral of the probability density function or through the application of numerical integration techniques (for example, the trapezoidal Riemann sum rule—Appendix I4).

The tabular method was derived prior to the ubiquitous availability and use of computers for mathematical problem solving (for example, integration). This method uses a table of common values, referred to as the standard normal distribution table (Appendix I4). The values in this table were derived from the analytical solution of the integral of the normal probability density function. Details of the application of the tabular method for hydrologic-based problems are provided in Hann (1977). Example calculations of the probability of occurrence using Tarawa Terrace results for the mathematical and tabular methods are presented in Appendix I4.

In the graphical method, a histogram is used to estimate the probability density function. The limiting value of relative frequency or probability is defined as the ordinate value of the histogram for a selected interval or bin (Appendix I4, Figure I4.2*c*). In the ensuing discussion of Tarawa Terrace results, the application of the graphical method is described in detail, and this method is used to estimate probabilities for specific PCE concentrations of finished water at the Tarawa Terrace WTP.

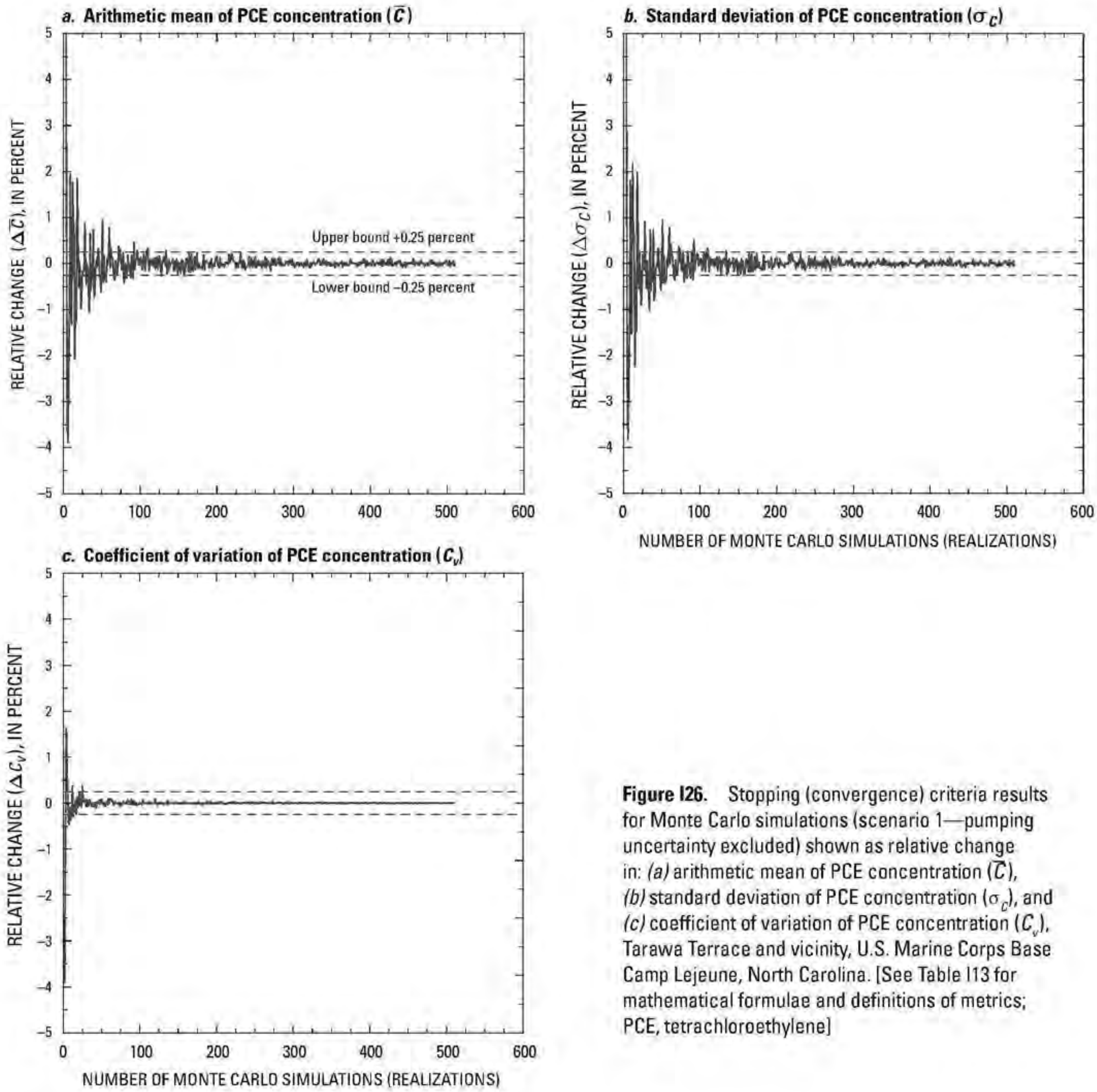

Figure I26. Stopping (convergence) criteria results for Monte Carlo simulations (scenario 1—pumping uncertainty excluded) shown as relative change in: *(a)* arithmetic mean of PCE concentration ($\overline{C}$), *(b)* standard deviation of PCE concentration (σ_C), and *(c)* coefficient of variation of PCE concentration (C_v), Tarawa Terrace and vicinity, U.S. Marine Corps Base Camp Lejeune, North Carolina. [See Table I13 for mathematical formulae and definitions of metrics; PCE, tetrachloroethylene]

Scenario 1: Pumping Uncertainty Excluded

Probabilistic analysis results of PCE concentrations in finished water for the Tarawa Terrace WTP are shown as a series of histograms for selected times: January 1958, January 1968, January 1979, and January 1985 (Figure I27). These histograms show the probability of a range of PCE-concentrations occurring during a specific month and year. For example, the probability of a PCE concentration of about 100 μg/L, occurring in finished water at the Tarawa Terrace WTP during January 1979 can be identified according to the following procedure:

1. Locate the nearest concentration range or bin that includes the 100-μg/L PCE-concentration value along the x-axis of the graph in Figure I27*c* (in this example, the histogram bar between 96 and 105 μg/L).
2. Move vertically upward until intersecting the top of the histogram bar derived from the MC simulation results.
3. Move horizontally to the left until intersecting the y-axis. For this example, the probability is between 14% and 15%.

In this example, the value on the y-axis of Figure I27*c* at the point of intersection—between 14% and 15%—is the probability that finished water at the Tarawa Terrace WTP was contaminated with a PCE concentration of about 100 μg/L during January 1979. This result, obtained using the graphical (histogram) method, is approximately the same as the result obtained using the more exact mathematical or tabular method described in Appendix I4 (13.45% and 13.66%, respectively).

As a comparison, the same procedure described above is used to determine the probability that finished water was contaminated with the same concentration of PCE (100 μg/L) during January 1985 (Figure I27*d*). For this situation, the probability that finished water at the Tarawa Terrace WTP was contaminated with a PCE concentration of about 100 μg/L during January 1985 is determined to be less than 2%. In other words, for conditions occurring during January 1985, a PCE concentration in the range of 100 μg/L is on the lower end (or "tail") of the normal distribution curve (Figure I27*d*).

MC simulation results for scenario 1 for PCE concentrations in finished water at the Tarawa Terrace WTP for all stress periods are listed in Appendix I5. In this appendix, comparisons can be made between the calibrated values reported by Faye (2008)—derived from the deterministic, single-value output—and the distributed-value output considering uncertainty and variability using the probabilistic analysis. In Appendix I5, the $P_{2.5}$, P_{50}, and $P_{97.5}$ values represent PCE concentrations in finished water at the Tarawa Terrace WTP for MC simulations at the 2.5 percentile, 50 percentile, and 97.5 percentile, respectively. Three points are noteworthy:

1. Because the calibrated parameter values were used as the mean values for input parameter PDFs and all input parameters were characterized by a normal (Gaussian) distribution except for α_L (Table I15), the 50 percentile or P_{50} values of simulated PCE concentration are close in value to the calibrated PCE concentration values.
2. The range of PCE concentrations for 95% of the MC simulations can be determined by subtracting the simulated concentration for $P_{2.5}$ from the simulated concentration for $P_{97.5}$. For example, during January 1968, the PCE concentrations corresponding to $P_{2.5}$ and $P_{97.5}$ for scenario 1 are 38.91 μg/L and 76.43 μg/L, respectively, resulting in a range of 37.52 μg/L. This range is interpreted as representing 95% of all realizations that were simulated during January 1968. Thus, based on a probabilistic analysis, the simulated PCE concentration in finished water at the Tarawa Terrace WTP during January 1968 was about 8 to 15 times greater than the current MCL for PCE of 5 μg/L.
3. Using values reported in Appendix I5, for scenario 1 (pumping uncertainty excluded), 95% of the MC simulations show that the current MCL for PCE of 5 μg/L was first exceeded in finished water at the Tarawa Terrace WTP during the period October 1957–August 1958. These results include November 1957, the date of first exceedance determined from the calibrated contaminant fate and transport model (Faye 2008) that was based on a deterministic approach (single-value parameter input and output).

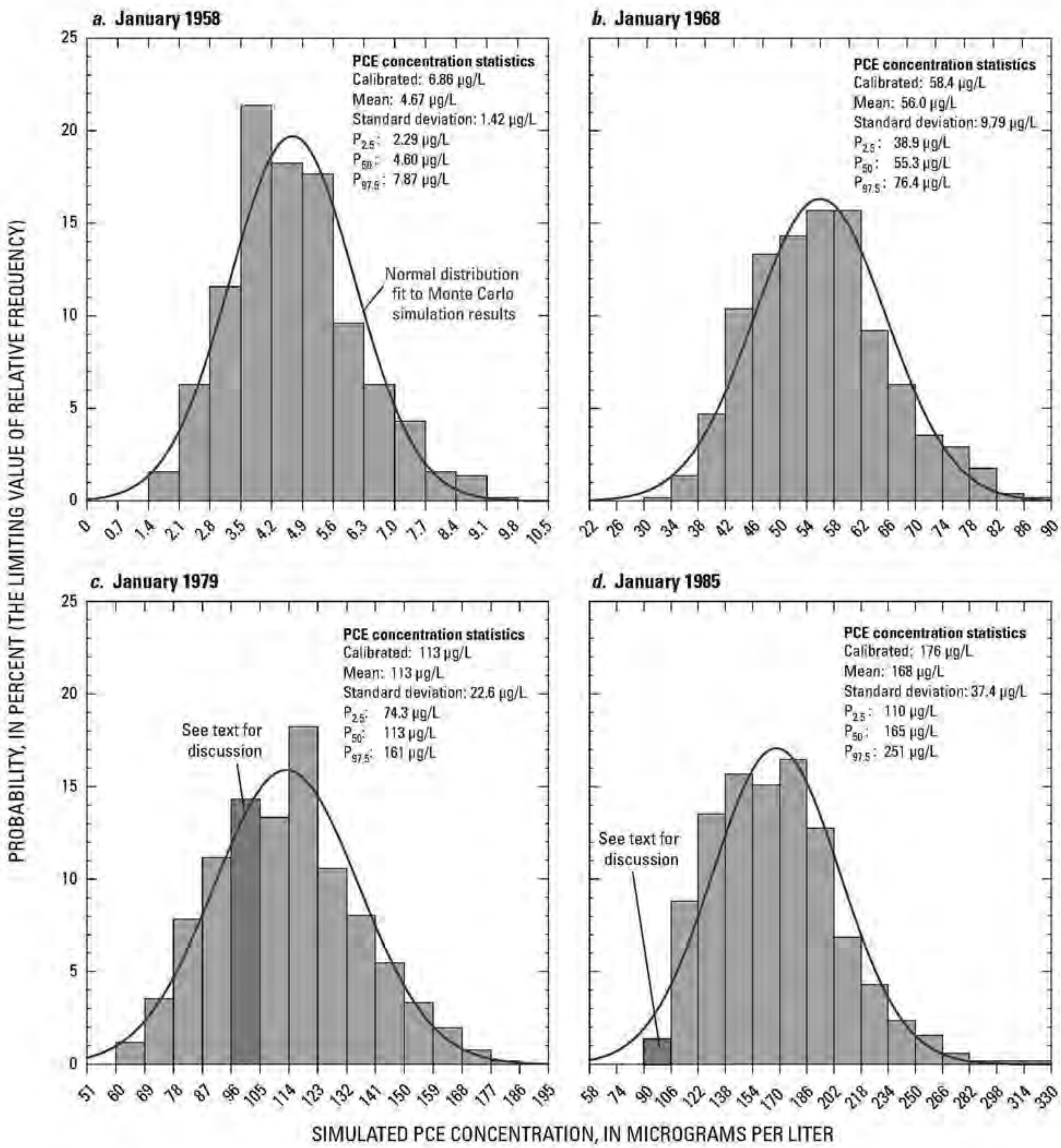

Figure I27. Probability of occurrence of tetrachloroethylene contamination in finished water at the water treatment plant derived from scenario 1 (pumping uncertainty excluded) probabilistic analysis using Monte Carlo simulation for *(a)* January 1958, *(b)* January 1968, *(c)* January 1979, and *(d)* January 1985, Tarawa Terrace, U.S. Marine Corps Base Camp Lejeune, North Carolina. [PCE, tetrachloroethylene; µg/L, micrograms per liter; $P_{2.5}$, P_{50}, and $P_{97.5}$ concentrations at 2.5, 50, and 97.5 percent, respectively; calibrated concentration from Maslia et al. 2007, Appendix A2]

For purposes of a health study or exposure assessment, epidemiologists and health scientists are interested in the probability that a person or population was exposed to a contaminant exceeding a given health guideline or criteria. An example of this is the probability that residents of Tarawa Terrace were exposed to drinking water contaminated with PCE exceeding the current MCL of 5 μg/L. To address this issue, the MC simulation results previously described can be presented in the form of the complementary cumulative probability function and plotted as a series of probability "type curves" (Figure I28). The complementary cumulative probability function describes the probability of exceeding a certain value, or shows how often a random variable (for example, the concentration of PCE in finished water) is above a certain value. Using results shown in Figure I28, the probability that the PCE concentration in finished water at the Tarawa Terrace WTP exceeded a value of 5 μg/L during January 1958 is determined in the following manner.

1. Locate the probabilistic type curve for January 1958 in Figure I28*a*.
2. Locate the 5-μg/L PCE concentration along the x-axis of the graph in Figure I28*a*.
3. Follow the vertical line until it intersects with the January 1958 complementary cumulative probability function type curve (point A, Figure I28*a*).
4. Follow the horizontal line until it intersects the y-axis—for this example, the probability is 39%.

In this case, the probability is 39% that the PCE concentration in finished water at the Tarawa Terrace WTP exceeded the current MCL of 5 μg/L during January 1958. Because the vertical MCL line does not intersect any other type curves on the graph (Figure I28*a*), the probability of exceeding the MCL for PCE is at least 99.8%, or a near certainty for all years following 1958 until water-supply wells TT-23 and TT-26 were removed from service in February 1985.[27]

Because of contaminated groundwater, water-supply well TT-26 was removed from regular service during February 1985 (Maslia et al. 2007, Table A6). This caused an immediate reduction in the PCE concentration in finished water at the Tarawa Terrace WTP because of the dilution of contaminated WTP water with water from other water-supply wells that were not contaminated or were contaminated with much lower concentrations of PCE than was water-supply well TT-26. As a result, PCE concentrations in finished water at the Tarawa Terrace WTP during February 1985–February 1987 (when the WTP was permanently closed) were significantly reduced compared with January 1985 concentrations (Maslia et al. 2007, Figure A18). Probabilistic type curves representing the complementary cumulative probability function for selected months during January 1985–February 1987 shown in Figure I28*b* also confirm this observation. For example, using the procedure described previously, the probability of exceeding the current MCL for PCE of 5 μg/L during February 1985 is about 10% (point F in Figure I28*b*), compared to a probability of 39% during January 1958 and a probability of greater than 99.8% during January 1985.

The probability type curves shown in Figure I28 also can be used to ascertain uncertainty and variability associated with simulated PCE concentrations in finished water at the Tarawa Terrace WTP. For example, referring to points B and C in Figure I28*a*, during January 1958, there is a 97.5% probability that the concentration of PCE in finished water at the Tarawa Terrace WTP exceeded 2 μg/L (point B), and correspondingly, a 2.5% probability that the concentration exceeded 8 μg/L (point C). Thus, during January 1958, 95% of MC simulation results indicate that the concentration of PCE in finished water at the Tarawa Terrace WTP was in the range of 2–8 μg/L.[28] Stated in terms of uncertainty and variability, during January 1958, the uncertainty is 5% (100% minus 95% of all MC simulation results), and the corresponding variability in PCE concentration in finished water at the Tarawa Terrace WTP is 2–8 μg/L. As a comparison, this same analysis is conducted for January 1968 (points D and E). For simulated conditions existing during January 1968 (the start of the epidemiological case-control study), 95% of MC simulation results indicate that the concentration of PCE in finished water at the Tarawa Terrace WTP was in the range of 40–80 μg/L. Stated in terms of uncertainty and variability, during January 1968, the uncertainty is 5% (100% minus 95% of all MC simulation results), and the corresponding variability in PCE concentration in finished water at the Tarawa Terrace WTP is 40–80 μg/L.

[27] Except for July and August 1980 and January and February 1983 when water-supply well TT-26 was out of service—see Figure A18 in Maslia et al. (2007).

[28] In this example, point B (Figure I28*a*) represents 97.5 percent of Monte Carlo simulations, and point C represents 2.5 percent of Monte Carlo simulations. Thus, the range of results representing 95 percent of Monte Carlo simulations is obtained by subtracting the probability-axis value of point C from point B or 97.5%–2.5%.

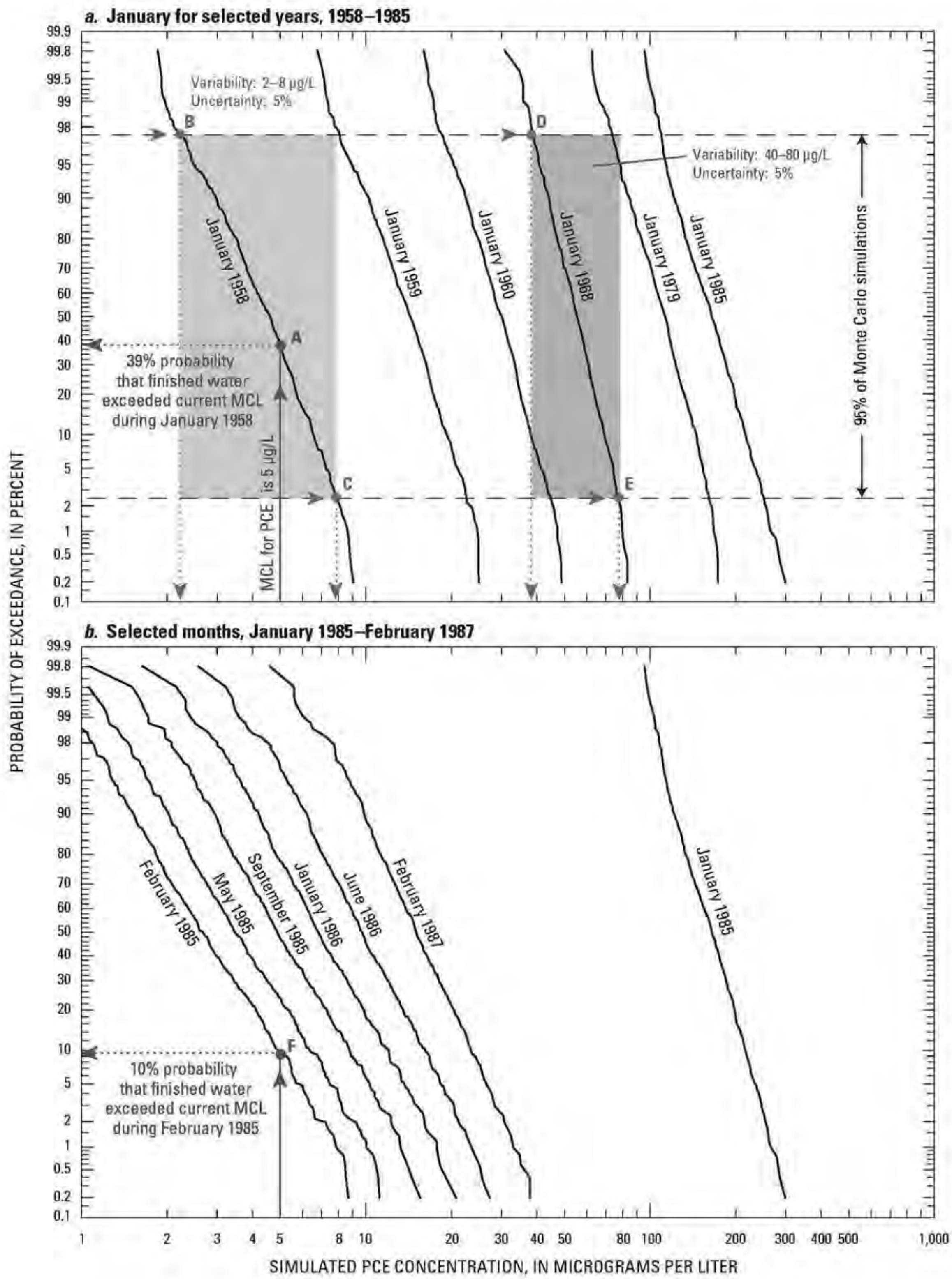

Figure I28. Probabilities of exceeding tetrachloroethylene concentrations in finished water at the water treatment plant derived from scenario 1 (pumping uncertainty excluded) probabilistic analysis using Monte Carlo simulation for *(a)* selected years, 1958–1985, and *(b)* selected months, January 1985–February 1987, Tarawa Terrace, U.S. Marine Corps Base Camp Lejeune, North Carolina (see text for discussion of points A–F). [PCE, tetrachloroethylene; MCL, maximum contaminant level; µg/L, micrograms per liter; %, percent]

The probabilistic analysis conducted using MC simulation was applied to the entire period of operation of the Tarawa Terrace WTP (January 1953–February 1987). The PCE concentration in finished water determined using the deterministic analysis (single-value parameter input and output) also can be expressed and presented in terms of a range of probabilities for the entire duration of WTP operations. Figure I29 shows the concentration of PCE in finished water at the Tarawa Terrace WTP in terms of the MC simulation results. Several results shown on this graph are worthy of further explanation.

1. The range of PCE concentrations derived from the probabilistic analysis using MC simulation is shown as a band of solutions in Figure I29 and represents 95% of all simulated results.
2. The current MCL for PCE (5 μg/L) was first exceeded in finished water during October 1957–August 1958; these solutions include November 1957, the exceedance date determined using the calibrated fate and transport model (Faye 2008), which is a deterministic modeling analysis approach.
3. The PCE concentration in Tarawa Terrace WTP finished water during January 1985, simulated using the probabilistic analysis, ranges from about 110–251 μg/L (95 percent of Monte Carlo simulations; Appendix I5). This range includes the maximum calibrated value of 183 μg/L (derived without considering uncertainty and variability using MT3DMS) and the maximum measured value of 215 μg/L (Faye 2008).

Results of the probabilistic analysis, which were obtained by using MC simulation with pumping uncertainty excluded (scenario 1), quantitatively define the uncertainty and variability of the deterministically derived results reported by Faye and Valenzuela (2007) and Faye (2008). These probabilistic results provide additional confidence that the deterministically derived results (for example, the historically reconstructed PCE concentrations in Tarawa Terrace finished water) are reasonable and conform well to field observations and data.

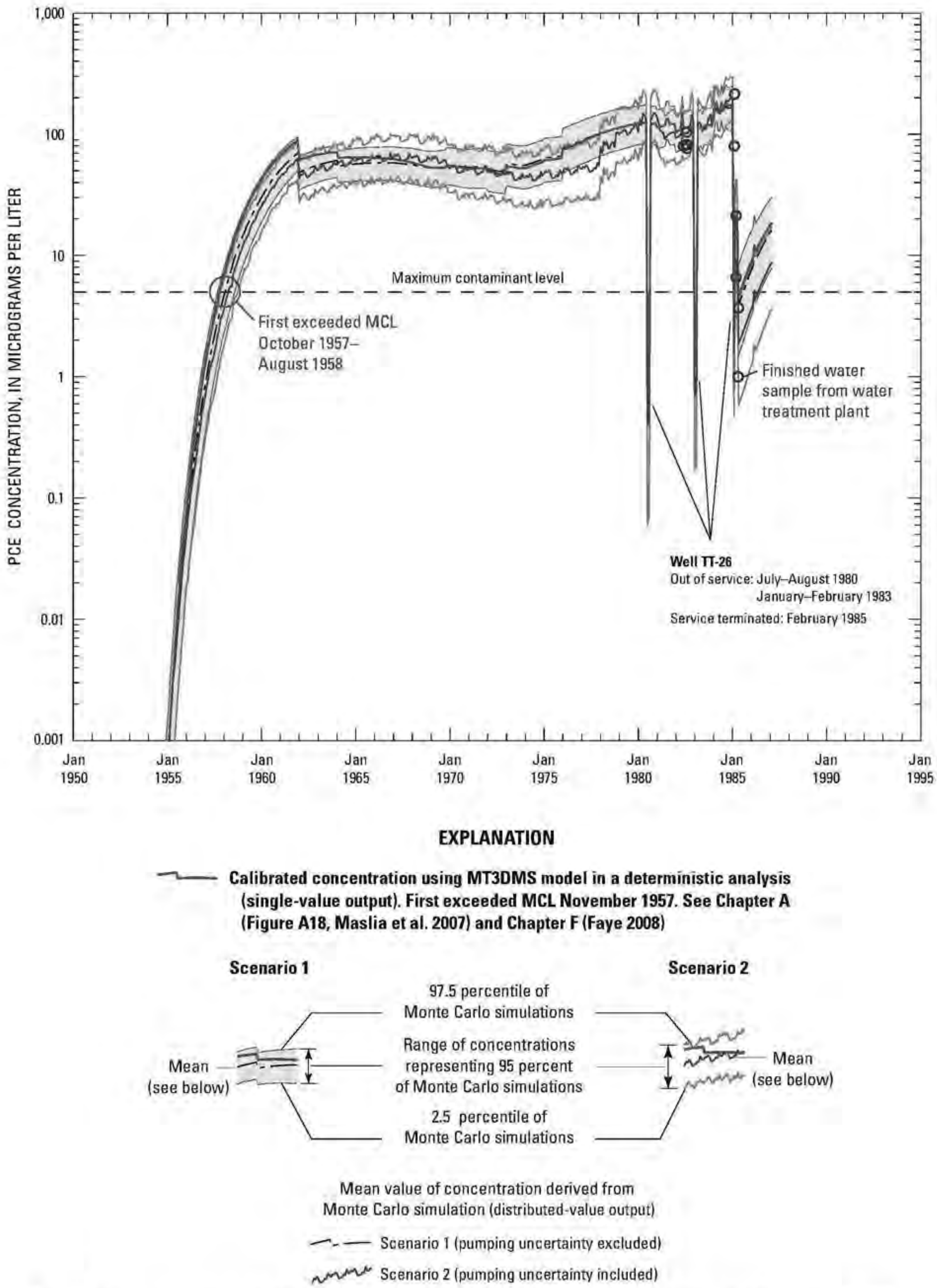

Figure I29. Concentrations of tetrachloroethylene in finished water at the water treatment plant derived from scenario 1 (pumping uncertainty excluded) and scenario 2 (pumping uncertainty included) probabilistic analyses using Monte Carlo simulation, Tarawa Terrace, U.S. Marine Corps Base Camp Lejeune, North Carolina. [See Appendix I5 for tabular listing; PCE, tetrachloroethylene; MCL, maximum contaminant level]

Scenario 2: Pumping Uncertainty Included

For the scenario 2 probabilistic analysis, pumping was characterized as an uncertain and varying input parameter (for example, Figure I24). For this scenario, probabilistic analysis results for finished water at the Tarawa Terrace WTP also are shown as a series of histograms for the same selected times used for scenario 1 results: January 1958, January 1968, January 1979, and January 1985 (Figure I30). These histograms show the probability of a range of PCE-concentration values occurring during a specific month and year. The histograms of PCE concentrations in finished water under scenario 1 (pumping uncertainty excluded) and scenario 2 (pumping uncertainty included) are similar when compared to the theoretical normal distribution fit to MC simulation results. However, under scenario 2 conditions, with the exception of results for January 1958, the range in PCE concentrations for 95% of all MC simulation results ($P_{97.5}$ minus $P_{2.5}$) indicate greater variation. For example, for January 1979, the range of 95% of all MC simulation results is 107 µg/L for scenario 2 compared with a corresponding variation of 87 µg/L for scenario 1. Similarly, for January 1985, the range of 95% of all MC simulation results is 170 µg/L for scenario 2 compared with a corresponding range of 141 µg/L for scenario 1. This increase in variation is most likely a consequence of characterizing pumping as an uncertain input parameter (scenario 2 conditions) rather than as a known quantity (scenario 1 conditions).

The probabilistic analysis conducted using MC simulation for scenario 2 conditions was applied to the entire period of operation of the Tarawa Terrace WTP (January 1953–February 1987). Similar to scenario 1, scenario 2 results also can be expressed and presented in terms of a range of probabilities for the entire duration of WTP operations. Figure I29 shows the concentration of PCE in finished water at the Tarawa Terrace WTP in terms of the MC simulation results, and comparisons can be made between scenario 1 and scenario 2 results. Tabular values for both scenario 1 and scenario 2 results in terms of the $P_{2.5}$, P_{50}, and $P_{97.5}$ values and comparisons with the deterministically calibrated values of PCE in finished water at the Tarawa Terrace WTP derived using the deterministic modeling analysis (Faye 2008) are listed in Appendix I5. Several results shown on Figure I29 are worthy of further explanation:

1. The range of PCE concentrations derived from the probabilistic analysis using MC simulations for scenario 1 and scenario 2 represent 95% of all possible results.

2. Both scenario 1 and scenario 2 indicated a date range for first exceeding the MCL for PCE (5 µg/L) of October 1957–August 1985; this range also includes the date of November 1957, derived using the deterministic modeling analysis (Faye 2008).

3. The PCE concentration in Tarawa Terrace WTP finished water during January 1985, simulated using the scenario 2 probabilistic analysis, ranges from 123–293 µg/L (95 percent of Monte Carlo simulations—see Appendix I5). As with scenario 1 results, this range includes the maximum calibrated value of 183 µg/L (derived without considering uncertainty and variability using MT3DMS) and the maximum measured value of 215 µg/L (Faye 2008).

Calibrated time-varying PCE concentrations in finished water at the Tarawa Terrace WTP (Maslia et al. 2007; Faye 2008), mean values of MC simulation results from scenario 1 (pumping uncertainty excluded), and mean values of MC simulation results from scenario 2 (pumping uncertainty included) are shown for comparison in Figure I31. Results of these comparisons indicate that the PCE concentration in finished water exceeded the current MCL for PCE of 5 µg/L during February 1958 for scenario 1 and during April 1958 for scenario 2. Recall, that for the calibrated model (single-valued, deterministic results), PCE concentration in finished water exceeded the current MCL for PCE of 5 µg/L during November 1957 (Figure I31, Inset A). Thus, compared to the calibrated, single-valued, deterministic results, accounting for input parameter uncertainty and excluding pumping uncertainty (scenario 1) resulted in a delay of 3 months (November 1957–February 1958) before finished water at the WTP exceeded the current MCL for PCE. When pumping uncertainty is included as a variant (scenario 2), the delay was 5 months (November 1957–April 1958), when compared with calibrated model results.

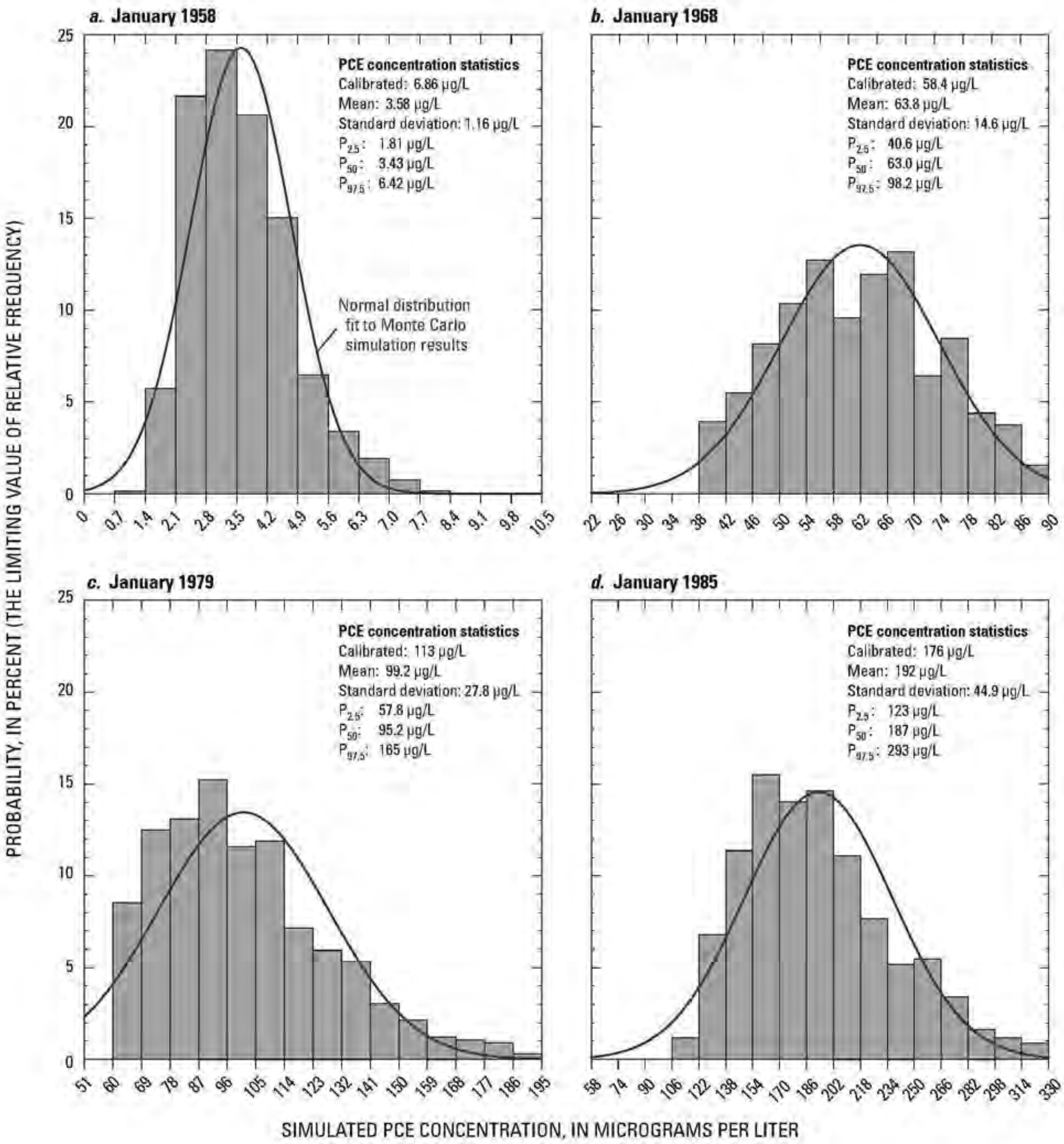

Figure I30. Probability of occurrence of tetrachloroethylene contamination in finished water at the water treatment plant derived from scenario 2 (pumping uncertainty included) probabilistic analysis using Monte Carlo simulation for *(a)* January 1958, *(b)* January 1968, *(c)* January 1979, and *(d)* January 1985, Tarawa Terrace, U.S. Marine Corps Base Camp Lejeune, North Carolina. [PCE, tetrachloroethylene; µg/L, micrograms per liter; $P_{2.5}$, P_{50}, and $P_{97.5}$ concentrations at 2.5, 50, and 97.5 percent, respectively; calibrated concentration from Maslia et al. 2007, Appendix A2]

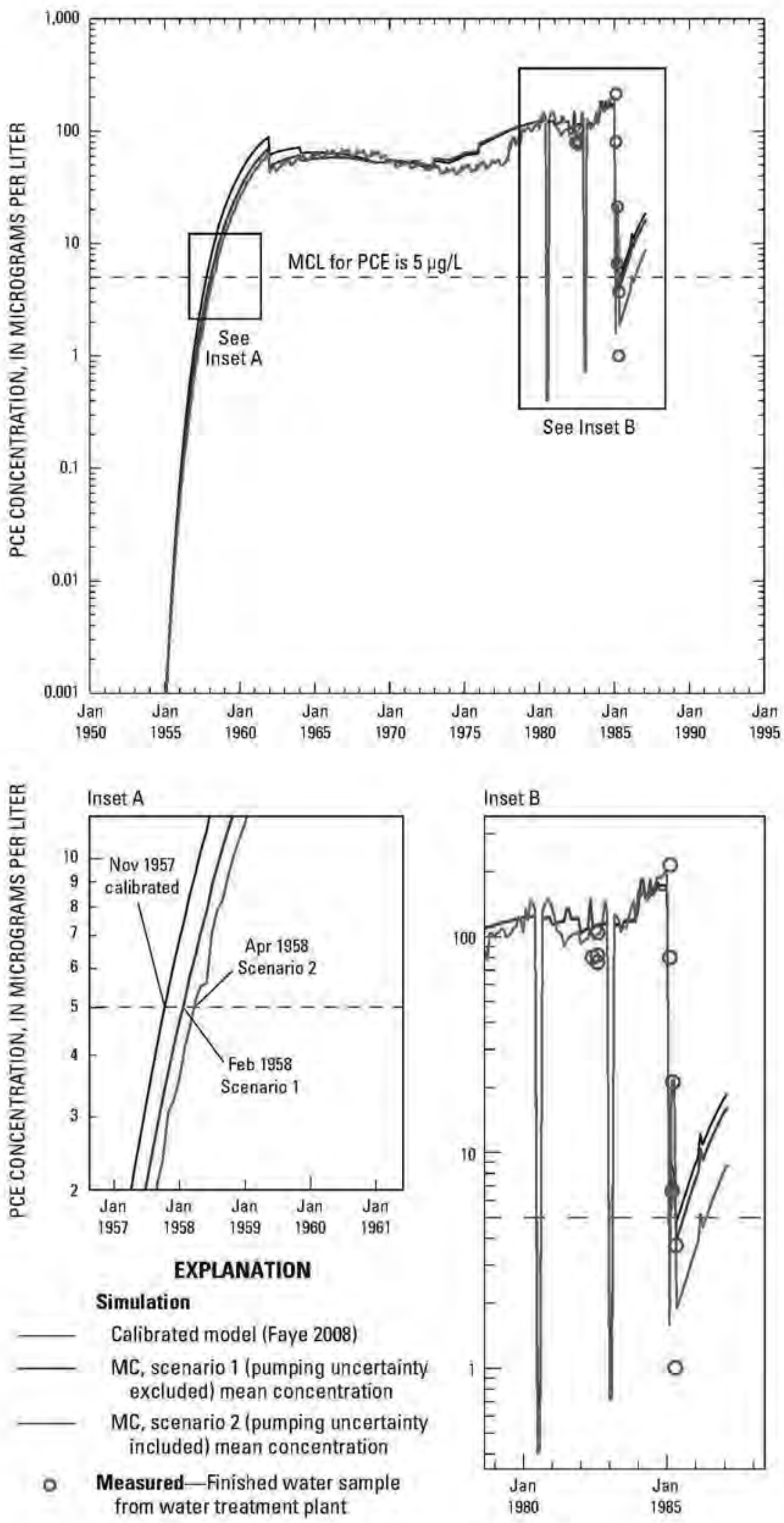

Figure I31. Concentration of tetrachloroethylene in finished water at the water treatment plant derived from deterministic (calibrated model) and probabilistic (Monte Carlo simulation) analysis, Tarawa Terrace, U.S. Marine Corps Base Camp Lejeune, North Carolina. [PCE, tetrachloroethylene; MCL, maximum contaminant level; µg/L, micrograms per liter; MC, Monte Carlo]

A series of probabilistic type curves, such as those shown in Figure I28, also were constructed for results of scenario 2. As previously explained, these type curves can be used to estimate the probability that a specified PCE concentration (for example, the MCL of 5 μg/L) was exceeded. Probabilistic type curves derived from results of scenario 2 (pumping uncertainty included) are plotted along with results from scenario 1 (pumping uncertainty excluded) in Figure I32. Using the procedure previously described for scenario 1, the probability that the current MCL for PCE (5 μg/L) is exceeded for a given date is determined as follows for scenario 2 results.

1. Locate the scenario 2 probabilistic type curve for January 1958 in Figure I32.
2. Locate the 5 μg/L PCE concentration along the x-axis of the graph in Figure I32.
3. Follow the vertical line until it intersects with the January 1958 complementary cumulative probability function type curve for scenario 2 (point A, Figure I32).
4. Follow the horizontal line until it intersects the y-axis—for the scenario 2 example, 11%.

The same procedure is used to determine the probability of exceeding the 5 μg/L PCE concentration for scenario 1 results (pumping uncertainty excluded). For this scenario, it is 39%. Thus, when including pumping uncertainty (scenario 2) as a model parameter of variation, there is about a fourfold reduction in the probability of exceeding the MCL for PCE in finished water at the Tarawa Terrace WTP during January 1958.

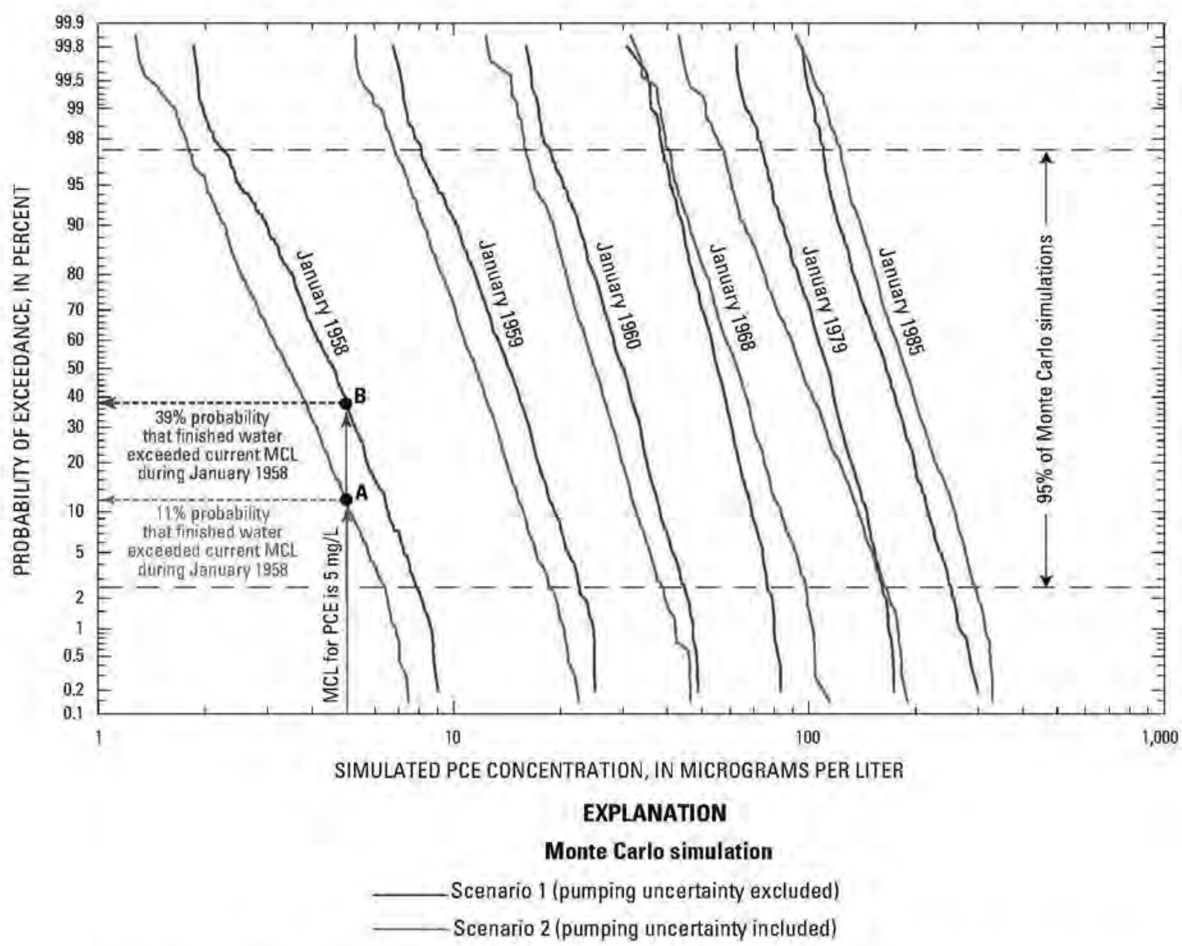

Figure I32. Probabilities of exceeding tetrachloroethylene concentration in finished water at the water treatment plant derived from probabilistic analysis (Monte Carlo simulation) with pumping uncertainty excluded (scenario 1) and included (scenario 2), Tarawa Terrace, U.S. Marine Corps Base Camp Lejeune, North Carolina. [See text for discussion of points A and B; PCE, tetrachloroethylene; MCL, maximum contaminant level; μg/L, micrograms per liter; %, percent]

Summary and Conclusions

This chapter (Chapter I) of the Tarawa Terrace report series was written to provide detailed and specific information relative to model parameter sensitivity, variability, and uncertainty associated with simulations of groundwater flow, contaminant fate and transport, and distribution of drinking water. The literature abounds with a plethora of books, research articles, and conference proceedings specifically dedicated to the topic of sensitivity, variability, uncertainty, and probabilistic analysis techniques. Some of these references are cited in the "References" section of this report. It is not the focus of this report, however, to develop an all encompassing dissertation on the aforementioned topics. Rather, the aim of this chapter report is to provide readers with an understanding of how parameter sensitivity, variability, and uncertainty have been taken into account and investigated in the course of assessing deterministically derived calibrated model results for Tarawa Terrace and vicinity. These calibrated model results are based on the application of groundwater-flow, contaminant fate and transport, and water-distribution system models described in the Chapter A (Maslia et al. 2007), Chapter C (Faye and Valenzuela 2007), Chapter F (Faye 2008), and Chapter J (Sautner et al. In press 2009) reports. Results also are based on associated data and information described in other reports—Chapter B (Faye 2007), Chapter D (Lawrence 2007), Chapter E (Faye and Green 2007), Chapter G (Jang and Aral 2008), and Chapter H (Wang and Aral 2008).

The approach used in developing the deterministically derived calibrated groundwater-flow and contaminant fate and transport models relied solely on available information (current and historical) to develop the geohydrologic framework and conceptual models of groundwater flow and contaminant fate and transport. A time-consuming and costly drilling program to gather additional site data was not part of this investigation. Thus, in addition to parameter variability in the study area, relying on available data and information also leads to parameter uncertainty, owing in part to the paucity of historical information and data.

To investigate model input parameter sensitivity, variability, and uncertainty, and model output variability and uncertainty, several methods were used. These methods ranged from the less sophisticated one-at-a-time parameter variation wherein a selected input parameter was independently varied to assess sensitivity, to a more complex parameterization using the advanced, nonlinear parameter estimation package PEST, to sophisticated probabilistic techniques that rely on numerical methods such as sequential Gaussian (SG) simulation, pseudo-random number generators (PRNGs), and Monte Carlo (MC) simulation to investigate parameter input and output uncertainty. Each of the methods has advantages and disadvantages. For example, varying one input parameter at a time is computationally efficient and provides some qualitative insight into the relative importance of selected model parameters. A probabilistic analysis, on the other hand, can be computationally expensive, requiring many hours to many days to conduct an MC simulation; however, it does provide detailed quantitative results about the range and likelihood (probability) of model outputs. This quantitative information is needed by epidemiologists to assess the reliability of historically reconstructed drinking water concentrations as part of the case-control epidemiological study. The methods presented in this report are summarized below:

1. a sensitivity analysis conducted using parameters of the groundwater-flow and contaminant fate and transport models—this sensitivity analysis included 11 parameters associated with the groundwater-flow model and 7 parameters associated with the contaminant fate and transport model;
2. a sensitivity analysis conducted to quantify the effect of the finite-difference grid cell size on groundwater-flow model output;
3. a sensitivity analysis conducted to quantify the effect of time-step size on contaminant fate and transport model output;
4. a sensitivity analysis conducted to quantify the relative importance of water-distribution system model parameters by conducting analyses of storage-tank mixing models and by using the parameter estimation package, PEST; and
5. Monte Carlo analyses using selected groundwater-flow and contaminant fate and transport model parameters with and without considering pumping uncertainty.

The sensitivity analysis method was used in this study to ascertain the dependency of model output, such as tetrachloroethylene (PCE) concentration in finished water at the Tarawa Terrace water treatment plant (WTP), on certain model input parameters (for example, horizontal hydraulic conductivity or mass-loading rate). The sensitivity analysis approach used is referred to as a one-at-a-time design or experiment and was conducted by changing the values of input parameters of the calibrated models one at a time and then quantifying the variation in the output parameter (Tables I5–I7; Figures I4–I6). Results from these sensitivity analyses indicated that horizontal hydraulic conductivity was the most sensitive parameter for the groundwater-flow model (Figure I4*a*, *b*) and reaction rate and mass-loading rate were the most sensitive parameters for the contaminant fate and transport model (Figure I4*c*, *d*).

Properties of numerical models such as the design of the computational grid (cell size) and temporal discretization (time-step size) also can have an effect on model output, and quantifying and understanding the effect of the aforementioned numerical properties on output variables are important. Therefore, sensitivity analyses were conducted on the groundwater-flow and contaminant fate and transport models by varying the calibrated model cell size and time-step size (Figure I8 and Table I8, respectively). Results of the cell-size sensitivity analysis indicated that refining the calibrated model grid from cell sizes of 50 ft per side to 25 ft per side did not appreciably provide improved accuracy of computation in terms of simulated drawdown at water-supply wells (Figure I8). Refining time-step sizes from 30 and 31 days used in the calibrated

models to 1 day indicated that PCE concentrations at water-supply wells TT-23 and TT-26 were unaffected by numerical oscillations that could be caused by inappropriate temporal discretization (Table I8).

Two types of sensitivity analyses were conducted on results obtained from applying the EPANET 2 model (Rossman 2000) to the Tarawa Terrace and Holcomb Boulevard water-distribution systems. These analyses consisted of ascertaining the effect of: (1) storage-tank mixing model choice and (2) sensitivity of the model to material roughness coefficients (C-factor) and demand-pattern factors using the advanced parameter estimation modeling package, PEST (Doherty 2005). Sensitivity analysis results comparing four storage-tank models (continuous stirred-tank reactor; two-compartment storage tank; first-in, first-out plug-flow storage tank; and last-in, first-out plug-flow storage tank) with measured data indicated that the choice of mixing model does make a difference (Figures I12 and I13) and that water-quality dynamics associated with monitoring locations and source characterization also can affect modeling results. Using PEST to estimate and optimize C-factor values indicated that the Tarawa Terrace water-distribution system model is relatively insensitive to C-factor values (Table I9). Still, the model was more sensitive to polyvinyl chloride pipe C-factor variation than to cast iron pipe C-factor variation (Figure I14). With respect to demand-pattern factors, PEST was used to optimize values by minimizing the sum of squared differences between measured and simulated hydraulic head. Overall, the PEST-derived demand-pattern factors resulted in lower root-mean-square values, greater correlation coefficients, and closer matches between measured and simulated hydraulic heads in the storage tanks (Figure I16 and Table I10).

A probabilistic analysis was used to generate uncertainties in model inputs (for example, horizontal hydraulic conductivity) so that estimates of uncertainty and variability in model output (for example, PCE concentration in finished water at the Tarawa Terrace WTP) could be made. MC simulation was used to quantify model uncertainty and variability. In the probabilistic analysis, selected input parameters of the deterministically derived calibrated groundwater-flow and contaminant fate and transport models were characterized using the SG simulation and MC simulation methods. Results were obtained in terms of distributed-value output that was used to assess model uncertainty and parameter variability. Customized computer codes were developed for incorporating the two-stage MC simulation process into the Tarawa Terrace models (Figure I18). The probabilistic analysis described herein can be summarized in four steps: (1) selection of uncertain input parameters; (2) generation of uncertain input parameters using SG simulation, PRNG, or statistical analysis of historical pumping variation; (3) incorporating the statistical distributions of input parameters into the groundwater-flow and contaminant fate and transport models; and (4) using MC simulation to obtain physically plausible distributions of model output (that is, potentiometric heads, groundwater velocities, PCE concentrations in groundwater, and PCE concentrations in finished water at the Tarawa Terrace WTP).

For the probabilistic analysis, eight input parameters were assumed to be uncertain and variable: (1) horizontal hydraulic conductivity, (2) infiltration, (3) distribution coefficient, (4) bulk density, (5) effective porosity, (6) reaction rate, (7) mass-loading rate, and (8) longitudinal dispersivity (Table I15). Two MC simulation scenarios were investigated. For scenario 1, water-supply well pumping uncertainty was excluded from the probabilistic analysis; for scenario 2, water-supply well pumping uncertainty was included in the probabilistic analysis (Figure I24).

For scenario 1 (pumping uncertainty excluded), 95% of MC simulation results indicate the maximum contaminant level for PCE of 5 μg/L was first exceeded in finished water during October 1957–August 1958 (Figure I29; Appendix I5). For scenario 2 (pumping uncertainty included) 95% of MC simulation results indicate the current MCL for PCE of 5 μg/L was first exceeded in finished water during November 1957–October 1958 (Appendix I5). Furthermore, results for both scenario 1 and scenario 2 show the PCE concentration in finished water during January 1985, simulated using the probabilistic analysis, ranged from about 110 to 293 μg/L (95% of MC simulations, Appendix I5). This range includes the maximum calibrated value of 183 μg/L (derived without considering uncertainty and variability using MT3DMS) and the maximum measured value of 215 μg/L (Faye 2008). Therefore, these probabilistic analysis results, obtained by using MC simulation and including and excluding pumping uncertainty, provide additional confidence that the historically reconstructed PCE concentrations determined by Faye (2008) using the single-valued deterministic approach are reasonable and conform well to field observations and data.

Based on the results from the probabilistic analyses using a two-stage MC simulation approach, the following conclusions are made.

- PCE concentrations in finished water at the Tarawa Terrace WTP deterministically derived from the calibrated model (Faye 2008) are contained within the 95 percentile range ($P_{2.5}$– $P_{97.5}$) of PCE results obtained from the probabilistically derived MC simulation results (Appendix I5).
- Finished water delivered by the Tarawa Terrace WTP exceeded the current MCL for PCE of 5 μg/L as early as October 1957 and as late as October 1958 (Appendix I5) when considering pumping as both a certain and uncertain model input parameter.
- The PCE concentration in Tarawa Terrace WTP finished water during January 1985, simulated using scenario 1 probabilistic analysis (pumping uncertainty excluded), ranges from about 110 to 251 μg/L (95% of MC simulations). Using scenario 2 probabilistic analysis (pumping uncertainty included), the PCE concentration ranges from about 123 to 293 μg/L (95% of MC simulations) for January 1985. These ranges include the calibrated value of 183 μg/L (deterministic, single-value output reported in Maslia et al. [2007]) and the maximum measured value of 215 μg/L (Faye 2008).

Acknowledgments

A study of this complexity and magnitude is dependent upon the assistance, input, and suggestions of many colleagues. Thus, the authors of this report and all other chapter reports acknowledge the managers and staff of the U.S. Geological Survey Water Science Centers in Raleigh, North Carolina, and Atlanta, Georgia. In particular, the contributions of Melinda J. Chapman, Douglas A. Harned, and Stephen S. Howe are acknowledged for providing the majority of well, water-level, and pumpage data used in this study. Keith W. McFadden and Jonathan W. Musser are acknowledged for assistance with spatial analyses in preparing illustrations and with developing geodatabases, Web-based applications, and the querying system contained on the electronic media accompanying this report. Gregory C. Mayer and Edward H. Martin also are acknowledged for their administrative assistance.

The authors acknowledge the staff of the Environmental Management Division, U.S. Marine Corps Base Camp Lejeune, North Carolina. In particular, Scott A. Brewer, Brynn Ashton, Scott R. Williams, and Rick Cheng for their assistance and cooperation during the course of this study, especially for providing a large number of technical reports, maps, and historical documents, which summarize the results of groundwater remedial investigations at and in the vicinity of Tarawa Terrace.

The authors acknowledge the contributions of the U.S. Environmental Protection Agency, Region IV, Atlanta, Georgia, for providing reports and documents summarizing the results of investigations of groundwater contamination in the vicinity of ABC One-Hour Cleaners and in the northern part of Tarawa Terrace.

The authors acknowledge colleagues at ATSDR, Eastern Research Group, Inc., the Multimedia Environmental Simulations Laboratory at the Georgia Institute of Technology, and the Oak Ridge Institute for Science and Education for providing assistance and advice with all aspects of this study.

Thomas M. Plummer, Commander, U.S. Public Health Service, Indian Health Service, U.S. Department of Health and Human Services, assisted with planning, field instrumentation, and conducting tests of water-distribution systems serving Camp Lejeune, August 18–28, 2004.

Caryl J. Wipperfurth and Kimberly A. Waltenbaugh, U.S. Geological Survey Enterprise Publishing Network, assisted with the preparation of text, illustrations, and electronic media.

Availability of Model Input Data Files and Simulation Results

Calibrated model input data files developed for simulating predevelopment groundwater flow, transient groundwater flow, the fate and transport of PCE as a single species, and the distribution of water and contaminants in a water-distribution system are provided with this report in a CD–ROM format. Input files and selected output files used with the parameter estimation model, PEST, also are provided on the CD–ROM. Public-domain model codes used with these input files are available on the Internet at the following Web sites:

- Predevelopment and transient groundwater flow
  - Model code: MODFLOW-96 and MODFLOW-2000
  - Web site: *http://water.usgs.gov/nrp/gwsoftware/modflow.html*
- Fate and transport of PCE as a single species
  - Model code: MT3DMS
  - Web site: *http://hydro.geo.ua.edu/*
- Distribution of water and contaminants in a water-distribution system
  - Model code: EPANET 2
  - Web site: *http://www.epa.gov/nrmrl/wswrd/epanet.html*
- Model-independent parameter estimation
  - Model code: PEST
  - Web site: *http://www.sspa.com/pest/*

Readers desiring information about the model input data files contained on the CD-ROM or simulation results may also contact the Project Officer of ATSDR's Exposure-Dose Reconstruction Program at the following address:

Morris L. Maslia, P.E., D.WRE, DEE
Agency for Toxic Substances and Disease Registry
4770 Buford Highway, N.E., Mail Stop F-59
Atlanta, Georgia 30341-3717
Telephone: (770) 488-3842
Fax: (770) 488-1536
Email: *mmaslia@cdc.gov*

References

Absoft Pro FORTRAN v10.0. Absoft Corporation. Rochester Hills, MI. 2005. [cited 2008 July 30]; Available from *http://www.absoft.com/*

Anderson MP, and Woessner WW. Applied Groundwater Modeling. San Diego, CA: Academic Press, Inc.; 1992.

Barnes R. Variogram Tutorial. Golden Software, Inc. Golden, CO. 2003. [cited 2008 August 2]; Available from *http://www.goldensoftware.com/variogramTutorial.pdf*

Boulos PF, Grayman WM, Bowcock RW, Clapp JW, Rossman LA, Clark RM, Deininger RA, and Dhingra AK. Hydraulic Mixing and Free Chlorine Residual in Reservoirs. Journal of the American Water Works Association. 1996; 88(7):48–59.

Boulos PF, Lansey KE, and Karney BW. Comprehensive Water Distribution System Analysis Handbook for Engineers and Planners. Pasadena, CA: MWH Soft; 2006.

Cesario L. Modeling, Analysis, and Design of Water Distribution Systems. Denver, CO: American Water Works Association; 1995.

Chiang W-H, and Kinzelbach W. 3D-Groundwater Modeling with PMWIN: A Simulation System for Modeling Groundwater Flow and Pollution. New York: Springer-Verlag Berlin Heidelberg; 2001.

Clark RM, and Grayman WM. Modeling Water Quality in Drinking Water Distribution Systems. Denver, CO: American Water Works Association; 1998.

CLW, Camp Lejeune Water Documents, 0001–8761 (not consecutively available), provided on DVD format, in Maslia ML, Sautner JB, Faye RE, Suárez-Soto RJ, Aral MM, Grayman WM, Jang W, Wang J, Bove FJ, Ruckart PZ, Valenzuela C, Green JW Jr, and Krueger AL. Analyses of Groundwater Flow, Contaminant Fate and Transport, and Distribution of Drinking Water at Tarawa Terrace and Vicinity, U.S. Marine Corps Base Camp Lejeune, North Carolina: Historical Reconstruction and Present-Day Conditions—Chapter A: Summary of Findings. Atlanta, GA: Agency for Toxic Substances and Disease Registry; 2007.

Cooley RL. A Method for Estimating Parameters and Assessing Reliability for Models of Steady-State Groundwater Flow, 1. Theory and Numerical Properties. Water Resources Research. 1977;13(2):318–324.

Cooley RL. A Method for Estimating Parameters and Assessing Reliability for Models of Steady-State Groundwater Flow, 2. Application of Statistical Analysis. Water Resources Research. 1979;15(3):603–617.

Cooley RL. Comparison of Several Methods of Solving Nonlinear Regression Groundwater Flow Problems. Water Resources Research. 1985; 21(10):1525–1538.

Cowles MK, and Carlin BP. Markov Chain Monte Carlo Convergence Diagnostics: A Comparative Review. Journal of the American Statistical Association. 1996;91:883–904.

Cullen AC, and Frey HC. Probabilistic Techniques in Exposure Assessment: A Handbook for Dealing with Variability and Uncertainty in Models and Inputs. New York: Plenum Press; 1999.

Daus AD, and Frind EO. An Alternating Direction Galerkin Technique for Simulation of Contaminant Transport in Complex Ground Water Systems. Water Resources Research. 1985;21(5):653–654.

Davis JC. Statistics and Data Analysis in Geology. 2nd ed. New York: John Wiley & Sons; 1973.

Deutsch CV, and Journel AG. GSLIB Geostatistical Software Library and User's Guide. 2nd ed. New York: Oxford University Press; 1998.

Doherty J. Groundwater Data Utilities/Part B: Program Descriptions. 2005. [cited 2007 January 31]: Available from *http://www.sspa.com/pest/utilities.shtml*

ECG, Inc. Marine Corps Base Camp Lejeune and Marine Corps Air Station, New River, Water Conservation Analysis. Vienna, VA: ECG, Inc.; 1999.

Faye RE. Analyses of Groundwater Flow, Contaminant Fate and Transport, and Distribution of Drinking Water at Tarawa Terrace and Vicinity, U.S. Marine Corps Base Camp Lejeune, North Carolina: Historical Reconstruction and Present-Day Conditions—Chapter B: Geohydrologic Framework of the Castle Hayne Aquifer System. Atlanta, GA: Agency for Toxic Substances and Disease Registry; 2007.

Faye RE. Analyses of Groundwater Flow, Contaminant Fate and Transport, and Distribution of Drinking Water at Tarawa Terrace and Vicinity, U.S. Marine Corps Base Camp Lejeune, North Carolina: Historical Reconstruction and Present-Day Conditions—Chapter F: Simulation of the Fate and Transport of Tetrachloroethylene (PCE). Atlanta, GA: Agency for Toxic Substances and Disease Registry; 2008.

Faye RE, and Green JW Jr. Analyses of Groundwater Flow, Contaminant Fate and Transport, and Distribution of Drinking Water at Tarawa Terrace and Vicinity, U.S. Marine Corps Base Camp Lejeune, North Carolina: Historical Reconstruction and Present-Day Conditions—Chapter E: Occurrence of Contaminants in Groundwater. Atlanta, GA: Agency for Toxic Substances and Disease Registry; 2007.

Faye RE, and Valenzuela C. Analyses of Groundwater Flow, Contaminant Fate and Transport, and Distribution of Drinking Water at Tarawa Terrace and Vicinity, U.S. Marine Corps Base Camp Lejeune, North Carolina: Historical Reconstruction and Present-Day Conditions—Chapter C: Simulation of Groundwater Flow. Atlanta, GA: Agency for Toxic Substances and Disease Registry; 2007.

Gelhar LW, Welty C, and Rehfeldt KR. A Critical Review of Data on Field-Scale Dispersion in Aquifers. Water Resources Research. 1992;28(7):1955–1973.

Golden Software, Inc. Surfer User's Guide. Golden, CO: Golden Software, Inc.; 1999.

Grayman WM, and Clark RM. Using Computer Models to Determine the Effect of Storage on Water Quality. Journal of the American Water Works Association. 1993;85(7):67–77.

Grayman WM, Deininger RA, Green A, Boulos PF, Bowcock RW, and Godwin CC. Water Quality and Mixing Models for Tanks and Reservoirs. Journal of the American Water Works Association. 1996;88(7):60–73.

Grayman WM, Rossman LA, Deininger RA, Smith CD, Arnold CN, and Smith JF. Mixing and Aging of Water in Distribution System Storage Facilities. Journal of the American Water Works Association. 2004;96(9):70–80.

Grayman WM, Maslia ML, and Sautner JB. Calibrating Distribution System Models with Fire-Flow Tests. Opflow, American Water Works Association. 2006 April:32(4)10–12.

Harbaugh AW, Banta ER, Hill MC, and McDonald MG. MODFLOW-2000, The U.S. Geological Survey Modular Ground-Water Model: User Guide to Modularization Concepts and the Ground-Water Flow Process. Reston, VA: U.S. Geological Survey Open-File Report 00–92; 2000.

Harbaugh AW, and McDonald MG. Programmer's Documentation for MODFLOW-96, an Update to the U.S. Geological Survey Modular Finite-Difference Ground-Water Flow Model. Reston, VA: U.S. Geological Survey Open-File Report 96–486; 1996.

Henry Von Oesen and Associates, Inc. Study of Two Water Plants, Tarawa Terrace-Montford Point, Camp Lejeune, North Carolina: Henry Von Oesen and Associates, Inc.; 1979.

Hill MC, and Tiedman CR. Effective Groundwater Model Calibration. Hoboken, NJ: John Wiley & Sons; 2007.

Hoffman F. Retardation of Volatile Organic Compounds in Groundwater in Low Organic Carbon Sediments—Interim Report. Oak Ridge, TN: U.S. Department of Energy, Lawrence Livermore National Laboratory; 1995.

Howard PH, Boethling RS, and Jarvis WF. Handbook of Environmental Degradation Rates 1st ed. Ann Arbor, MI: Lewis Publishers; 1991.

IMSL. FORTRAN Numerical Library, V 5. Visual Numerics, Inc. San Ramon, CA. 2003. [cited: 2008 July 30]; Available from *http://www.visualnumerics.com*

Jang W, and Aral MM. Analyses of Groundwater Flow, Contaminant Fate and Transport, and Distribution of Drinking Water at Tarawa Terrace and Vicinity, U.S. Marine Corps Base Camp Lejeune, North Carolina: Historical Reconstruction and Present-Day Conditions—Chapter G: Simulation of Three-Dimensional Multispecies, Multiphase Mass Transport of Tetrachloroethylene (PCE) and Associated Degradation By-Products. Atlanta, GA: Agency for Toxic Substances and Disease Registry; 2008.

Kennedy MS, Moegling S, Sarikelle S, and Suravallop K. Assessing the Effects of Storage Tank Design on Water Quality. Journal of the American Water Works Association. 1993:85(7)78–88.

Kitanidis PK. Introductions to Geostatistics Application in Hydrogeology. New York, NY: Cambridge University Press; 1997.

Lawrence SJ. Analyses of Groundwater Flow, Contaminant Fate and Transport, and Distribution of Drinking Water at Tarawa Terrace and Vicinity, U.S. Marine Corps Base Camp Lejeune, North Carolina: Historical Reconstruction and Present-Day Conditions—Chapter D: Properties of Degradation Pathways of Common Organic Compounds in Groundwater. Atlanta, GA: Agency for Toxic Substances and Disease Registry; 2007.

Maslia ML. Expert Peer Review Panel Evaluating ATSDR's Water-Modeling Activities in Support of the Current Study of Childhood Birth Defects and Cancer at U.S. Marine Corps Base Camp Lejeune, North Carolina: Atlanta, GA: Agency for Toxic Substances and Disease Registry; 2005.

Maslia ML and Aral MM. Analytical Contaminant Transport Analysis System (ACTS)—Multimedia Environmental Fate and Transport. Practice Periodical of Hazardous, Toxic, and Radioactive Waste Management. 2004 July:181–198.

Maslia ML, Sautner JB, and Aral MM. Analysis of the 1998 Water-Distribution System Serving the Dover Township Area, New Jersey: Field-Data Collection Activities and Water-Distribution System Modeling. Atlanta, GA: Agency for Toxic Substances and Disease Registry; 2000.

Maslia ML, Sautner JB, Aral MM, Gillig RE, Reyes JJ, and Williams RC. Historical Reconstruction of the Water-Distribution System Serving the Dover Township Area, New Jersey: January 1962–December 1996. Atlanta, GA: Agency for Toxic Substances and Disease Registry; 2001 October.

Maslia ML, Sautner JB, Valenzuela C, Bove FJ, and Aral MM. Field Data Collection Activities for Water-Distribution Systems Serving Marine Corps Base Camp Lejeune, North Carolina. Preliminary Test and Tracer Study of the Hadnot Point Water-Distribution System: Draft Work Plan. Atlanta, GA: Agency for Toxic Substances and Disease Registry; 2004.

Maslia ML, Sautner JB, Valenzuela C, Grayman WM, Aral MM, and Green JW Jr. Use of Continuous Recording Water-Quality Monitoring Equipment for Conducting Water-Distribution System Tracer Tests: The Good, the Bad, and the Ugly. Proceedings: World Environmental and Water Resources Congress; 2005 May 15–19; Anchorage, AK; 2005.

Maslia ML, Sautner JB, Faye RE, Suárez-Soto RJ, Aral MM, Grayman WM, Jang W, Wang J, Bove F, Ruckart PZ, Valenzuela C, Green JW Jr, and Krueger AL. Analyses of Groundwater Flow, Contaminant Fate and Transport, and Distribution of Drinking Water at Tarawa Terrace and Vicinity, U.S. Marine Corps Base Camp Lejeune, North Carolina: Historical Reconstruction and Present-Day Conditions—Chapter A: Summary of Findings. Atlanta, GA: Agency for Toxic Substances and Disease Registry; 2007.

Maslia ML, Sautner JB, Faye RE, Suárez-Soto RJ, Aral MM, Grayman WM, Jang W, Wang J, Bove F, Ruckart PZ, Valenzuela C, Green JW Jr, and Krueger AL. Analyses of Groundwater Flow, Contaminant Fate and Transport, and Distribution of Drinking Water at Tarawa Terrace and Vicinity, U.S. Marine Corps Base Camp Lejeune, North Carolina: Historical Reconstruction and Present-Day Conditions—Chapter K: Supplemental Information. Atlanta, GA: Agency for Toxic Substances and Disease Registry; In press 2009.

Masters GM. Introduction to Environmental Engineering and Science. 2nd ed. Upper Saddle River, NJ: Prentice Hall; 1998.

Molak V. Fundamentals of Risk Analysis and Risk Management. Boca Raton, FL: Lewis Publishers; 1997.

Morris DA, and Johnson AI. Summary of Hydrologic and Physical Properties of Rock and Soil Materials, as Analyzed by the Hydrologic Laboratory of the U.S. Geological Survey, 1948–60. Washington, DC: U.S. Geological Survey Water-Supply Paper 1839–D; 1967.

North Carolina Rural Economic Development Center. Water 2030 Report North Carolina Water Supply and Demand, 2005–2030. 2006. [cited 14 August 2008]; Available from *http://www.ncruralcenter.org/pubs/*

Nyhoff L, and Leestma S. FORTRAN 77 for Engineers and Scientists, with an Introduction to FORTRAN 90. 4th ed. Upper Saddle River, New Jersey: Prentice Hall; 1996.

Olea RA. Geostatistics for Engineers and Earth Scientists. Boston, MA: Kluwer Academic Publishers; 1999.

Palisade Corporation. @RISK Advanced Risk Analysis for Spreadsheets. Newfield, NY: Palisade Corporation; 2004. p. 503.

Palisade Corporation. Guide to Using @RISK: Risk Analysis and Simulation Add-In for Microsoft® Excel. Version 5.0. Ithica, NY; May 2008.

Pankow JF, and Cherry JA. Dense Chlorinated Solvents and Other DNAPLs in Groundwater: History, Behavior, and Remediation: Waterloo Press; 1996.

Roberts PJW, and Tian X. Application of Three-Dimensional Laser-Induced Fluorescence to Stratified Turbulent Mixing Process. Proceedings: American Society of Civil Engineers, Hydraulic Measurements and Experimental Methods Conference, 2002 July 28–August 1, Estes Park, CO.

Roberts PWJ, Tian X, Soitropoulos F, and Duer M. Physical Modeling of Mixing in Water Storage Tanks. Denver, CO: American Water Works Association Research Foundation Report; 2005.

Rogers JF, Kilough GG, Thompson SJ, Addy CL, McKeown RE, and Cowen DJ. Estimating Environmental Exposures to Sulfur Dioxide from Multiple Industrial Sources for a Case-Control Study. Journal of Exposure Analysis and Environmental Epidemiology. 1999;9:535–545.

Rossman LA. EPANET 2 Users Manual. Cincinnati: U.S. Environmental Protection Agency, Nation Risk Management Research Laboratory, Report No.: EPA/600–R–00/057; 2000 September.

Rossman LA, and Grayman WM. Scale-Model Studies of Mixing on Drinking Water Storage Tanks. Journal of Environmental Engineering, American Society of Civil Engineers. 1999;125(8):755–761.

Saltelli A, Chan K, and Scott EM, eds. Sensitivity Analysis. Chichester, England: John Wiley & Sons, Ltd; 2000.

Sautner JB, Maslia ML, Valenzuela C, Grayman WM, Aral MM, and Green JW Jr. Field Testing of Water-Distribution Systems at the U.S. Marine Corps Base Camp Lejeune, North Carolina, in Support of an Epidemiologic Study. Proceedings: World Environmental and Water Resources Congress; 2005 May 15–19, Anchorage, AK.

Sautner JB, Maslia ML, and Grayman WM. Storage Tank Mixing Models: Comparison of Tracer Data with Model Simulation. Proceedings: World Environmental and Water Resources Congress; 2007 May 15–19, Tampa, FL.

Sautner JB, Valenzuela C, Maslia ML, and Grayman WM. Analyses of Groundwater Flow, Contaminant Fate and Transport, and Distribution of Drinking Water at Tarawa Terrace and Vicinity, U.S. Marine Corps Base Camp Lejeune, North Carolina: Historical Reconstruction and Present-Day Conditions—Chapter J: Field Tests, Data Analyses, and Simulation of Distribution of Drinking Water. Atlanta, GA: Agency for Toxic Substances and Disease Registry; In press 2009.

Schnoor JL. Environmental Modeling. New York: John Wiley & Sons, Inc.; 1996.

Schwartz FW, and Zhang H. Fundamentals of Ground Water. New York: John Wiley & Sons, Inc.; 2003.

Tung Y-K, and Yen B-C. Hydrosystems Engineering Uncertainty Analysis. New York: McGraw-Hill; 2005.

Uner E. Generating Random Numbers. 2004. [cited 2008 August 1]; Available from *http://www.embedded.com/columns*

U.S. Environmental Protection Agency (USEPA). Guiding Principles for Monte Carlo Analysis. Washington, DC: U.S. Environmental Protection Agency, Report No.: EPA 630–R–97–001; 1997 March.

Walski TM. Analysis of Water Distribution Systems. Malabar, FL: Krieger Publishing Company; 1992.

Walski TM, Chase DV, and Savic DA. Water Distribution Modeling, 1st ed. Waterbury, CT: Haestad Press; 2001.

Wang J, and Aral MM. Analyses of Groundwater Flow, Contaminant Fate and Transport, and Distribution of Drinking Water at Tarawa Terrace and Vicinity, U.S. Marine Corps Base Camp Lejeune, North Carolina: Historical Reconstruction and Present-Day Conditions—Chapter H: Effect of Groundwater Pumping Schedule Variation on Arrival of Tetrachloroethylene (PCE) at Water-Supply Wells and the Water Treatment Plant. Atlanta, GA: Agency for Toxic Substances and Disease Registry; 2008.

Wikipedia. The Free Encyclopedia. Pseudorandom Number Generator. 2008. [cited: 2008 August 1]; Available from *http://en.wikipedia.org/wiki/Pseudorandom_random_generator*

Zhang D. Stochastic Methods for Flow in Porous Media: Coping with Uncertainties. San Diego, CA: Academic Press; 2002.

Zheng C, and Wang PP. MT3DMS: A Modular Three-Dimensional Multi-Species Model for Simulation of Advection, Dispersion, and Chemical Reactions of Contaminants in Groundwater Systems: Documentation and User's Guide. Vicksburg, MS: U.S. Army Engineer Research and Development Center; 1999. Report No.: SERDP-99.

Appendixes

Appendix I1. Simulation stress periods and corresponding month and year.

[Jan, January; Feb, February; Mar, March; Apr, April; Aug, August; Sept, September; Oct, October; Nov, November; Dec, December]

Stress period	Month and year	Stress period	Month and year	Stress period	Month and year	Stress period	Month and year	Stress period	Month and year	Stress period	Month and year
1	Jan 1951	49	Jan 1955	97	Jan 1959	145	Jan 1963	193	Jan 1967	241	Jan 1971
2	Feb 1951	50	Feb 1955	98	Feb 1959	146	Feb 1963	194	Feb 1967	242	Feb 1971
3	Mar 1951	51	Mar 1955	99	Mar 1959	147	Mar 1963	195	Mar 1967	243	Mar 1971
4	Apr 1951	52	Apr 1955	100	Apr 1959	148	Apr 1963	196	Apr 1967	244	Apr 1971
5	May 1951	53	May 1955	101	May 1959	149	May 1963	197	May 1967	245	May 1971
6	June 1951	54	June 1955	102	June 1959	150	June 1963	198	June 1967	246	June 1971
7	July 1951	55	July 1955	103	July 1959	151	July 1963	199	July 1967	247	July 1971
8	Aug 1951	56	Aug 1955	104	Aug 1959	152	Aug 1963	200	Aug 1967	248	Aug 1971
9	Sept 1951	57	Sept 1955	105	Sept 1959	153	Sept 1963	201	Sept 1967	249	Sept 1971
10	Oct 1951	58	Oct 1955	106	Oct 1959	154	Oct 1963	202	Oct 1967	250	Oct 1971
11	Nov 1951	59	Nov 1955	107	Nov 1959	155	Nov 1963	203	Nov 1967	251	Nov 1971
12	Dec 1951	60	Dec 1955	108	Dec 1959	156	Dec 1963	204	Dec 1967	252	Dec 1971
13	Jan 1952	61	Jan 1956	109	Jan 1960	157	Jan 1964	205	Jan 1968	253	Jan 1972
14	Feb 1952	62	Feb 1956	110	Feb 1960	158	Feb 1964	206	Feb 1968	254	Feb 1972
15	Mar 1952	63	Mar 1956	111	Mar 1960	159	Mar 1964	207	Mar 1968	255	Mar 1972
16	Apr 1952	64	Apr 1956	112	Apr 1960	160	Apr 1964	208	Apr 1968	256	Apr 1972
17	May 1952	65	May 1956	113	May 1960	161	May 1964	209	May 1968	257	May 1972
18	June 1952	66	June 1956	114	June 1960	162	June 1964	210	June 1968	258	June 1972
19	July 1952	67	July 1956	115	July 1960	163	July 1964	211	July 1968	259	July 1972
20	Aug 1952	68	Aug 1956	116	Aug 1960	164	Aug 1964	212	Aug 1968	260	Aug 1972
21	Sept 1952	69	Sept 1956	117	Sept 1960	165	Sept 1964	213	Sept 1968	261	Sept 1972
22	Oct 1952	70	Oct 1956	118	Oct 1960	166	Oct 1964	214	Oct 1968	262	Oct 1972
23	Nov 1952	71	Nov 1956	119	Nov 1960	167	Nov 1964	215	Nov 1968	263	Nov 1972
24	Dec 1952	72	Dec 1956	120	Dec 1960	168	Dec 1964	216	Dec 1968	264	Dec 1972
25	Jan 1953	73	Jan 1957	121	Jan 1961	169	Jan 1965	217	Jan 1969	265	Jan 1973
26	Feb 1953	74	Feb 1957	122	Feb 1961	170	Feb 1965	218	Feb 1969	266	Feb 1973
27	Mar 1953	75	Mar 1957	123	Mar 1961	171	Mar 1965	219	Mar 1969	267	Mar 1973
28	Apr 1953	76	Apr 1957	124	Apr 1961	172	Apr 1965	220	Apr 1969	268	Apr 1973
29	May 1953	77	May 1957	125	May 1961	173	May 1965	221	May 1969	269	May 1973
30	June 1953	78	June 1957	126	June 1961	174	June 1965	222	June 1969	270	June 1973
31	July 1953	79	July 1957	127	July 1961	175	July 1965	223	July 1969	271	July 1973
32	Aug 1953	80	Aug 1957	128	Aug 1961	176	Aug 1965	224	Aug 1969	272	Aug 1973
33	Sept 1953	81	Sept 1957	129	Sept 1961	177	Sept 1965	225	Sept 1969	273	Sept 1973
34	Oct 1953	82	Oct 1957	130	Oct 1961	178	Oct 1965	226	Oct 1969	274	Oct 1973
35	Nov 1953	83	Nov 1957	131	Nov 1961	179	Nov 1965	227	Nov 1969	275	Nov 1973
36	Dec 1953	84	Dec 1957	132	Dec 1961	180	Dec 1965	228	Dec 1969	276	Dec 1973
37	Jan 1954	85	Jan 1958	133	Jan 1962	181	Jan 1966	229	Jan 1970	277	Jan 1974
38	Feb 1954	86	Feb 1958	134	Feb 1962	182	Feb 1966	230	Feb 1970	278	Feb 1974
39	Mar 1954	87	Mar 1958	135	Mar 1962	183	Mar 1966	231	Mar 1970	279	Mar 1974
40	Apr 1954	88	Apr 1958	136	Apr 1962	184	Apr 1966	232	Apr 1970	280	Apr 1974
41	May 1954	89	May 1958	137	May 1962	185	May 1966	233	May 1970	281	May 1974
42	June 1954	90	June 1958	138	June 1962	186	June 1966	234	June 1970	282	June 1974
43	July 1954	91	July 1958	139	July 1962	187	July 1966	235	July 1970	283	July 1974
44	Aug 1954	92	Aug 1958	140	Aug 1962	188	Aug 1966	236	Aug 1970	284	Aug 1974
45	Sept 1954	93	Sept 1958	141	Sept 1962	189	Sept 1966	237	Sept 1970	285	Sept 1974
46	Oct 1954	94	Oct 1958	142	Oct 1962	190	Oct 1966	238	Oct 1970	286	Oct 1974
47	Nov 1954	95	Nov 1958	143	Nov 1962	191	Nov 1966	239	Nov 1970	287	Nov 1974
48	Dec 1954	96	Dec 1958	144	Dec 1962	192	Dec 1966	240	Dec 1970	288	Dec 1974

Appendix I1. Simulation stress periods and corresponding month and year.—Continued

[Jan, January; Feb, February; Mar, March; Apr, April; Aug, August; Sept, September; Oct, October; Nov, November; Dec, December]

Stress period	Month and year	Stress period	Month and year	Stress period	Month and year	Stress period	Month and year	Stress period	Month and year
289	Jan 1975	337	Jan 1979	385	Jan 1983	433	Jan 1987	481	Jan 1991
290	Feb 1975	338	Feb 1979	386	Feb 1983	434	Feb 1987	482	Feb 1991
291	Mar 1975	339	Mar 1979	387	Mar 1983	435	Mar 1987	483	Mar 1991
292	Apr 1975	340	Apr 1979	388	Apr 1983	436	Apr 1987	484	Apr 1991
293	May 1975	341	May 1979	389	May 1983	437	May 1987	485	May 1991
294	June 1975	342	June 1979	390	June 1983	438	June 1987	486	June 1991
295	July 1975	343	July 1979	391	July 1983	439	July 1987	487	July 1991
296	Aug 1975	344	Aug 1979	392	Aug 1983	440	Aug 1987	488	Aug 1991
297	Sept 1975	345	Sept 1979	393	Sept 1983	441	Sept 1987	489	Sept 1991
298	Oct 1975	346	Oct 1979	394	Oct 1983	442	Oct 1987	490	Oct 1991
299	Nov 1975	347	Nov 1979	395	Nov 1983	443	Nov 1987	491	Nov 1991
300	Dec 1975	348	Dec 1979	396	Dec 1983	444	Dec 1987	492	Dec 1991
301	Jan 1976	349	Jan 1980	397	Jan 1984	445	Jan 1988	493	Jan 1992
302	Feb 1976	350	Feb 1980	398	Feb 1984	446	Feb 1988	494	Feb 1992
303	Mar 1976	351	Mar 1980	399	Mar 1984	447	Mar 1988	495	Mar 1992
304	Apr 1976	352	Apr 1980	400	Apr 1984	448	Apr 1988	496	Apr 1992
305	May 1976	353	May 1980	401	May 1984	449	May 1988	497	May 1992
306	June 1976	354	June 1980	402	June 1984	450	June 1988	498	June 1992
307	July 1976	355	July 1980	403	July 1984	451	July 1988	499	July 1992
308	Aug 1976	356	Aug 1980	404	Aug 1984	452	Aug 1988	500	Aug 1992
309	Sept 1976	357	Sept 1980	405	Sept 1984	453	Sept 1988	501	Sept 1992
310	Oct 1976	358	Oct 1980	406	Oct 1984	454	Oct 1988	502	Oct 1992
311	Nov 1976	359	Nov 1980	407	Nov 1984	455	Nov 1988	503	Nov 1992
312	Dec 1976	360	Dec 1980	408	Dec 1984	456	Dec 1988	504	Dec 1992
313	Jan 1977	361	Jan 1981	409	Jan 1985	457	Jan 1989	505	Jan 1993
314	Feb 1977	362	Feb 1981	410	Feb 1985	458	Feb 1989	506	Feb 1993
315	Mar 1977	363	Mar 1981	411	Mar 1985	459	Mar 1989	507	Mar 1993
316	Apr 1977	364	Apr 1981	412	Apr 1985	460	Apr 1989	508	Apr 1993
317	May 1977	365	May 1981	413	May 1985	461	May 1989	509	May 1993
318	June 1977	366	June 1981	414	June 1985	462	June 1989	510	June 1993
319	July 1977	367	July 1981	415	July 1985	463	July 1989	511	July 1993
320	Aug 1977	368	Aug 1981	416	Aug 1985	464	Aug 1989	512	Aug 1993
321	Sept 1977	369	Sept 1981	417	Sept 1985	465	Sept 1989	513	Sept 1993
322	Oct 1977	370	Oct 1981	418	Oct 1985	466	Oct 1989	514	Oct 1993
323	Nov 1977	371	Nov 1981	419	Nov 1985	467	Nov 1989	515	Nov 1993
324	Dec 1977	372	Dec 1981	420	Dec 1985	468	Dec 1989	516	Dec 1993
325	Jan 1978	373	Jan 1982	421	Jan 1986	469	Jan 1990	517	Jan 1994
326	Feb 1978	374	Feb 1982	422	Feb 1986	470	Feb 1990	518	Feb 1994
327	Mar 1978	375	Mar 1982	423	Mar 1986	471	Mar 1990	519	Mar 1994
328	Apr 1978	376	Apr 1982	424	Apr 1986	472	Apr 1990	520	Apr 1994
329	May 1978	377	May 1982	425	May 1986	473	May 1990	521	May 1994
330	June 1978	378	June 1982	426	June 1986	474	June 1990	522	June 1994
331	July 1978	379	July 1982	427	July 1986	475	July 1990	523	July 1994
332	Aug 1978	380	Aug 1982	428	Aug 1986	476	Aug 1990	524	Aug 1994
333	Sept 1978	381	Sept 1982	429	Sept 1986	477	Sept 1990	525	Sept 1994
334	Oct 1978	382	Oct 1982	430	Oct 1986	478	Oct 1990	526	Oct 1994
335	Nov 1978	383	Nov 1982	431	Nov 1986	479	Nov 1990	527	Nov 1994
336	Dec 1978	384	Dec 1982	432	Dec 1986	480	Dec 1990	528	Dec 1994

Appendix I2. Initial estimated and PEST-derived demand-pattern factors used in water-distribution system model simulations, September 22–October 12, 2004, Tarawa Terrace, U.S. Marine Corps Base Camp Lejeune, North Carolina.[1]

[PEST, parameter estimation modeling software developed by Doherty (2005); —, not applicable]

September 22			September 24			September 26			September 28			September 30			October 2		
Hour	Initial	PEST	Hour	Initial	PEST	Hour	Initial	PEST	Hour	Initial	PEST	Hour	Initial	PEST	Hour	Initial	PEST
0000	—	—	0000	0.12	0.41	0000	1.70	1.13	0000	1.31	[2]1.84	0000	0.96	0.99	0000	1.59	1.46
0100	—	—	0100	0.15	0.45	0100	0.00	0.00	0100	0.00	0.00	0100	0.35	0.36	0100	0.00	0.00
0200	—	—	0200	0.61	0.52	0200	0.02	0.01	0200	0.28	0.05	0200	0.02	0.07	0200	0.00	0.00
0300	—	—	0300	0.45	0.40	0300	0.10	0.29	0300	0.61	0.83	0300	0.80	0.41	0300	0.12	0.27
0400	—	—	0400	0.39	0.70	0400	0.32	0.84	0400	0.85	0.32	0400	1.86	1.77	0400	0.20	0.56
0500	—	—	0500	1.69	1.04	0500	1.27	0.77	0500	0.67	0.93	0500	1.89	1.86	0500	0.51	0.19
0600	1.75	1.77	0600	0.66	0.62	0600	0.25	0.00	0600	1.32	1.90	0600	1.89	1.89	0600	0.74	1.01
0700	1.30	0.98	0700	1.09	0.79	0700	0.58	0.45	0700	0.81	0.86	0700	1.89	1.89	0700	1.14	1.37
0800	0.22	0.00	0800	1.25	1.61	0800	1.29	2.05	0800	0.78	0.74	0800	1.89	1.89	0800	1.17	0.96
0900	0.98	1.06	0900	1.66	1.83	0900	1.51	2.07	0900	1.26	0.96	0900	1.91	1.94	0900	1.50	1.47
1000	1.41	1.50	1000	1.78	2.45	1000	1.29	1.01	1000	1.17	0.87	1000	0.42	0.85	1000	2.60	1.88
1100	0.98	1.08	1100	1.27	1.55	1100	2.01	1.79	1100	1.13	1.62	1100	1.34	0.71	1100	1.40	1.53
1200	1.18	1.12	1200	1.11	0.41	1200	0.97	0.75	1200	1.02	0.75	1200	1.00	1.05	1200	1.46	1.31
1300	1.64	1.40	1300	1.21	1.60	1300	0.82	1.27	1300	1.19	0.98	1300	0.96	0.70	1300	1.29	1.14
1400	0.70	0.74	1400	1.64	2.03	1400	1.36	0.75	1400	0.94	1.24	1400	1.33	1.24	1400	1.21	1.17
1500	0.47	1.18	1500	0.62	0.86	1500	1.36	1.53	1500	1.47	1.44	1500	1.09	1.08	1500	1.03	1.21
1600	1.39	1.15	1600	0.83	0.73	1600	1.38	1.80	1600	1.04	0.87	1600	0.89	0.67	1600	0.95	0.86
1700	1.11	0.95	1700	1.50	0.53	1700	0.94	0.70	1700	0.96	1.17	1700	0.77	2.01	1700	1.55	1.41
1800	1.37	1.26	1800	2.14	1.85	1800	0.67	1.67	1800	1.24	0.88	1800	0.42	0.88	1800	0.86	0.52
1900	1.74	1.57	1900	1.51	2.44	1900	0.45	1.44	1900	1.51	2.03	1900	1.59	1.50	1900	1.03	1.31
2000	1.09	1.38	2000	0.41	0.00	2000	2.25	0.38	2000	1.37	1.44	2000	1.74	1.47	2000	1.54	1.30
2100	1.33	1.04	2100	0.91	0.26	2100	1.29	1.66	2100	1.14	0.52	2100	1.89	1.77	2100	1.89	1.73
2200	0.97	0.55	2200	1.36	2.36	2200	0.83	0.28	2200	1.04	0.80	2200	1.89	1.85	2200	1.86	1.77
2300	0.00	0.00	2300	0.00	0.00	2300	0.78	0.88	2300	0.20	0.46	2300	1.89	1.88	2300	1.68	1.59

September 23			September 25			September 27			September 29			October 1			October 3		
Hour	Initial	PEST	Hour	Initial	PEST	Hour	Initial	PEST	Hour	Initial	PEST	Hour	Initial	PEST	Hour	Initial	PEST
0000	0.00	0.00	0000	0.65	0.00	0000	0.38	0.00	0000	1.87	2.14	0000	1.86	1.83	0000	0.00	0.00
0100	0.00	0.00	0100	0.69	1.23	0100	0.39	0.33	0100	0.00	0.00	0100	1.89	1.87	0100	0.02	0.00
0200	0.02	0.00	0200	0.56	0.00	0200	0.56	0.99	0200	0.15	0.00	0200	1.89	1.89	0200	0.15	0.39
0300	0.15	0.40	0300	1.17	1.62	0300	0.41	0.00	0300	0.12	0.07	0300	0.43	0.26	0300	0.17	0.50
0400	0.27	0.72	0400	0.00	0.49	0400	0.78	1.11	0400	0.26	0.00	0400	0.25	0.00	0400	0.93	0.68
0500	0.74	0.56	0500	0.31	0.00	0500	0.96	1.33	0500	0.30	0.45	0500	1.14	0.46	0500	0.20	0.32
0600	1.62	1.34	0600	0.00	0.00	0600	0.97	1.03	0600	1.23	1.12	0600	0.80	0.78	0600	0.51	0.31
0700	0.74	0.25	0700	0.10	0.27	0700	0.94	0.82	0700	0.95	1.30	0700	1.18	1.59	0700	0.77	0.99
0800	0.84	1.29	0800	2.11	1.61	0800	0.72	0.53	0800	0.84	0.07	0800	0.67	0.18	0800	1.45	1.38
0900	1.36	1.60	0900	1.52	1.53	0900	0.98	0.63	0900	0.00	0.33	0900	0.93	1.40	0900	1.54	1.72
1000	1.82	1.65	1000	1.66	1.63	1000	0.90	1.23	1000	0.70	1.25	1000	1.39	1.57	1000	1.71	1.79
1100	1.33	1.94	1100	1.39	1.39	1100	1.51	1.72	1100	1.20	1.20	1100	1.41	1.65	1100	1.79	1.86
1200	1.30	1.96	1200	1.46	1.38	1200	1.04	0.24	1200	2.18	2.35	1200	1.91	1.88	1200	1.31	1.88
1300	1.70	1.75	1300	1.80	1.74	1300	0.85	1.33	1300	0.93	0.78	1300	1.35	1.95	1300	1.37	1.32
1400	0.85	0.91	1400	0.00	0.57	1400	1.20	1.06	1400	0.52	1.29	1400	1.86	1.85	1400	1.00	1.20
1500	0.88	0.97	1500	1.13	1.19	1500	0.89	1.34	1500	0.37	1.17	1500	1.89	1.88	1500	1.62	1.45
1600	2.00	1.16	1600	0.78	0.99	1600	1.22	0.77	1600	2.40	0.86	1600	1.89	1.88	1600	1.72	1.40
1700	1.77	1.52	1700	1.49	1.04	1700	1.35	1.68	1700	2.03	2.00	1700	1.86	1.83	1700	1.40	1.54
1800	0.73	0.96	1800	1.64	1.34	1800	1.25	1.55	1800	0.00	0.46	1800	1.89	1.88	1800	1.12	1.42
1900	1.21	1.26	1900	0.74	1.16	1900	0.83	1.18	1900	0.70	1.81	1900	1.22	1.15	1900	1.10	1.20
2000	2.10	1.70	2000	1.25	0.94	2000	1.63	1.05	2000	0.74	0.77	2000	0.89	0.92	2000	1.59	1.36
2100	2.85	2.69	2100	0.27	0.33	2100	1.31	1.09	2100	1.91	1.18	2100	1.89	2.03	2100	1.50	1.43
2200	0.18	0.00	2200	0.85	0.85	2200	1.18	1.24	2200	0.37	0.00	2200	1.86	1.87	2200	1.07	0.77
2300	0.00	0.06	2300	0.24	0.00	2300	0.77	0.27	2300	0.84	0.62	2300	1.89	1.87	2300	0.30	0.57

Appendix I2. Initial estimated and PEST-derived demand-pattern factors used in water-distribution system model simulations, September 22–October 12, 2004, Tarawa Terrace, U.S. Marine Corps Base Camp Lejeune, North Carolina.[1]—Continued

[PEST, parameter estimation modeling software developed by Doherty (2005); —, not applicable]

October 4			October 6			October 8			October 10			October 12		
Hour	Initial	PEST	Hour	Initial	PEST	Hour	Initial	PEST	Hour	Initial	PEST	Hour	Initial	PEST
0000	0.69	0.41	0000	0.58	0.91	0000	1.03	0.66	0000	1.79	2.02	0000	0.23	0.00
0100	0.17	0.29	0100	0.70	0.41	0100	0.15	0.01	0100	0.05	0.01	0100	0.19	0.00
0200	1.03	0.71	0200	0.12	0.16	0200	0.25	0.69	0200	0.05	[3]0.13	0200	0.10	0.07
0300	0.20	0.23	0300	0.71	0.61	0300	0.86	0.60	0300	0.73	0.18	0300	0.12	0.35
0400	0.72	0.98	0400	0.54	0.65	0400	0.15	0.19	0400	0.07	0.00	0400	0.47	0.96
0500	1.53	1.14	0500	0.83	0.54	0500	0.79	0.50	0500	0.15	0.29	0500	1.20	1.16
0600	1.01	0.78	0600	0.63	1.15	0600	0.57	1.20	0600	0.17	0.50	0600	1.10	0.94
0700	1.18	1.21	0700	1.59	1.50	0700	1.62	1.07	0700	0.81	0.59	0700	0.66	0.27
0800	1.12	1.53	0800	1.24	1.57	0800	0.97	0.84	0800	0.66	1.14	0800	0.42	0.91
0900	1.23	1.01	0900	0.85	0.82	0900	0.82	1.58	0900	1.92	1.52	0900	1.40	1.36
1000	1.01	0.73	1000	0.96	0.70	1000	1.24	0.83	1000	1.39	1.36	1000	1.47	1.60
1100	1.05	1.57	1100	0.99	1.28	1100	1.23	1.30	1100	1.76	1.80	1100	1.34	1.34
1200	1.49	1.23	1200	1.48	1.41	1200	1.64	1.40	1200	1.91	1.92	1200	0.66	0.36
1300	0.81	1.26	1300	0.89	0.78	1300	0.94	0.88	1300	0.13	0.86	1300	0.62	1.41
1400	1.12	0.84	1400	0.95	1.12	1400	0.42	0.92	1400	0.30	0.76	1400	1.59	0.93
1500	0.86	0.53	1500	0.71	0.84	1500	0.91	1.02	1500	1.24	1.53	1500	0.94	0.39
1600	1.17	1.35	1600	1.37	1.24	1600	1.28	1.04	1600	0.86	0.81	1600	0.62	1.38
1700	1.49	1.40	1700	1.61	1.51	1700	0.74	0.78	1700	1.13	1.18	1700	1.35	1.24
1800	1.68	1.68	1800	1.39	1.14	1800	1.16	0.99	1800	1.01	1.04	1800	0.71	0.30
1900	1.11	1.58	1900	0.90	0.81	1900	0.66	0.59	1900	0.88	0.77	1900	0.74	1.66
2000	1.03	0.75	2000	0.99	1.65	2000	0.62	0.81	2000	1.02	0.89	2000	0.40	1.33
2100	1.11	1.14	2100	1.54	1.37	2100	1.08	0.92	2100	0.64	0.78	2100	1.86	1.17
2200	1.31	1.07	2200	1.01	1.24	2200	0.51	0.51	2200	0.79	0.61	2200	1.27	0.40
2300	0.22	0.31	2300	0.71	0.28	2300	0.82	0.68	2300	0.66	0.33	2300	0.59	0.19

October 5			October 7			October 9			October 11		
Hour	Initial	PEST	Hour	Initial	PEST	Hour	Initial	PEST	Hour	Initial	PEST
0000	0.86	0.59	0000	0.17	0.19	0000	0.40	0.44	0000	0.43	0.08
0100	0.20	0.33	0100	0.48	0.26	0100	0.22	0.61	0100	0.12	0.24
0200	0.33	0.44	0200	0.43	0.55	0200	0.61	0.33	0200	0.12	0.37
0300	0.53	0.44	0300	0.25	0.68	0300	0.12	0.17	0300	0.68	0.90
0400	0.98	0.91	0400	1.19	0.85	0400	1.04	0.79	0400	1.79	0.74
0500	1.06	1.13	0500	0.57	1.06	0500	0.87	0.46	0500	0.24	0.30
0600	1.15	0.80	0600	1.29	1.12	0600	0.15	0.12	0600	0.39	0.26
0700	0.50	1.02	0700	0.86	0.41	0700	0.68	0.68	0700	0.64	0.75
0800	1.14	1.12	0800	1.19	1.37	0800	0.86	1.17	0800	0.72	0.73
0900	1.21	1.27	0900	1.34	1.35	0900	1.27	1.93	0900	1.23	1.29
1000	1.38	1.56	1000	1.13	1.33	1000	0.88	0.87	1000	1.46	1.19
1100	1.19	1.03	1100	0.99	1.10	1100	1.15	1.03	1100	1.03	0.89
1200	0.89	0.50	1200	0.96	0.88	1200	1.21	1.30	1200	1.35	1.63
1300	0.97	1.47	1300	1.17	1.03	1300	1.49	1.17	1300	2.28	2.44
1400	1.37	1.29	1400	1.08	1.11	1400	1.89	1.69	1400	1.26	1.27
1500	0.96	0.78	1500	1.18	1.00	1500	1.89	1.83	1500	1.08	0.94
1600	0.88	1.46	1600	0.66	0.49	1600	1.86	1.82	1600	0.84	0.66
1700	1.13	1.31	1700	0.90	1.61	1700	1.89	1.87	1700	1.14	1.21
1800	1.59	1.37	1800	1.54	1.40	1800	1.89	1.89	1800	1.37	1.66
1900	1.82	1.59	1900	1.72	1.45	1900	1.76	1.83	1900	1.37	1.37
2000	1.47	1.64	2000	1.23	0.91	2000	0.90	0.74	2000	0.64	0.29
2100	1.02	0.76	2100	0.50	1.04	2100	0.10	0.00	2100	0.95	1.01
2200	0.92	0.11	2200	0.71	0.47	2200	0.17	0.45	2200	1.06	1.28
2300	0.45	0.65	2300	0.30	0.60	2300	0.17	0.52	2300	0.91	0.66

[1]Initial values for demand-pattern factors estimated from water-balance analysis derived from information and data contained in a water-conservation analysis conducted by EGG, Inc. (1999)

[2]Demand-pattern factor modified to 1.80 for calibrated model

[3]Demand-pattern factor modified to 0.15 for calibrated model

Appendix I3. Probability density functions for uncertain model input parameters (variants) derived using pseudo-random number generators.

Infiltration (I_R): Dry year–1968

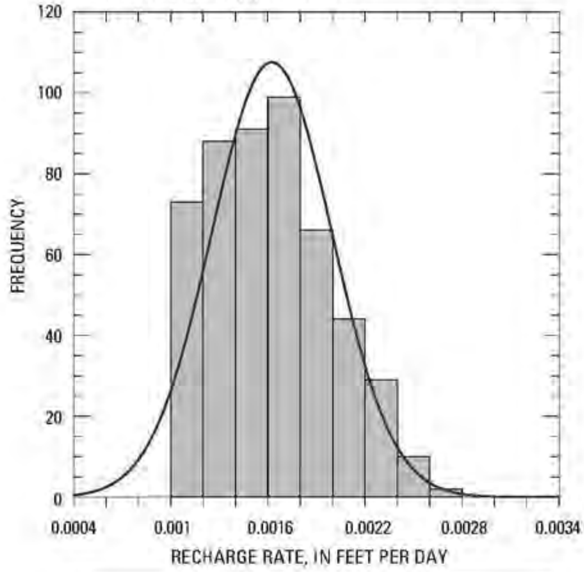

STATISTICS	Theoretical	Monte Carlo simulation
Distribution	Normal	Normal
Number of realizations	Not applicable	500
Minimum	–Infinity	0.001
Maximum	+ Infinity	0.005
Mean	0.0015	0.0016
Mode	0.0015	#N/A
Median	0.0015	0.0016
Standard deviation	0.0005	0.0004

Infiltration (I_R): Wet year–1974

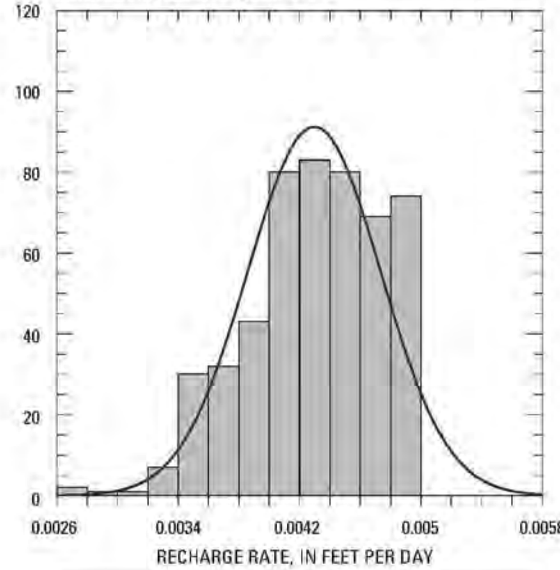

STATISTICS	Theoretical	Monte Carlo simulation
Distribution	Normal	Normal
Number of realizations	Not applicable	500
Minimum	–Infinity	0.001
Maximum	+ Infinity	0.005
Mean	0.0044	0.0043
Mode	0.0044	#N/A
Median	0.0044	0.0043
Standard deviation	0.0005	0.0004

Distribution coefficient (K_d)

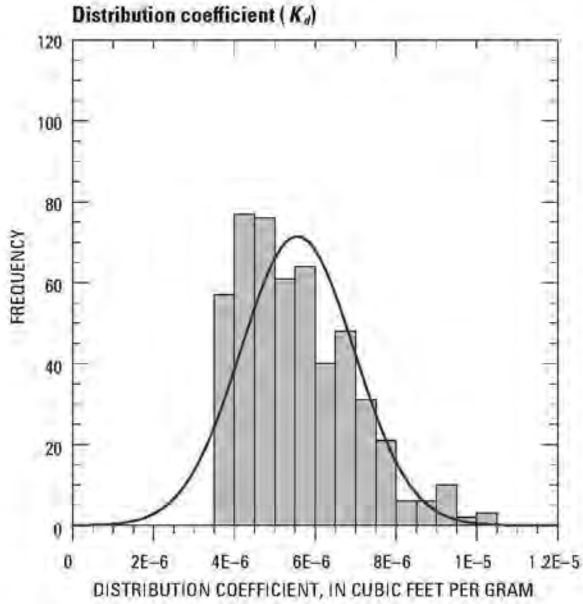

STATISTICS	Theoretical	Monte Carlo simulation
Distribution	Normal	Normal
Number of realizations	Not applicable	500
Minimum	–Infinity	3.5315E-06
Maximum	+ Infinity	2.6839E-06
Mean	5E-06	5.5550E-06
Mode	5E-06	#N/A
Median	5E-06	5.3030E-06
Standard deviation	1.7657E-06	1.3876E-06

Bulk density (ρ_b)

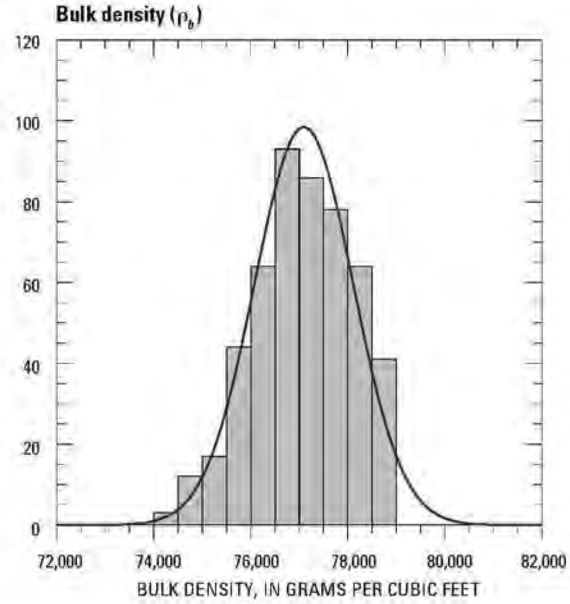

STATISTICS	Theoretical	Monte Carlo simulation
Distribution	Normal	Normal
Number of realizations	Not applicable	500
Minimum	–Infinity	69,943
Maximum	+ Infinity	79,004
Mean	77,112	77,097
Mode	77,112	77,512
Median	77,112	77,104
Standard deviation	1,100	1,009

Appendix I3. Probability density functions for uncertain model input parameters (variants) derived using pseudo-random number generators.—Continued

Effective porosity (n_E)

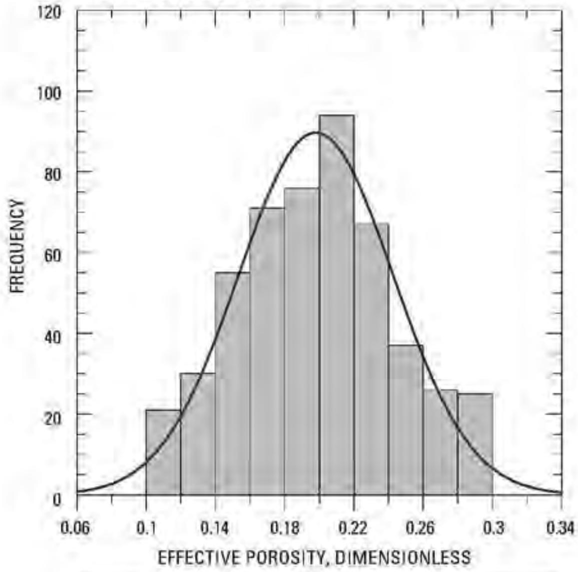

STATISTICS	Theoretical	Monte Carlo simulation
Distribution	Normal	Normal
Number of realizations	Not applicable	500
Minimum	−Infinity	0.1
Maximum	+ Infinity	0.3
Mean	0.2	0.1980
Mode	0.2	#N/A
Median	0.2	0.1992
Standard deviation	0.05	0.0444

Reaction rate (r)

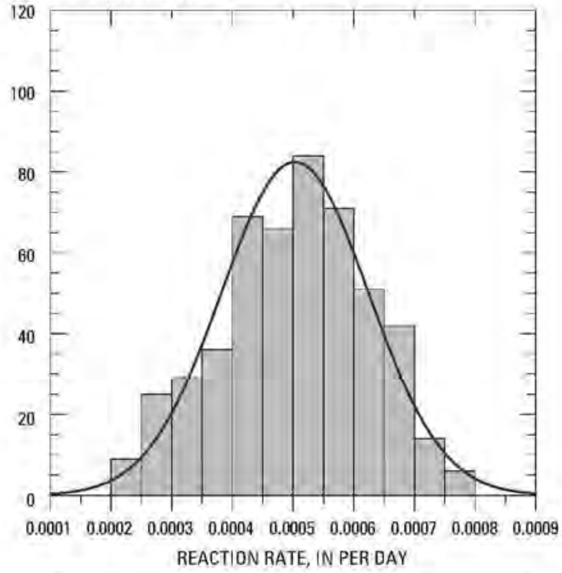

STATISTICS	Theoretical	Monte Carlo simulation
Distribution	Normal	Normal
Number of realizations	Not applicable	500
Minimum	−Infinity	2.3000E-04
Maximum	+ Infinity	7.7000E-04
Mean	5E-04	5.0309E-04
Mode	5E-04	#N/A
Median	5E-04	5.1309E-04
Standard deviation	1.35E-04	1.2059E-04

Mass-loading rate ($q_s C_s$)

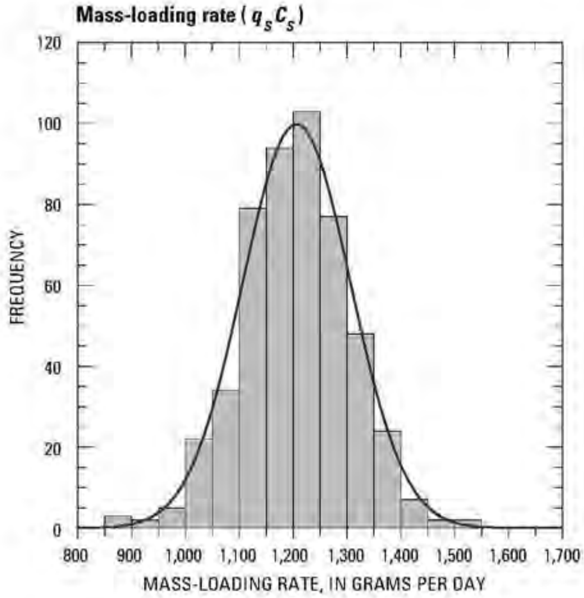

STATISTICS	Theoretical	Monte Carlo simulation
Distribution	Normal	Normal
Number of realizations	Not applicable	500
Minimum	−Infinity	200
Maximum	+Infinity	2,200
Mean	1,200	1,206.3168
Mode	1,200	1,190.2700
Median	1,200	1,207.9450
Standard deviation	100	98.3915

Longitudinal dispersivity (α_L)

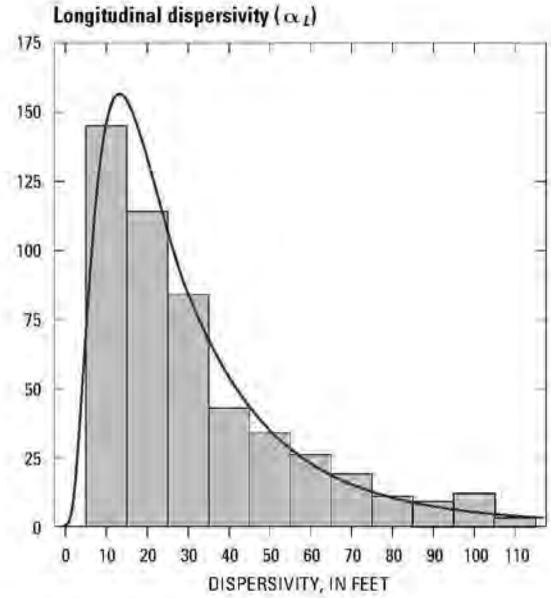

STATISTICS	Theoretical	Monte Carlo simulation
Distribution	Lognormal	Lognormal
Number of realizations	Not applicable	500
Minimum	0	5
Maximum	+ Infinity	125
Mean	34.56	31.3200
Mode	13.08	#N/A
Median	25	23.8500
Standard deviation	32.98	23.5900

Appendix I4. Methods for deriving probabilities of occurrence using simulated tetrachloroethylene (PCE) concentrations in finished drinking water, Tarawa Terrace, U.S. Marine Corps Base Camp Lejeune, North Carolina. [*P*, probability; Z, evaluated value in the standard normal distribution; ∞, infinity]

Appendix I4 presents two methods for determining the probability of occurrence of a specified concentration. In these methods, Monte Carlo simulation results for stress period 337, January 1979, are used for example calculations. For this stress period, the mean (μ) and standard deviation (σ) for 510 Monte Carlo realizations are 113 and 22.6 µg/L, respectively. The concentration of interest, 100 µg/L, occurs in the interval (or bin) between 96 and 105 µg/L, shown in the histogram representing Monte Carlo simulation results for January 1979 (Figure I27*c*).

A. Integration of the probability density function

1. The probability density function for the normal distribution is defined by the following formula:

$$\mathrm{Y} = \frac{1}{\sigma\sqrt{2\pi}} e^{-\frac{(x-\mu)^2}{2\sigma^2}}, \tag{I4.1}$$

where:
- Y is the value of the probability density function,
- σ is the standard deviation of simulated concentrations,
- x is the selected simulated concentration, and
- μ is the mean of simulated concentrations.

2. Obtain the mean (μ = 113 µg/L) and standard deviation (σ = 22.6 µg/L) for the January 1979 Monte Carlo simulation results. That is, the mean and standard deviation for the 510 concentration values for stress period 337, representing January 1979.

3. Using Equation I4.1 and substituting the values for the mean and standard deviation described in step 2 above, the probability density function for this set of simulations can be written as:

$$\mathrm{Y}(x) = \frac{1}{22.6\sqrt{2\pi}} e^{-\frac{(x-113)^2}{2(22.6)^2}} \tag{I4.2}$$

4. Then the probability of occurrence for the interval of 96–105 µg/L is obtained using the following integral:

$$P(96 \le x \le 105) = \int_{96}^{105} \frac{1}{22.6\sqrt{2\pi}} e^{-\frac{(x-113)^2}{2(22.6)^2}} dx \tag{I4.3}$$

5. This integral can be solved analytically or approximated numerically for this case.[1] Using the trapezoidal Riemann sum rule we can obtain the probability of occurrence. Figure I4.1 shows the procedure used to determine the area under the curve that represents probability.

$$\mathrm{Y}(96) = \frac{1}{22.6\sqrt{2\pi}} e^{-\frac{(96-113)^2}{2(22.6)^2}} = 0.013303 \text{ L/µg} \tag{I4.4}$$

$$\mathrm{Y}(105) = \frac{1}{22.6\sqrt{2\pi}} e^{-\frac{(105-113)^2}{2(22.6)^2}} = 0.016580 \text{ L/µg} \tag{I4.5}$$

[1]Numerical methods are advantageous for integrals that are difficult to evaluate or cannot be solved analytically.

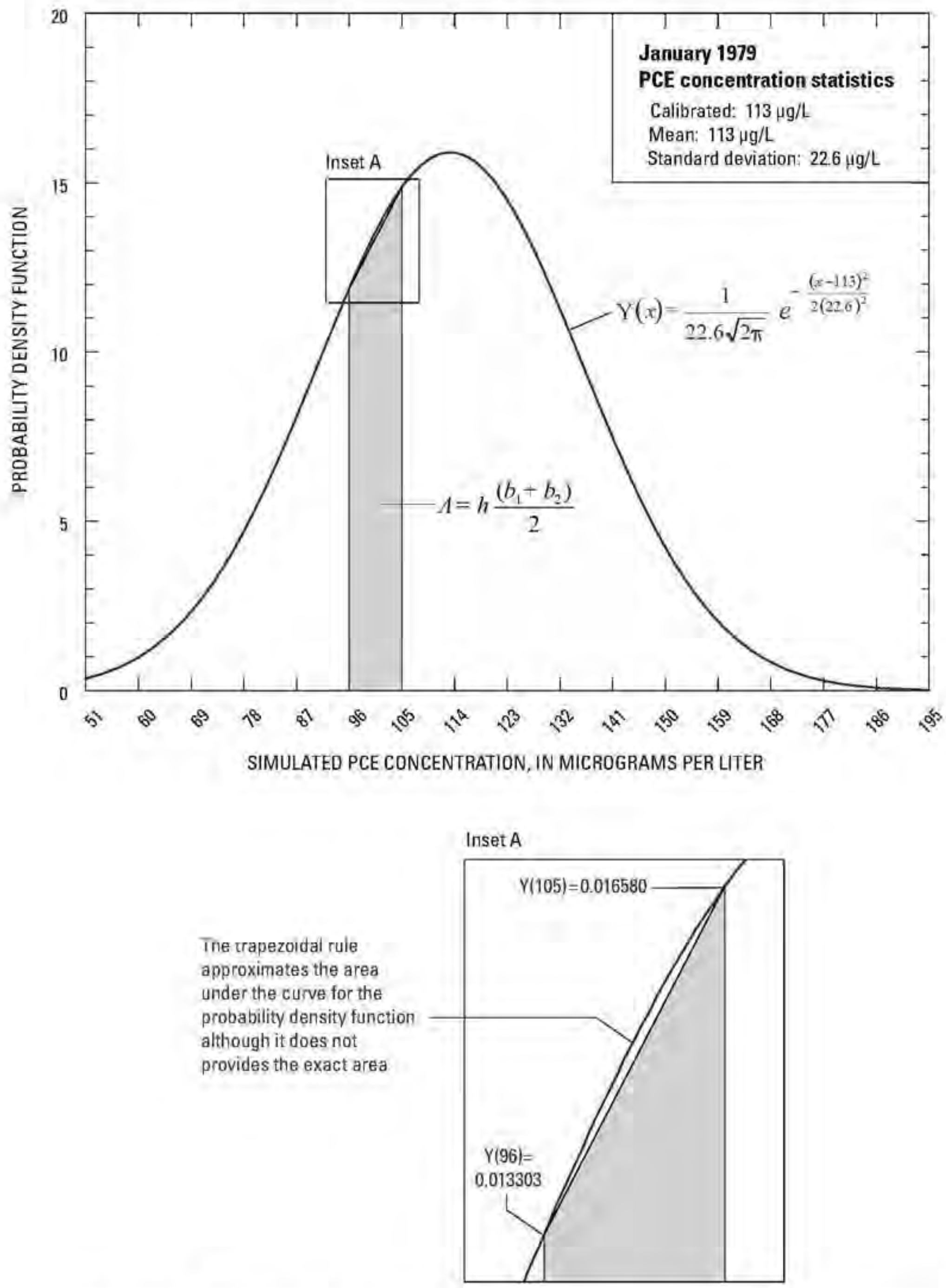

Figure I4.1. Probability of occurrence of tetrachloroethylene (PCE) contamination in finished water at the water treatment plant derived from the integration of the probability density function, Tarawa Terrace, U.S. Marine Corps Base Camp Lejeune, North Carolina.

Using the area formula for a trapezoid,

$$A = h\frac{(b_1 + b_2)}{2}, \tag{I4.6}$$

where,

- A is the area under the curve or probability of occurrence,
- h is the height of the trapezoid (9 μg/L [105 μg/L – 96 μg/L]), and
- b_1, b_2 are the bases of the trapezoid (0.013303 L/μg and 0.016580 L/μg, respectively).

Therefore, the probability of occurrence for concentrations between 96–105 μg/L is approximated as:

$$\mathrm{A} = 9\mu g/L\frac{(0.013303 + 0.0165850\,\mathrm{L}/\mu g)}{2} = 0.134496 = 13.45\% \tag{I4.7}$$

B. Table of the standard normal distribution

Another approach that can be used to obtain the probability of occurrence is by using the standard normal distribution table (Table I4.1). The following procedure, described in Haan (1977), summarizes the use of the standard normal table:

1. To use the standard normal distribution,[2] transform selected simulated concentration values as follows (using the simulated mean of μ = 113 μg/L and standard deviation of σ = 22.6 μg/L):

$$x = 96\mu g/L, \text{transforms to: } Z = \frac{x-\mu}{\sigma} = \frac{96-113}{22.6} = -0.7522 \tag{I4.8}$$

$$x = 105\mu g/L, \text{transforms to: } Z = \frac{x-\mu}{\sigma} = \frac{105-113}{22.6} = -0.3540 \tag{I4.9}$$

The standard normal distribution is symmetric about a mean = 0. Tables with negative values (such as those using Equations I4.8 and I4.9) usually are not published because all values can be obtained by using one side of the graph and complementary table values, as discussed below.

2. Obtain the probability from $-\infty$ to Z from the standard normal probability table (Table I4.1). In Figure I4.2 a section of Table I4.1 is shown, specific to this example:

$$P(x \le 96) = P(Z \le -0.7522) \tag{I4.10}$$

$$= 1 - P(Z \le 0.7522) = 1 - 0.7734 = 0.2266$$

This value represents the shaded area under the curve from $-\infty$ to 96 μg/L or the probability that the concentration will be less than or equal to 96 μg/L.

$$P(x \le 105) = P(Z \le -0.3540) \tag{I4.11}$$

$$= 1 - P(Z \le 0.3540) = 1 - 0.6368 = 0.3632$$

This value represents the shaded area under the curve from $-\infty$ to 105 μg/L or the probability that the concentration will be less than or equal to 105 μg/L.

3. The probability of occurrence is obtained by subtracting the two areas such that:

$$P(96 \le x \le 105) = P(x \le 105) - P(x \le 96) \tag{I4.12}$$

$$= 0{,}3632 - 0.2266 = 0.1366 = 13.66\% \tag{I4.13}$$

[2] A standard normal distribution has a mean of 0 and a standard deviation of 1.

Table I4.1. Standard normal distribution, probability content from $-\infty$ to Z.

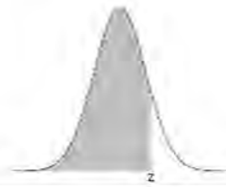

Z[1]	0.00	0.01	0.02	0.03	0.04	0.05	0.06	0.07	0.08	0.09
0.0	0.5000	0.5040	0.5080	0.5120	0.5160	0.5199	0.5239	0.5279	0.5319	0.5359
0.1	0.5398	0.5438	0.5478	0.5517	0.5557	0.5596	0.5636	0.5675	0.5714	0.5753
0.2	0.5793	0.5832	0.5871	0.5910	0.5948	0.5987	0.6026	0.6064	0.6103	0.6141
0.3	0.6179	0.6217	0.6255	0.6293	0.6331	0.6368	0.6406	0.6443	0.6480	0.6517
0.4	0.6554	0.6591	0.6628	0.6664	0.6700	0.6736	0.6772	0.6808	0.6844	0.6879
0.5	0.6915	0.6950	0.6985	0.7019	0.7054	0.7088	0.7123	0.7157	0.7190	0.7224
0.6	0.7257	0.7291	0.7324	0.7357	0.7389	0.7422	0.7454	0.7486	0.7517	0.7549
0.7	0.7580	0.7611	0.7642	0.7673	0.7704	0.7734	0.7764	0.7794	0.7823	0.7852
0.8	0.7881	0.7910	0.7939	0.7967	0.7995	0.8023	0.8051	0.8078	0.8106	0.8133
0.9	0.8159	0.8186	0.8212	0.8238	0.8264	0.8289	0.8315	0.8340	0.8365	0.8389
1.0	0.8413	0.8438	0.8461	0.8485	0.8508	0.8531	0.8554	0.8577	0.8599	0.8621
1.1	0.8643	0.8665	0.8686	0.8708	0.8729	0.8749	0.8770	0.8790	0.8810	0.8830
1.2	0.8849	0.8869	0.8888	0.8907	0.8925	0.8944	0.8962	0.8980	0.8997	0.9015
1.3	0.9032	0.9049	0.9066	0.9082	0.9099	0.9115	0.9131	0.9147	0.9162	0.9177
1.4	0.9192	0.9207	0.9222	0.9236	0.9251	0.9265	0.9279	0.9292	0.9306	0.9319
1.5	0.9332	0.9345	0.9357	0.9370	0.9382	0.9394	0.9406	0.9418	0.9429	0.9441
1.6	0.9452	0.9463	0.9474	0.9484	0.9495	0.9505	0.9515	0.9525	0.9535	0.9545
1.7	0.9554	0.9564	0.9573	0.9582	0.9591	0.9599	0.9608	0.9616	0.9625	0.9633
1.8	0.9641	0.9649	0.9656	0.9664	0.9671	0.9678	0.9686	0.9693	0.9699	0.9706
1.9	0.9713	0.9719	0.9726	0.9732	0.9738	0.9744	0.9750	0.9756	0.9761	0.9767
2.0	0.9772	0.9778	0.9783	0.9788	0.9793	0.9798	0.9803	0.9808	0.9812	0.9817
2.1	0.9821	0.9826	0.9830	0.9834	0.9838	0.9842	0.9846	0.9850	0.9854	0.9857
2.2	0.9861	0.9864	0.9868	0.9871	0.9875	0.9878	0.9881	0.9884	0.9887	0.9890
2.3	0.9893	0.9896	0.9898	0.9901	0.9904	0.9906	0.9909	0.9911	0.9913	0.9916
2.4	0.9918	0.9920	0.9922	0.9925	0.9927	0.9929	0.9931	0.9932	0.9934	0.9936
2.5	0.9938	0.9940	0.9941	0.9943	0.9945	0.9946	0.9948	0.9949	0.9951	0.9952
2.6	0.9953	0.9955	0.9956	0.9957	0.9959	0.9960	0.9961	0.9962	0.9963	0.9964
2.7	0.9965	0.9966	0.9967	0.9968	0.9969	0.9970	0.9971	0.9972	0.9973	0.9974
2.8	0.9974	0.9975	0.9976	0.9977	0.9977	0.9978	0.9979	0.9979	0.9980	0.9981
2.9	0.9981	0.9982	0.9982	0.9983	0.9984	0.9984	0.9985	0.9985	0.9986	0.9986
3.0	0.9987	0.9987	0.9987	0.9988	0.9988	0.9989	0.9989	0.9989	0.9990	0.9990

[1]For a negative Z-value, use the complementary table value that is defined as 1 – P(Z)

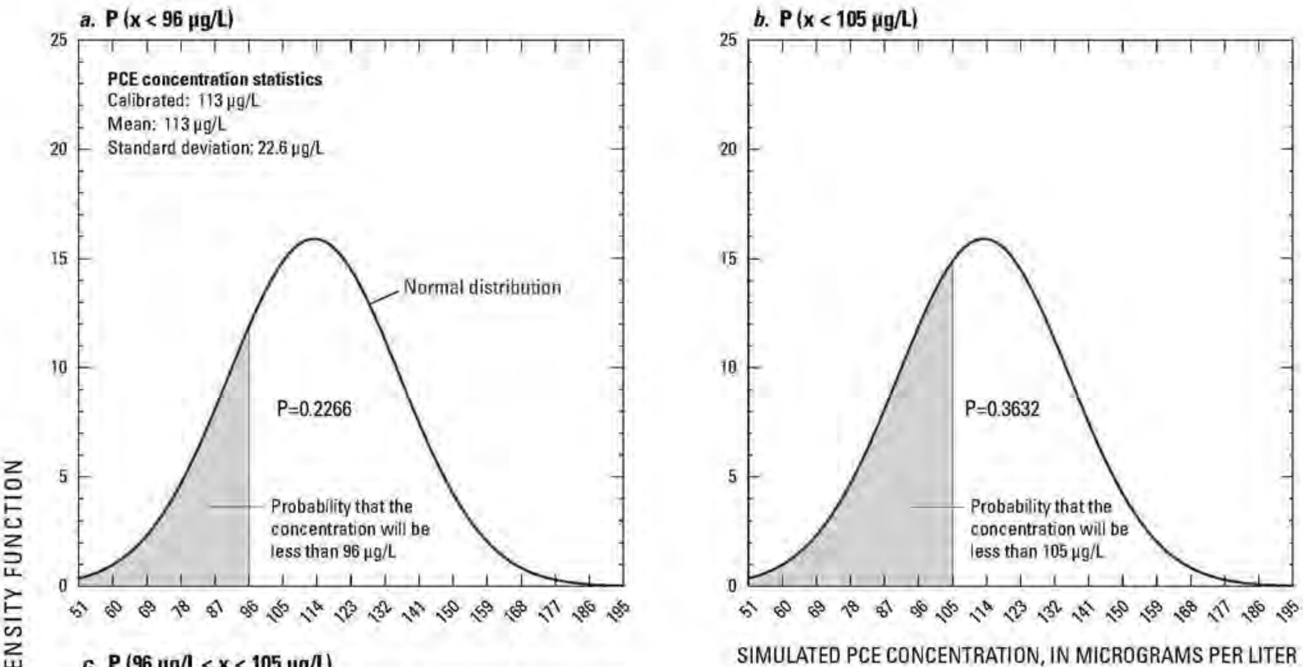

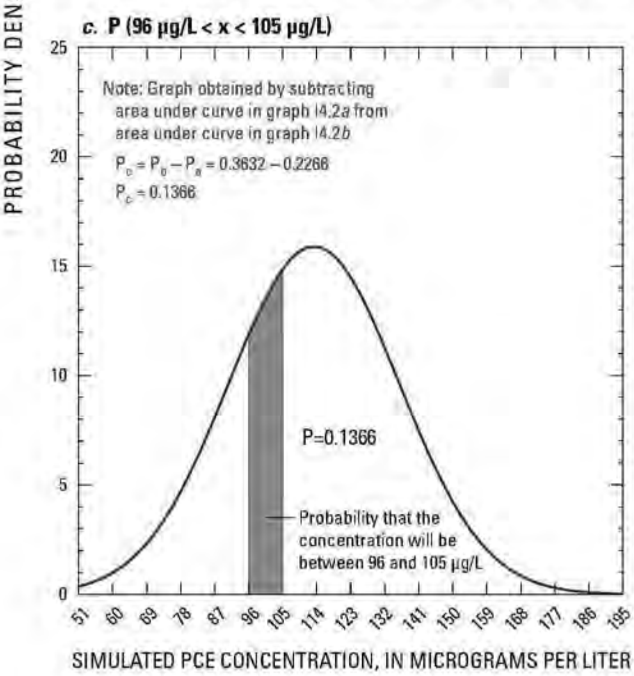

STANDARD NORMAL DISTRIBUTION

Z[1]	0.00	0.01	0.02	0.03	0.04	0.05
0.0	0.5000	0.5040	0.5080	0.5120	0.5160	0.5199
0.1	0.5398	0.5438	0.5478	0.5517	0.5557	0.5596
0.2	0.5793	0.5832	0.5871	0.5910	0.5948	0.5987
0.3	0.6179	0.6217	0.6255	0.6293	0.6331	0.6368
0.4	0.6554	0.6591	0.6628	0.6664	0.6700	0.6736
0.5	0.6915	0.6950	0.6985	0.7019	0.7054	0.7088
0.6	0.7257	0.7291	0.7324	0.7357	0.7389	0.7422
0.7	0.7580	0.7611	0.7642	0.7673	0.7704	0.7734

[1] For a negative Z-value, use the complementary table value that is defined as 1 − P(Z)

Figure I4.2. Probability of occurrence of tetrachloroethylene (PCE) contamination in finished water at the water treatment plant derived from the table of the standard normal distribution, Tarawa Terrace, U.S. Marine Corps Base Camp Lejeune, North Carolina.

Appendix I5. Simulated concentrations of tetrachloroethylene in finished water at the water treatment plant, Tarawa Terrace, U.S. Marine Corps Base Camp Lejeune, North Carolina.

[PCE, tetrachloroethylene; µg/L, microgram per liter; $P_{2.5}$, Monte Carlo simulation results for the 2.5 percentile; P_{50}, Monte Carlo simulation results for the 50 percentile; $P_{97.5}$, Monte Carlo simulation results for the 97.5 percentile; WTP, water treatment plant; Jan, January; Feb, February; Mar, March; Apr, April; Aug, August; Sept, September; Oct, October; Dec, December]

Stress period	Month and year	Calibrated PCE concentration, in µg/L[1]	Range of concentrations derived from Monte Carlo simulations[2]					
			Monte Carlo simulation (Scenario 1)[3]			Monte Carlo simulation (Scenario 2)[4]		
			$P_{2.5}$, in µg/L	P_{50}, in µg/L	$P_{97.5}$, in µg/L	$P_{2.5}$, in µg/L	P_{50}, in µg/L	$P_{97.5}$, in µg/L
1-12	Jan–Dec 1951				WTP not operating			
13	Jan 1952	0.00	0.00	0.00	0.00	0.00	0.00	0.00
14	Feb 1952	0.00	0.00	0.00	0.00	0.00	0.00	0.00
15	Mar 1952	0.00	0.00	0.00	0.00	0.00	0.00	0.00
16	Apr 1952	0.00	0.00	0.00	0.00	0.00	0.00	0.00
17	May 1952	0.00	0.00	0.00	0.00	0.00	0.00	0.00
18	June 1952	0.00	0.00	0.00	0.00	0.00	0.00	0.00
19	July 1952	0.00	0.00	0.00	0.00	0.00	0.00	0.00
20	Aug 1952	0.00	0.00	0.00	0.00	0.00	0.00	0.00
21	Sept 1952	0.00	0.00	0.00	0.00	0.00	0.00	0.00
22	Oct 1952	0.00	0.00	0.00	0.00	0.00	0.00	0.00
23	Nov 1952	0.00	0.00	0.00	0.00	0.00	0.00	0.00
24	Dec 1952	0.00	0.00	0.00	0.00	0.00	0.00	0.00
25	Jan 1953	0.00	0.00	0.00	0.00	0.00	0.00	0.00
26	Feb 1953	0.00	0.00	0.00	0.00	0.00	0.00	0.00
27	Mar 1953	0.00	0.00	0.00	0.00	0.00	0.00	0.00
28	Apr 1953	0.00	0.00	0.00	0.00	0.00	0.00	0.00
29	May 1953	0.00	0.00	0.00	0.00	0.00	0.00	0.00
30	June 1953	0.00	0.00	0.00	0.00	0.00	0.00	0.00
31	July 1953	0.00	0.00	0.00	0.00	0.00	0.00	0.00
32	Aug 1953	0.00	0.00	0.00	0.00	0.00	0.00	0.00
33	Sept 1953	0.00	0.00	0.00	0.00	0.00	0.00	0.00
34	Oct 1953	0.00	0.00	0.00	0.00	0.00	0.00	0.00
35	Nov 1953	0.00	0.00	0.00	0.00	0.00	0.00	0.00
36	Dec 1953	0.00	0.00	0.00	0.00	0.00	0.00	0.00
37	Jan 1954	0.00	0.00	0.00	0.00	0.00	0.00	0.00
38	Feb 1954	0.00	0.00	0.00	0.00	0.00	0.00	0.00
39	Mar 1954	0.00	0.00	0.00	0.00	0.00	0.00	0.00
40	Apr 1954	0.00	0.00	0.00	0.00	0.00	0.00	0.00
41	May 1954	0.00	0.00	0.00	0.00	0.00	0.00	0.00
42	June 1954	0.00	0.00	0.00	0.00	0.00	0.00	0.00
43	July 1954	0.00	0.00	0.00	0.00	0.00	0.00	0.00
44	Aug 1954	0.00	0.00	0.00	0.00	0.00	0.00	0.00
45	Sept 1954	0.00	0.00	0.00	0.00	0.00	0.00	0.00
46	Oct 1954	0.00	0.00	0.00	0.00	0.00	0.00	0.00
47	Nov 1954	0.00	0.00	0.00	0.00	0.00	0.00	0.00
48	Dec 1954	0.00	0.00	0.00	0.00	0.00	0.00	0.00
49	Jan 1955	0.00	0.00	0.00	0.00	0.00	0.00	0.00
50	Feb 1955	0.00	0.00	0.00	0.00	0.00	0.00	0.00
51	Mar 1955	0.00	0.00	0.00	0.00	0.00	0.00	0.00
52	Apr 1955	0.00	0.00	0.00	0.01	0.00	0.00	0.01
53	May 1955	0.00	0.00	0.00	0.01	0.00	0.00	0.01
54	June 1955	0.01	0.00	0.00	0.01	0.00	0.00	0.01
55	July 1955	0.01	0.00	0.01	0.02	0.00	0.01	0.02
56	Aug 1955	0.01	0.00	0.01	0.03	0.00	0.01	0.02
57	Sept 1955	0.02	0.00	0.01	0.04	0.00	0.01	0.03
58	Oct 1955	0.03	0.01	0.02	0.05	0.01	0.02	0.04
59	Nov 1955	0.04	0.01	0.03	0.07	0.01	0.03	0.07
60	Dec 1955	0.06	0.01	0.04	0.09	0.01	0.03	0.09

Appendix I5. Simulated concentrations of tetrachloroethylene in finished water at the water treatment plant, Tarawa Terrace, U.S. Marine Corps Base Camp Lejeune, North Carolina.—Continued

[PCE, tetrachloroethylene; µg/L, microgram per liter; $P_{2.5}$, Monte Carlo simulation results for the 2.5 percentile; P_{50}, Monte Carlo simulation results for the 50 percentile; $P_{97.5}$, Monte Carlo simulation results for the 97.5 percentile; WTP, water treatment plant; Jan, January; Feb, February; Mar, March; Apr, April; Aug, August; Sept, September; Oct, October; Dec, December]

Stress period	Month and year	Calibrated PCE concentration, in µg/L[1]	Range of concentrations derived from Monte Carlo simulations[2]					
			Monte Carlo simulation (Scenario 1)[3]			Monte Carlo simulation (Scenario 2)[4]		
			$P_{2.5}$, in µg/L	P_{50}, in µg/L	$P_{97.5}$, in µg/L	$P_{2.5}$, in µg/L	P_{50}, in µg/L	$P_{97.5}$, in µg/L
61	Jan 1956	0.08	0.02	0.05	0.12	0.02	0.04	0.12
62	Feb 1956	0.10	0.02	0.07	0.16	0.02	0.06	0.15
63	Mar 1956	0.13	0.03	0.09	0.21	0.03	0.08	0.18
64	Apr 1956	0.17	0.04	0.12	0.26	0.04	0.10	0.24
65	May 1956	0.23	0.05	0.15	0.33	0.05	0.12	0.29
66	June 1956	0.29	0.07	0.20	0.42	0.06	0.15	0.34
67	July 1956	0.36	0.09	0.25	0.52	0.08	0.18	0.41
68	Aug 1956	0.46	0.12	0.31	0.65	0.10	0.23	0.51
69	Sept 1956	0.57	0.15	0.38	0.79	0.13	0.29	0.65
70	Oct 1956	0.70	0.18	0.47	0.96	0.16	0.35	0.78
71	Nov 1956	0.85	0.23	0.57	1.16	0.22	0.47	1.03
72	Dec 1956	1.04	0.28	0.69	1.38	0.24	0.54	1.14
73	Jan 1957	1.25	0.35	0.83	1.63	0.31	0.63	1.38
74	Feb 1957	1.47	0.41	0.97	1.89	0.37	0.77	1.69
75	Mar 1957	1.74	0.49	1.16	2.21	0.43	0.88	1.84
76	Apr 1957	2.04	0.59	1.36	2.57	0.53	1.09	2.08
77	May 1957	2.39	0.70	1.59	2.97	0.60	1.20	2.40
78	June 1957	2.77	0.83	1.84	3.40	0.64	1.31	2.51
79	July 1957	3.21	0.98	2.12	3.87	0.74	1.50	3.08
80	Aug 1957	3.69	1.15	2.45	4.42	0.87	1.73	3.38
81	Sept 1957	4.21	1.33	2.80	4.99	1.07	2.11	3.83
82	Oct 1957	4.79	1.54	3.20	5.64	1.20	2.31	4.48
83	Nov 1957	5.41	1.77	3.61	6.32	1.46	2.95	5.33
84	Dec 1957	6.10	2.02	4.08	7.07	1.61	3.08	5.81
85	Jan 1958	6.86	2.29	4.60	7.87	1.81	3.43	6.42
86	Feb 1958	7.60	2.57	5.11	8.67	2.04	3.97	7.10
87	Mar 1958	8.47	2.88	5.71	9.58	2.36	4.36	7.74
88	Apr 1958	9.37	3.22	6.33	10.56	2.68	5.04	8.73
89	May 1958	10.37	3.61	7.02	11.61	2.99	5.37	9.15
90	June 1958	11.39	4.00	7.73	12.67	2.98	5.43	9.32
91	July 1958	12.91	4.59	8.78	14.26	4.03	6.88	11.46
92	Aug 1958	14.12	5.09	9.61	15.49	4.55	7.67	12.57
93	Sept 1958	15.35	5.62	10.47	16.74	4.62	8.07	13.12
94	Oct 1958	16.69	6.19	11.39	18.13	5.24	8.98	14.89
95	Nov 1958	18.03	6.79	12.32	19.54	5.71	9.88	16.33
96	Dec 1958	19.49	7.45	13.33	21.07	6.32	10.83	17.27
97	Jan 1959	20.97	8.11	14.36	22.62	6.84	11.56	18.53
98	Feb 1959	22.35	8.77	15.34	23.97	7.74	12.87	20.40
99	Mar 1959	23.92	9.53	16.47	25.59	7.80	13.07	20.81
100	Apr 1959	25.49	10.24	17.59	27.22	8.26	14.30	23.52
101	May 1959	27.15	11.08	18.81	29.01	8.82	15.02	23.60
102	June 1959	28.81	11.94	20.01	30.78	10.46	16.86	25.74
103	July 1959	30.56	12.79	21.37	32.69	11.14	17.71	27.35
104	Aug 1959	32.36	13.70	22.77	34.63	12.06	18.88	28.65
105	Sept 1959	34.14	14.62	24.11	36.56	12.39	19.29	28.82
106	Oct 1959	36.01	15.60	25.59	38.60	13.35	20.99	31.36
107	Nov 1959	37.85	16.60	27.04	40.57	13.30	22.66	35.03
108	Dec 1959	39.78	17.68	28.50	42.59	14.48	23.99	36.02

Appendix I5. Simulated concentrations of tetrachloroethylene in finished water at the water treatment plant, Tarawa Terrace, U.S. Marine Corps Base Camp Lejeune, North Carolina.—Continued

[PCE, tetrachloroethylene; µg/L, microgram per liter; $P_{2.5}$, Monte Carlo simulation results for the 2.5 percentile; P_{50}, Monte Carlo simulation results for the 50 percentile; $P_{97.5}$, Monte Carlo simulation results for the 97.5 percentile; WTP, water treatment plant; Jan, January; Feb, February; Mar, March; Apr, April; Aug, August; Sept, September; Oct, October; Dec, December]

Stress period	Month and year	Calibrated PCE concentration, in µg/L[1]	Range of concentrations derived from Monte Carlo simulations[2]					
			Monte Carlo simulation (Scenario 1)[3]			Monte Carlo simulation (Scenario 2)[4]		
			$P_{2.5}$, in µg/L	P_{50}, in µg/L	$P_{97.5}$, in µg/L	$P_{2.5}$, in µg/L	P_{50}, in µg/L	$P_{97.5}$, in µg/L
109	Jan 1960	41.86	18.82	30.15	44.74	15.99	24.99	38.89
110	Feb 1960	43.85	19.92	31.62	46.80	16.98	27.00	41.00
111	Mar 1960	46.03	21.13	33.16	49.07	17.85	26.94	41.01
112	Apr 1960	48.15	22.35	34.81	51.31	18.45	29.03	43.84
113	May 1960	50.37	23.59	36.60	53.65	19.84	30.13	44.48
114	June 1960	52.51	24.80	38.35	55.92	22.20	33.22	47.21
115	July 1960	54.74	26.08	40.12	58.27	23.30	34.55	50.18
116	Aug 1960	56.96	27.37	42.13	60.60	24.49	36.32	51.82
117	Sept 1960	59.09	28.64	43.80	62.82	24.27	35.66	51.64
118	Oct 1960	61.30	29.98	45.51	65.09	26.27	38.51	55.86
119	Nov 1960	63.42	31.31	47.25	67.22	26.43	40.46	59.79
120	Dec 1960	65.61	32.81	48.96	69.64	26.91	43.02	60.66
121	Jan 1961	67.69	34.22	50.74	71.88	28.21	43.30	63.65
122	Feb 1961	69.54	35.52	52.42	73.96	30.97	45.69	70.43
123	Mar 1961	71.56	36.93	54.16	76.28	31.47	45.72	66.14
124	Apr 1961	73.49	38.31	55.82	78.51	32.33	47.92	70.86
125	May 1961	75.49	39.76	57.54	80.74	32.37	49.12	70.32
126	June 1961	77.39	41.04	59.14	82.99	38.28	53.02	73.49
127	July 1961	79.36	42.45	60.87	84.92	36.88	54.13	75.55
128	Aug 1961	81.32	43.86	62.61	86.79	38.78	56.07	77.30
129	Sept 1961	83.19	45.25	64.23	88.82	38.62	54.74	76.56
130	Oct 1961	85.11	46.69	65.85	90.84	40.37	58.11	80.91
131	Nov 1961	86.95	48.10	67.44	92.75	39.55	59.92	87.09
132	Dec 1961	88.84	49.61	69.03	94.71	42.20	62.63	86.40
133	Jan 1962	60.88	34.23	47.47	64.96	27.60	42.46	62.20
134	Feb 1962	62.10	35.17	48.52	66.43	30.36	45.91	68.03
135	Mar 1962	62.94	35.84	49.35	67.26	31.00	45.13	66.06
136	Apr 1962	63.59	36.33	50.10	68.07	32.57	48.08	68.30
137	May 1962	64.17	36.80	50.73	68.98	31.10	46.57	66.06
138	June 1962	64.70	37.21	51.33	69.81	29.45	43.47	61.90
139	July 1962	65.23	37.65	51.82	70.45	28.63	44.36	62.01
140	Aug 1962	65.74	38.07	52.41	71.23	29.87	45.14	64.88
141	Sept 1962	66.22	38.47	52.91	71.97	32.00	47.51	67.91
142	Oct 1962	66.71	38.89	53.53	72.74	30.29	47.30	68.59
143	Nov 1962	67.18	39.30	54.16	73.38	35.13	53.53	77.51
144	Dec 1962	67.65	39.72	54.77	74.05	33.21	50.53	75.06
145	Jan 1963	68.06	40.19	55.24	74.67	32.41	49.74	74.10
146	Feb 1963	68.39	40.63	55.56	75.17	34.46	52.70	77.58
147	Mar 1963	68.73	41.15	56.03	75.76	35.61	52.41	73.73
148	Apr 1963	69.03	41.66	56.47	76.32	36.91	55.39	79.81
149	May 1963	69.33	42.03	56.98	77.17	34.47	53.02	77.36
150	June 1963	69.62	42.25	57.46	77.94	34.18	49.23	70.00
151	July 1963	69.90	42.45	57.98	78.48	32.75	49.62	71.03
152	Aug 1963	70.17	42.67	58.43	79.00	34.06	51.05	73.06
153	Sept 1963	70.43	42.87	58.82	79.47	36.62	52.90	76.53
154	Oct 1963	70.69	43.17	59.15	79.90	36.26	52.47	77.15
155	Nov 1963	70.93	43.60	59.49	80.31	38.46	59.09	84.58
156	Dec 1963	71.17	43.90	59.88	80.88	36.71	56.06	80.60

Appendix I5. Simulated concentrations of tetrachloroethylene in finished water at the water treatment plant, Tarawa Terrace, U.S. Marine Corps Base Camp Lejeune, North Carolina.—Continued

[PCE, tetrachloroethylene; µg/L, microgram per liter; $P_{2.5}$, Monte Carlo simulation results for the 2.5 percentile; P_{50}, Monte Carlo simulation results for the 50 percentile; $P_{97.5}$, Monte Carlo simulation results for the 97.5 percentile; WTP, water treatment plant; Jan, January; Feb, February; Mar, March; Apr, April; Aug, August; Sept, September; Oct, October; Dec, December]

Stress period	Month and year	Calibrated PCE concentration, in µg/L[1]	Range of concentrations derived from Monte Carlo simulations[2]					
			Monte Carlo simulation (Scenario 1)[3]			Monte Carlo simulation (Scenario 2)[4]		
			$P_{2.5}$, in µg/L	P_{50}, in µg/L	$P_{97.5}$, in µg/L	$P_{2.5}$, in µg/L	P_{50}, in µg/L	$P_{97.5}$, in µg/L
157	Jan 1964	71.40	44.18	60.32	81.34	35.81	55.22	80.71
158	Feb 1964	63.77	39.66	54.00	72.84	37.51	58.47	83.80
159	Mar 1964	63.95	39.92	54.36	73.38	37.37	57.84	81.58
160	Apr 1964	64.08	40.09	54.68	73.85	40.30	60.39	85.06
161	May 1964	64.19	40.31	54.98	74.28	39.56	57.23	84.15
162	June 1964	64.27	40.51	55.23	74.64	37.14	53.54	75.21
163	July 1964	64.34	40.61	55.45	74.98	35.59	54.24	76.87
164	Aug 1964	64.39	40.68	55.64	75.27	37.29	55.12	77.08
165	Sept 1964	64.43	40.75	55.82	75.62	39.55	57.96	80.84
166	Oct 1964	64.47	40.81	56.00	75.94	38.57	56.64	78.51
167	Nov 1964	64.49	40.88	56.18	76.19	42.49	63.10	91.13
168	Dec 1964	64.50	40.96	56.36	76.45	39.06	59.01	88.36
169	Jan 1965	64.50	41.10	56.58	76.70	37.87	59.05	88.52
170	Feb 1965	64.49	41.12	56.70	76.94	39.46	61.35	94.71
171	Mar 1965	64.47	41.14	56.78	77.17	41.20	60.99	89.98
172	Apr 1965	64.45	41.16	56.92	77.24	42.66	64.07	93.10
173	May 1965	64.42	41.20	57.06	77.13	41.03	61.17	87.07
174	June 1965	64.38	41.23	57.20	77.34	36.64	56.23	81.33
175	July 1965	64.33	41.26	57.22	77.80	38.15	57.32	81.83
176	Aug 1965	64.27	41.14	57.22	77.91	38.93	57.04	84.04
177	Sept 1965	64.20	41.03	57.22	77.92	41.40	60.36	84.29
178	Oct 1965	64.13	40.92	57.30	78.03	38.84	59.61	87.79
179	Nov 1965	64.05	40.85	57.34	78.10	44.47	66.00	95.45
180	Dec 1965	63.97	40.78	57.39	78.10	39.95	61.88	91.31
181	Jan 1966	63.88	40.81	57.48	78.26	39.34	61.61	91.59
182	Feb 1966	63.79	40.88	57.54	78.38	42.06	64.63	99.81
183	Mar 1966	63.68	41.01	57.62	78.45	41.44	63.87	94.47
184	Apr 1966	63.57	41.20	57.61	78.33	43.72	66.91	97.21
185	May 1966	63.46	41.28	57.64	78.43	42.05	64.21	91.37
186	June 1966	63.34	41.40	57.70	78.44	38.28	58.86	86.56
187	July 1966	63.21	41.54	57.70	78.65	39.70	58.20	87.29
188	Aug 1966	63.08	41.69	57.74	78.94	39.57	60.11	87.73
189	Sept 1966	62.94	41.79	57.79	78.91	41.82	62.94	91.60
190	Oct 1966	62.80	41.73	57.82	78.87	40.67	60.35	90.52
191	Nov 1966	62.65	41.67	57.78	78.78	44.43	68.76	99.82
192	Dec 1966	62.50	41.60	57.82	78.70	40.92	63.19	97.26
193	Jan 1967	62.25	41.42	57.70	78.67	40.95	62.45	96.88
194	Feb 1967	61.99	41.20	57.61	78.56	41.00	66.51	98.39
195	Mar 1967	61.67	40.98	57.36	78.37	43.47	64.42	95.01
196	Apr 1967	61.35	40.74	57.12	78.11	44.75	66.63	97.65
197	May 1967	61.02	40.52	56.84	77.78	42.71	64.23	95.11
198	June 1967	60.69	40.22	56.65	77.54	38.89	58.53	86.55
199	July 1967	60.37	40.03	56.43	77.45	38.46	59.64	87.57
200	Aug 1967	60.05	39.87	56.26	77.39	39.01	59.72	89.18
201	Sept 1967	59.74	39.69	56.04	77.26	40.93	61.91	90.19
202	Oct 1967	59.43	39.49	55.86	77.12	40.30	60.56	90.27
203	Nov 1967	59.13	39.31	55.71	76.98	44.01	68.01	99.90
204	Dec 1967	58.83	39.12	55.50	76.83	41.94	63.60	97.99

Appendix I5. Simulated concentrations of tetrachloroethylene in finished water at the water treatment plant, Tarawa Terrace, U.S. Marine Corps Base Camp Lejeune, North Carolina.—Continued

[PCE, tetrachloroethylene; µg/L, microgram per liter; $P_{2.5}$, Monte Carlo simulation results for the 2.5 percentile; P_{50}, Monte Carlo simulation results for the 50 percentile; $P_{97.5}$, Monte Carlo simulation results for the 97.5 percentile; WTP, water treatment plant; Jan, January; Feb, February; Mar, March; Apr, April; Aug, August; Sept, September; Oct, October; Dec, December]

Stress period	Month and year	Calibrated PCE concentration, in µg/L[1]	Range of concentrations derived from Monte Carlo simulations[2]					
			Monte Carlo simulation (Scenario 1)[3]			Monte Carlo simulation (Scenario 2)[4]		
			$P_{2.5}$, in µg/L	P_{50}, in µg/L	$P_{97.5}$, in µg/L	$P_{2.5}$, in µg/L	P_{50}, in µg/L	$P_{97.5}$, in µg/L
205	Jan 1968	58.41	38.91	55.32	76.43	40.60	63.04	98.22
206	Feb 1968	57.95	38.69	55.12	75.94	39.51	63.91	98.67
207	Mar 1968	57.43	38.44	54.74	75.51	41.62	63.54	94.21
208	Apr 1968	56.94	38.22	54.56	75.12	42.61	65.79	99.98
209	May 1968	56.45	37.99	54.20	74.61	39.39	62.35	92.79
210	June 1968	55.98	37.72	53.86	74.13	37.49	57.23	84.15
211	July 1968	55.49	37.46	53.50	73.63	37.51	56.92	83.56
212	Aug 1968	55.02	37.31	53.27	73.27	37.52	58.08	84.83
213	Sept 1968	54.58	37.16	53.00	73.05	40.06	60.24	89.84
214	Oct 1968	54.13	36.94	52.72	72.83	37.61	59.46	87.96
215	Nov 1968	53.71	36.71	52.49	72.61	42.84	64.11	96.77
216	Dec 1968	53.28	36.45	52.16	72.34	39.36	60.93	93.74
217	Jan 1969	53.07	36.40	52.03	72.40	37.42	60.60	90.38
218	Feb 1969	52.97	36.41	52.07	72.32	38.68	63.83	100.33
219	Mar 1969	52.94	36.41	52.21	72.23	40.85	62.20	90.15
220	Apr 1969	52.93	36.50	52.33	72.58	41.71	63.74	95.37
221	May 1969	52.93	36.55	52.41	72.94	40.51	60.54	94.64
222	June 1969	52.92	36.59	52.49	73.24	37.99	56.86	82.85
223	July 1969	52.90	36.61	52.54	73.52	35.02	57.32	85.75
224	Aug 1969	52.86	36.63	52.71	73.77	36.90	57.85	85.34
225	Sept 1969	52.81	36.64	52.74	73.98	39.74	59.97	89.19
226	Oct 1969	52.75	36.64	52.75	74.13	37.64	59.44	92.22
227	Nov 1969	55.19	38.34	55.24	77.72	36.74	55.89	84.87
228	Dec 1969	55.19	38.30	55.23	77.70	32.94	51.96	81.13
229	Jan 1970	55.01	38.10	55.14	77.54	32.78	50.97	81.62
230	Feb 1970	54.79	37.97	55.03	77.34	33.13	52.80	83.08
231	Mar 1970	54.49	37.71	54.76	77.08	32.85	52.72	79.35
232	Apr 1970	54.20	37.46	54.48	76.72	34.85	54.22	82.26
233	May 1970	53.90	37.21	54.17	76.27	33.91	51.26	78.11
234	June 1970	53.61	37.01	53.91	75.89	29.54	47.08	71.71
235	July 1970	53.32	36.82	53.59	75.68	28.77	46.80	72.48
236	Aug 1970	53.04	36.64	53.32	75.44	29.60	47.37	70.90
237	Sept 1970	52.78	36.47	53.06	75.25	31.55	49.00	74.82
238	Oct 1970	52.53	36.31	52.78	75.02	30.14	48.10	73.55
239	Nov 1970	52.29	36.19	52.67	74.93	32.50	53.01	81.51
240	Dec 1970	52.05	36.05	52.54	74.88	32.47	48.94	76.35
241	Jan 1971	51.96	35.96	52.53	75.02	30.00	48.86	77.29
242	Feb 1971	51.93	35.90	52.50	75.19	32.51	50.78	80.73
243	Mar 1971	51.95	35.87	52.60	75.42	32.25	49.82	78.27
244	Apr 1971	51.99	35.86	52.73	75.65	32.74	52.65	81.01
245	May 1971	52.03	35.86	52.88	75.88	30.15	49.32	76.96
246	June 1971	52.08	35.85	52.86	76.11	29.02	45.87	72.87
247	July 1971	52.12	35.92	52.88	76.35	29.03	45.64	72.37
248	Aug 1971	52.16	35.93	52.97	76.52	29.30	46.61	71.75
249	Sept 1971	52.20	35.93	53.07	76.72	30.33	48.38	74.56
250	Oct 1971	52.23	35.95	53.13	76.91	29.27	46.98	73.25
251	Nov 1971	52.26	35.98	53.25	77.05	32.40	52.55	82.47
252	Dec 1971	52.29	35.91	53.28	77.28	30.91	49.57	76.35

Appendix I5. Simulated concentrations of tetrachloroethylene in finished water at the water treatment plant, Tarawa Terrace, U.S. Marine Corps Base Camp Lejeune, North Carolina.—Continued

[PCE, tetrachloroethylene; µg/L, microgram per liter; $P_{2.5}$, Monte Carlo simulation results for the 2.5 percentile; P_{50}, Monte Carlo simulation results for the 50 percentile; $P_{97.5}$, Monte Carlo simulation results for the 97.5 percentile; WTP, water treatment plant; Jan, January; Feb, February; Mar, March; Apr, April; Aug, August; Sept, September; Oct, October; Dec, December]

Stress period	Month and year	Calibrated PCE concentration, in µg/L[1]	Range of concentrations derived from Monte Carlo simulations[2]					
			Monte Carlo simulation (Scenario 1)[3]			Monte Carlo simulation (Scenario 2)[4]		
			$P_{2.5}$, in µg/L	P_{50}, in µg/L	$P_{97.5}$, in µg/L	$P_{2.5}$, in µg/L	P_{50}, in µg/L	$P_{97.5}$, in µg/L
253	Jan 1972	49.34	33.93	50.30	73.12	29.17	48.14	77.82
254	Feb 1972	49.01	33.72	50.06	72.93	30.19	50.33	81.13
255	Mar 1972	48.68	33.47	49.71	72.72	31.69	48.44	75.80
256	Apr 1972	48.40	33.25	49.54	72.47	30.79	50.77	79.48
257	May 1972	48.14	33.10	49.27	72.26	30.44	48.53	73.97
258	June 1972	47.90	32.98	49.08	72.17	27.68	44.98	68.87
259	July 1972	47.67	32.85	48.97	72.02	27.13	43.58	66.62
260	Aug 1972	47.45	32.72	48.78	71.78	26.91	43.63	68.46
261	Sept 1972	47.25	32.60	48.69	71.47	28.10	46.38	72.80
262	Oct 1972	47.05	32.49	48.58	71.34	28.15	44.90	70.07
263	Nov 1972	46.87	32.41	48.43	71.26	30.68	49.80	78.83
264	Dec 1972	46.69	32.29	48.21	71.16	28.36	46.21	76.56
265	Jan 1973	54.28	37.52	56.04	82.79	27.54	44.70	72.51
266	Feb 1973	54.19	37.39	55.96	82.69	29.05	47.31	78.50
267	Mar 1973	53.98	37.15	55.78	82.35	28.09	46.20	73.11
268	Apr 1973	53.76	36.91	55.44	81.94	28.95	46.73	77.52
269	May 1973	53.52	36.68	55.24	81.51	26.12	45.17	70.36
270	June 1973	53.30	36.46	55.22	81.10	25.61	40.75	66.70
271	July 1973	53.08	36.24	55.12	80.74	25.25	40.82	63.84
272	Aug 1973	52.87	36.03	54.99	80.59	25.02	41.47	64.39
273	Sept 1973	52.68	35.84	54.88	80.46	26.43	43.33	68.68
274	Oct 1973	52.51	35.66	54.87	80.34	26.17	41.28	65.28
275	Nov 1973	52.35	35.49	54.80	80.25	27.77	45.41	72.92
276	Dec 1973	52.20	35.33	54.72	80.17	25.66	42.21	68.89
277	Jan 1974	52.43	35.41	54.97	80.49	25.72	42.62	69.65
278	Feb 1974	52.82	35.59	55.42	80.98	26.19	43.80	72.53
279	Mar 1974	53.39	35.86	55.92	81.66	25.08	42.86	68.49
280	Apr 1974	53.99	36.16	56.60	82.41	28.14	45.59	71.28
281	May 1974	54.63	36.49	57.21	83.20	25.84	42.70	72.49
282	June 1974	55.25	36.80	57.69	84.15	25.00	40.00	64.50
283	July 1974	55.90	37.13	58.15	85.07	24.17	40.57	65.57
284	Aug 1974	56.53	37.50	58.85	85.98	24.29	40.75	65.98
285	Sept 1974	57.10	37.85	59.43	86.86	27.22	43.16	69.98
286	Oct 1974	57.70	38.22	60.00	87.74	25.22	42.68	67.27
287	Nov 1974	58.30	38.56	60.59	88.58	28.99	47.52	76.53
288	Dec 1974	58.92	38.98	61.11	89.45	25.07	44.15	72.46
289	Jan 1975	61.00	40.30	63.17	92.62	27.61	45.83	75.73
290	Feb 1975	61.24	40.39	63.33	92.97	28.46	48.17	80.43
291	Mar 1975	61.41	40.51	63.43	93.20	28.98	46.39	77.50
292	Apr 1975	61.57	40.61	63.45	93.38	29.37	48.59	82.56
293	May 1975	61.72	40.78	63.62	93.32	28.00	46.55	76.49
294	June 1975	61.88	40.92	63.77	93.48	24.95	42.93	67.44
295	July 1975	62.05	41.05	64.04	93.91	25.59	42.20	68.93
296	Aug 1975	62.25	41.13	64.22	94.27	26.21	42.72	68.78
297	Sept 1975	62.46	41.20	64.36	94.54	25.88	44.92	73.09
298	Oct 1975	62.69	41.18	64.65	94.84	26.24	43.56	70.58
299	Nov 1975	62.92	41.12	64.91	95.15	27.40	49.02	80.06
300	Dec 1975	63.18	41.12	65.11	95.44	26.23	45.41	76.07

Appendix I5. Simulated concentrations of tetrachloroethylene in finished water at the water treatment plant, Tarawa Terrace, U.S. Marine Corps Base Camp Lejeune, North Carolina.—Continued

[PCE, tetrachloroethylene; µg/L, microgram per liter; $P_{2.5}$, Monte Carlo simulation results for the 2.5 percentile; P_{50}, Monte Carlo simulation results for the 50 percentile; $P_{97.5}$, Monte Carlo simulation results for the 97.5 percentile; WTP, water treatment plant; Jan, January; Feb, February; Mar, March; Apr, April; Aug, August; Sept, September; Oct, October; Dec, December]

Stress period	Month and year	Calibrated PCE concentration, in µg/L[1]	Range of concentrations derived from Monte Carlo simulations[2]: Monte Carlo simulation (Scenario 1)[3]			Monte Carlo simulation (Scenario 2)[4]		
			$P_{2.5}$, in µg/L	P_{50}, in µg/L	$P_{97.5}$, in µg/L	$P_{2.5}$, in µg/L	P_{50}, in µg/L	$P_{97.5}$, in µg/L
301	Jan 1976	73.96	48.06	76.13	111.62	27.44	47.37	78.75
302	Feb 1976	74.94	48.64	77.01	112.96	28.08	50.08	82.73
303	Mar 1976	75.97	49.28	77.88	114.29	30.00	49.48	77.65
304	Apr 1976	76.97	49.90	78.87	115.66	29.89	51.83	83.45
305	May 1976	78.00	50.66	79.94	117.25	28.96	49.32	81.75
306	June 1976	79.02	51.42	80.86	118.78	27.37	44.69	74.98
307	July 1976	80.07	52.20	81.82	120.35	28.29	45.16	75.62
308	Aug 1976	81.13	52.86	82.70	121.82	27.95	46.57	76.48
309	Sept 1976	82.17	53.51	83.71	123.46	29.17	49.14	79.62
310	Oct 1976	83.25	54.25	84.81	124.74	28.92	48.10	80.30
311	Nov 1976	84.31	55.09	85.76	126.00	31.09	53.61	90.47
312	Dec 1976	85.41	55.90	86.67	127.61	28.21	50.51	82.95
313	Jan 1977	86.61	56.70	87.66	129.36	28.88	49.71	81.57
314	Feb 1977	87.70	57.45	88.70	131.09	30.18	52.13	85.43
315	Mar 1977	88.91	58.14	89.80	133.02	29.18	51.65	83.61
316	Apr 1977	90.10	58.86	90.90	134.30	32.23	54.40	88.91
317	May 1977	91.32	59.61	91.86	135.48	30.43	50.86	86.19
318	June 1977	92.53	60.38	93.08	136.61	28.97	47.43	78.24
319	July 1977	93.75	61.24	94.29	137.80	29.03	47.45	77.48
320	Aug 1977	94.99	62.11	95.48	139.43	28.20	48.28	81.51
321	Sept 1977	96.20	62.97	96.44	140.89	30.24	50.29	85.19
322	Oct 1977	97.42	63.86	97.49	142.51	28.33	51.14	82.53
323	Nov 1977	98.62	64.58	98.62	144.08	32.33	56.02	92.86
324	Dec 1977	99.84	65.31	99.65	145.59	29.86	53.22	90.47
325	Jan 1978	101.18	66.16	101.09	147.13	44.02	75.70	120.92
326	Feb 1978	102.77	67.25	102.62	148.91	39.93	67.26	112.31
327	Mar 1978	103.04	67.39	103.04	149.08	52.50	84.64	133.87
328	Apr 1978	104.31	68.24	104.52	150.32	46.79	76.94	126.94
329	May 1978	105.19	68.81	105.34	151.12	50.49	85.95	136.76
330	June 1978	106.88	70.00	107.10	153.19	42.45	73.13	119.19
331	July 1978	107.95	70.77	108.05	154.56	45.08	75.24	121.43
332	Aug 1978	108.69	71.12	108.58	155.63	48.54	80.46	135.92
333	Sept 1978	109.61	71.68	109.40	156.91	48.81	83.51	139.85
334	Oct 1978	111.18	72.89	110.78	158.60	44.55	75.04	121.83
335	Nov 1978	111.08	72.99	110.76	158.33	59.23	100.40	162.58
336	Dec 1978	111.93	73.52	111.71	159.48	58.45	100.01	162.64
337	Jan 1979	113.14	74.30	112.93	161.01	57.81	95.20	164.77
338	Feb 1979	114.05	74.80	113.75	162.04	58.23	99.50	166.62
339	Mar 1979	114.98	75.32	114.60	163.14	59.21	101.26	162.26
340	Apr 1979	115.82	76.01	115.14	164.14	64.03	105.77	169.77
341	May 1979	116.68	76.83	115.85	165.22	60.49	104.49	166.33
342	June 1979	117.47	77.56	116.62	166.12	57.29	95.08	158.63
343	July 1979	118.29	78.22	117.32	166.52	60.76	97.83	159.43
344	Aug 1979	119.08	78.87	117.95	167.11	60.40	101.30	162.28
345	Sept 1979	119.83	79.50	118.62	167.82	67.04	105.09	167.67
346	Oct 1979	120.59	80.14	119.49	168.59	63.07	104.48	172.01
347	Nov 1979	121.31	80.74	120.12	169.34	74.24	119.14	191.45
348	Dec 1979	122.04	81.35	120.77	170.09	68.90	113.89	186.42

Appendix I5. Simulated concentrations of tetrachloroethylene in finished water at the water treatment plant, Tarawa Terrace, U.S. Marine Corps Base Camp Lejeune, North Carolina.—Continued

[PCE, tetrachloroethylene; µg/L, microgram per liter; $P_{2.5}$, Monte Carlo simulation results for the 2.5 percentile; P_{50}, Monte Carlo simulation results for the 50 percentile; $P_{97.5}$, Monte Carlo simulation results for the 97.5 percentile; WTP, water treatment plant; Jan, January; Feb, February; Mar, March; Apr, April; Aug, August; Sept, September; Oct, October; Dec, December]

Stress period	Month and year	Calibrated PCE concentration, in µg/L[1]	Range of concentrations derived from Monte Carlo simulations[2]					
			Monte Carlo simulation (Scenario 1)[3]			Monte Carlo simulation (Scenario 2)[4]		
			$P_{2.5}$, in µg/L	P_{50}, in µg/L	$P_{97.5}$, in µg/L	$P_{2.5}$, in µg/L	P_{50}, in µg/L	$P_{97.5}$, in µg/L
349	Jan 1980	123.28	82.20	122.09	171.34	61.30	101.54	159.81
350	Feb 1980	122.98	81.93	121.80	171.45	77.70	131.23	206.13
351	Mar 1980	124.03	82.63	122.99	172.63	67.73	114.94	183.21
352	Apr 1980	123.90	82.42	123.27	172.41	86.02	143.61	229.05
353	May 1980	124.69	82.89	123.73	173.81	85.23	138.95	220.28
354	June 1980	125.83	83.92	124.67	175.54	80.14	128.55	203.28
355	July 1980	0.72	0.10	0.43	1.67	0.06	0.32	1.22
356	Aug 1980	0.75	0.11	0.45	1.73	0.07	0.34	1.28
357	Sept 1980	121.36	80.64	120.61	170.25	74.54	128.20	195.86
358	Oct 1980	121.72	80.95	121.00	170.55	82.88	137.09	215.09
359	Nov 1980	122.14	81.32	121.73	171.07	89.83	145.35	231.15
360	Dec 1980	122.95	81.96	122.56	171.97	87.97	143.51	226.80
361	Jan 1981	114.05	76.20	113.83	159.33	81.35	131.65	210.19
362	Feb 1981	114.39	76.42	114.22	159.76	71.73	120.32	185.47
363	Mar 1981	115.60	77.32	115.10	161.62	65.38	104.23	164.75
364	Apr 1981	116.55	78.07	116.07	163.34	61.89	101.55	158.35
365	May 1981	117.30	78.64	116.91	164.52	63.14	99.62	156.29
366	June 1981	118.36	79.53	117.92	165.37	54.95	86.73	140.98
367	July 1981	133.29	89.77	132.96	186.08	58.22	92.47	142.21
368	Aug 1981	134.31	90.57	133.94	187.73	59.68	95.47	151.17
369	Sept 1981	120.72	81.40	120.32	168.91	58.90	98.56	150.82
370	Oct 1981	121.04	81.71	120.86	169.57	61.42	99.80	157.59
371	Nov 1981	121.41	82.04	121.17	170.30	60.76	101.36	158.08
372	Dec 1981	121.81	82.41	121.56	171.08	63.30	102.27	160.36
373	Jan 1982	103.95	70.61	103.86	145.41	55.35	91.05	141.55
374	Feb 1982	105.86	71.96	105.76	147.68	56.60	92.63	140.40
375	Mar 1982	107.52	73.05	107.51	149.67	59.57	93.91	147.10
376	Apr 1982	108.83	74.01	108.79	151.25	58.43	97.00	147.50
377	May 1982	148.50	101.45	147.91	206.23	66.65	107.89	166.05
378	June 1982	110.78	75.70	110.41	153.60	61.01	99.03	151.27
379	July 1982	111.98	76.77	111.69	154.90	62.24	97.91	154.37
380	Aug 1982	113.07	77.74	112.66	156.03	63.70	99.09	152.90
381	Sept 1982	114.04	78.49	113.60	157.00	65.21	100.91	153.98
382	Oct 1982	114.60	79.03	114.14	157.69	67.41	108.99	165.07
383	Nov 1982	113.87	78.41	113.67	157.37	88.82	142.12	223.75
384	Dec 1982	115.16	79.21	114.95	158.89	79.98	128.05	193.75
385	Jan 1983	1.25	0.25	0.75	2.48	0.17	0.61	1.90
386	Feb 1983	1.29	0.27	0.78	2.56	0.18	0.63	1.94
387	Mar 1983	111.76	77.09	112.19	156.29	78.57	123.82	194.41
388	Apr 1983	112.66	77.92	112.99	157.31	74.18	119.77	182.63
389	May 1983	113.97	79.21	114.10	158.82	70.85	117.76	174.86
390	June 1983	106.10	74.18	106.03	147.67	68.30	103.53	162.13
391	July 1983	116.70	81.48	116.62	162.17	66.41	108.10	166.88
392	Aug 1983	117.72	82.09	117.54	163.39	67.97	107.12	161.29
393	Sept 1983	117.83	82.03	117.63	163.40	76.74	120.27	183.16
394	Oct 1983	117.97	82.03	117.88	163.53	84.95	133.04	207.24
395	Nov 1983	118.63	82.60	118.70	164.81	89.04	142.71	224.56
396	Dec 1983	120.78	84.23	120.74	167.35	72.65	113.38	171.38

Appendix I5. Simulated concentrations of tetrachloroethylene in finished water at the water treatment plant, Tarawa Terrace, U.S. Marine Corps Base Camp Lejeune, North Carolina.—Continued

[PCE, tetrachloroethylene; µg/L, microgram per liter; $P_{2.5}$, Monte Carlo simulation results for the 2.5 percentile; P_{50}, Monte Carlo simulation results for the 50 percentile; $P_{97.5}$, Monte Carlo simulation results for the 97.5 percentile; WTP, water treatment plant; Jan, January; Feb, February; Mar, March; Apr, April; Aug, August; Sept, September; Oct, October; Dec, December]

Stress period	Month and year	Calibrated PCE concentration, in µg/L[1]	Range of concentrations derived from Monte Carlo simulations[2]					
			Monte Carlo simulation (Scenario 1)[3]			Monte Carlo simulation (Scenario 2)[4]		
			$P_{2.5}$, in µg/L	P_{50}, in µg/L	$P_{97.5}$, in µg/L	$P_{2.5}$, in µg/L	P_{50}, in µg/L	$P_{97.5}$, in µg/L
397	Jan 1984	132.87	92.63	133.27	185.03	103.04	159.84	247.01
398	Feb 1984	180.39	126.52	180.97	249.43	94.25	150.35	230.69
399	Mar 1984	183.02	128.61	183.55	252.50	99.38	159.70	240.42
400	Apr 1984	151.46	106.37	151.54	208.97	97.90	155.71	236.45
401	May 1984	153.42	107.63	153.20	211.58	92.85	146.63	220.85
402	June 1984	182.13	127.45	181.99	250.57	94.11	152.75	228.36
403	July 1984	156.39	109.41	156.40	214.58	101.95	160.97	234.39
404	Aug 1984	170.47	106.73	158.25	238.65	108.76	168.54	261.54
405	Sept 1984	181.22	113.28	168.51	253.93	117.53	184.30	295.64
406	Oct 1984	173.73	108.42	161.84	245.02	120.12	182.33	281.84
407	Nov 1984	173.77	108.41	161.92	245.70	124.18	187.60	287.36
408	Dec 1984	173.18	107.82	161.69	246.06	127.85	193.50	301.23
409	Jan 1985	176.12	109.98	164.71	251.48	122.98	187.00	293.19
410	Feb 1985	3.64	1.13	2.67	6.57	0.47	1.41	3.74
411	Mar 1985	8.71	3.21	6.58	14.79	8.83	20.01	41.59
412	Apr 1985	8.09	2.99	6.16	13.70	9.00	20.41	42.30
413	May 1985	4.76	1.50	3.46	8.36	0.58	1.68	4.47
414	June 1985	5.14	1.65	3.80	9.21	0.64	1.81	4.78
415	July 1985	5.54	1.80	4.12	10.04	0.69	1.96	5.12
416	Aug 1985	6.01	1.98	4.50	10.97	0.76	2.14	5.56
417	Sept 1985	6.50	2.19	4.88	11.89	0.83	2.30	6.03
418	Oct 1985	7.06	2.43	5.33	12.88	0.92	2.53	6.53
419	Nov 1985	7.64	2.68	5.78	13.90	1.02	2.76	7.07
420	Dec 1985	8.27	2.93	6.32	14.99	1.13	3.00	7.59
421	Jan 1986	8.85	3.18	6.82	15.87	1.24	3.22	8.14
422	Feb 1986	9.42	3.45	7.30	16.67	1.35	3.46	8.69
423	Mar 1986	12.14	4.55	9.43	21.18	1.85	4.67	11.50
424	Apr 1986	10.83	4.09	8.44	18.71	1.64	4.08	9.90
425	May 1986	11.56	4.42	9.06	19.63	1.79	4.41	10.49
426	June 1986	12.28	4.77	9.70	20.59	1.94	4.76	11.08
427	July 1986	13.06	5.14	10.35	21.75	2.11	5.12	11.77
428	Aug 1986	13.84	5.54	11.01	23.04	2.29	5.51	12.50
429	Sept 1986	14.61	5.90	11.70	24.30	2.49	5.89	13.19
430	Oct 1986	15.42	6.28	12.41	25.59	2.71	6.33	13.94
431	Nov 1986	16.21	6.66	13.11	26.70	2.93	6.73	14.77
432	Dec 1986	17.03	7.06	13.77	27.86	3.17	7.20	15.65
433	Jan 1987	17.85	7.47	14.46	29.04	3.41	7.66	16.46
434	Feb 1987	18.49	7.82	15.02	29.91	3.62	8.04	17.16
435	Mar 1987	WTP closed						

[1]Results from Faye (2008) and reported in Maslia et al. (2007, Appendix A2)

[2]$P_{97.5}$ and $P_{2.5}$ represent the upper and lower bound, respectively, of 95 percent of Monte Carlo simulations; for a Gaussian (normal) distribution, the median (P_{50}) should equal the mean value

[3]Scenario 1 Monte Carlo simulation is for pumping uncertainty excluded

[4]Scenario 2 Monte Carlo simulation is for pumping uncertainty included

ATSDR

Analyses of Groundwater Flow, Contaminant Fate and Transport, and Distribution of Drinking Water at Tarawa Terrace and Vicinity,
U.S. Marine Corps Base Camp Lejeune, North Carolina: Historical Reconstruction and Present-Day Conditions—
Chapter I: Parameter Sensitivity, Uncertainty, and Variability Associated with Model Simulations of Groundwater Flow,
Contaminant Fate and Transport, and Distribution of Drinking Water